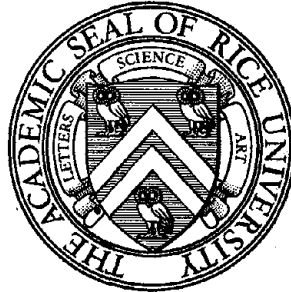# STRUCTURAL RESEARCH AT RICE

Report No. 40

SEISMIC RESPONSE OF CONNECTIONS IN INDETERMINATE R/C FRAME SUBASSEMBLIES

by

H. E. Zerbe and A. J. Durrani

Department of Civil Engineering
Rice University
Houston, Texas

April, 1990

SEISMIC RESPONSE OF CONNECTIONS IN INDETERMINATE R/C FRAME SUBASSEMBLIES

by

Hikmat Edward Zerbe

Ahmad Jan Durrani

Department of Civil Engineering
Rice University
Houston, Texas

April, 1990

i.a

SEISMIC RESPONSE OF CONNECTIONS IN INDETERMINATE R/C FRAME SUBASSEMBLIES

ABSTRACT

The behavior of beam-to-column connections under earthquake-type loading has been studied in the past by testing isolated interior or exterior connections. In such tests, the beams are allowed to elongate freely when subjected to large deformation reversal. In a real building, however, the beams may be partially restrained against such elongation. The current design procedures which have been developed on the basis of tests on isolated connections, therefore, ignore the effects of continuity and beam elongation on the performance of connections.

In this investigation, the behavior of connections was studied by testing indeterminate frame subassemblies under earthquake-type loading. Six half-scale multiple-connection subassemblies were tested. Each subassembly consisted of a two-bay frame isolated at the column mid-heights. Five single connection subassemblies were also tested to correlate the behavior of connections in multiple-connection subassemblies with the behavior of connections observed by testing isolated connections.

i. b

Tests have shown that restriction to elongation of beams in indeterminate systems resulted in axial compression in beams which in turn had a significant effect on the performance of connections. The joint shear increased in both interior and exterior connections and the column-to-beam flexural strength ratio decreased. The energy dissipation was not affected by the continuity, but the lateral load resistance increased significantly. The stiffness degradation was more controlled and gradual in the indeterminate subassemblies compared to that observed in isolated connections. Based on the observed mechanism of lateral load resistance and the observed behavior of connections, a procedure is presented to account for the presence of axial compression in the main beams in the design of beam-to-column connections.

ACKNOWLEDGMENTS

LIST OF CONTENTS

LIST OF TABLES

LIST OF FIGURES

NOTATION

A_s = Area of positive beam reinforcement

A_{sj} = Total cross-sectional area of joint lateral reinforcement

A_{st} = Area of negative beam reinforcement = $A_{sb} + 2A_{ss}$

A_{sb} = Area of beam top reinforcement

A_{ss} = Area of slab reinforcement within the effective slab width on one side of the beam

b_b = Width of beam

b_c = Width of column

b_e = Effective slab width in positive bending (slab in compression)

b_{eff} = Effective slab width in negative bending (slab in tension)

b_j = Effective width of joint = $(b_b + b_c)/2$ < $b_b + b_c/2$

$d - d'$ = Distance between beam top and bottom reinforcement

E = Modulus of elasticity of reinforcement before yield

E_{sh} = Modulus of elasticity of reinforcement at strain hardening

f'_c = Concrete compressive strength

f_y = Reinforcement yield strength

f_u = Reinforcement ultimate strength

H = Total column height

h_c = Depth of column

h_b = Depth of beam

h_s = Thickness of slab

M_b^+ = Positive moment in the beam (slab in compression)

M_b^- = Negative moment in the beam (slab in tension)

M_{nb}^+ = Beam positive flexural capacity (slab in compression)

M_{nb}^- = Beam negative flexural capacity (slab in tension)

M'_{nb} = Beam flexural capacity including the effect of axial compression

M_{nc} = Column flexural capacity

M_{yc} = Column yield flexural capacity

N = Axial force in the beam

N_{max} = Maximum axial force in the beam

R = Column to beam flexural strength ratio

T_n = Nominal torsional moment strength

V_{col} = Shear in the column

V_c = Shear in the center column

V_j = Lateral shear in the joint

V_L = Shear in the left column

V_R = Shear in the right column

v_j = Shear stress in the joint

α = Steel strength multiplier

ϵ_y = Strain of reinforcement at yield

ϵ_{sh} = Strain of reinforcement at strain hardening

γ = Shear strength factor

ρ = Ratio of joint lateral reinforcement

ϕ = Strength reduction factor

Chapter 1

INTRODUCTION

1.1 General

Multistory reinforced concrete frames are expected to undergo large inelastic deformation reversals during earthquakes of moderate to strong intensity. These deformations are mostly concentrated in areas such as beam-column joints and the beam flexural hinges. In order to preserve the integrity of a structure, such critical regions must be designed and detailed to dissipate the input earthquake energy without any significant loss of strength and stiffness.

The seismic response of beam-to-column connections has been traditionally studied by testing isolated interior or exterior connections under simulated earthquake-type loading (1-28). When a frame is subjected to lateral earthquake forces, the effect of gravity load, particularly for the intermediate and lower stories, is assumed to be relatively small and neglected. This assumption implies that the points of inflection occur at the mid-span of the beams and at the mid-height of the columns. The resulting testing arrangement

which is undoubtedly economical and convenient, represents an interior connection or an exterior connection where the beams and the upper and lower columns cantilever out from the joint. Since these test subassemblies are determinate, the forces acting on the joint can be easily computed. The current understanding of the behavior of connections and the procedure for the design of connections are almost entirely based on observations and conclusions drawn from such tests on isolated connections.

However, there are still many questions to be answered on the applicability of the behavior observed from tests on isolated connections to the response of connections in a real building. The connections in real buildings respond under a set of boundary conditions that can be quite different from what is assumed in the laboratory tests. The isolated connections tested in laboratory typically experience elongation of the main beams which results mostly from yielding of longitudinal bars in the flexural hinging region. Since the beams in such tests are free to elongate, no axial compression can develop in the beams. In a real building, this will occur only if flexural hinges in the beams at all floor levels would develop simultaneously and have identical plastic rotation. However, nonlinear analyses of frame buildings (29) have shown that not only do the hinges propagate

along the height of the building but they may also not occur simultaneously at the same floor level. Consequently, the floor beams which yielded first or experienced more inelastic deformation compared to beams at adjacent floors may be partially restrained against free elongation. This phenomenon could result in the development of axial compression in certain beams, which would increase their flexural capacity and affect the distribution of lateral load among the columns.

1.2 Objectives and Scope

The first objective of this investigation was to study the behavior of beam-to-column connections in multiple-connection frame subassemblies subjected to earthquake-type loading. Testing of such frame subassemblies represents a new generation of tests where the continuity in the test frame provides the connections with an indeterminate environment that more closely simulates the case of a real building. The variables investigated in this study included (1) the presence of transverse beams, (2) the presence of transverse beams and a floor slab, (3) the amount of joint transverse reinforcement, and (4) the location of beam flexural hinges with respect the column face.

The second objective of this investigation was to compare the behavior of connections when tested as isolated interior

or exterior connections, as has been done in the past, to their behavior when tested as multiple-connection frame subassemblies. The connections studied in this section included (1) beam-to-column connections without a floor slab, and (2) beam-to-column connections with transverse beams and a floor slab.

In order to accomplish these objectives, eleven half-scale beam-to-column connection subassemblies were tested under earthquake-type loading. Six of these subassemblies were two-bay frames isolated at column mid-heights. The other five test subassemblies were single interior or exterior connections which were isolated from column mid-heights and beam mid-spans.

1.3 Literature Review

During the 1960s, investigations of structural damage following several severe earthquakes, including earthquakes in Chile (30), Caracas (31), Tokachi-Oki (32), and San Fernando (33), have called attention to the importance of proper design and detailing of members and joints in moment resisting frames. Since then, a great number of research programs in many different countries have investigated the behavior of beam-to-column connections and developed design recommendations. These research programs significantly improved the understanding of

the behavior of frame structures subjected to earthquake-type loading and some of the recommendations have been incorporated in building codes (34-38).

In this section, the contribution of some of these research programs to the current understanding of the behavior of beam-to-column connections subjected to earthquake-type loading is reviewed.

Hanson and Conner (1) conducted some of the earliest tests on the behavior of connections by testing sixteen beam-to-column connection subassemblies. They brought out the importance of the joint transverse reinforcement in improving the seismic behavior of connections. They also noted that adequate energy dissipation in members adjacent to the joint can be achieved if proper attention was given to the rebar anchorage and the joint confinement.

During the mid 1970s most researchers concentrated on investigating the shear failure through the joint core and, thus, a better understanding of the joint shear mechanism was developed. The idea of shifting the beam flexural hinges away from the face of the columns to further protect the joint was also developed. Zhang and Jirsa (39), analyzed data from a large number of beam-column joints tested in six different countries. They concluded that the joint shear is resisted

by an inclined concrete compression strut and they developed
a formula which reflects the effect of all the factors that
influence the joint shear strength. Paulay, Park, and Priestley
(6), however, emphasized that the joint shear is resisted by
a combination of a concrete diagonal strut and a truss mechanism
consisting of horizontal and vertical reinforcement. They
also noted that the shear resistance of the concrete diagonal
strut diminished when plastic hinges formed in the beams
adjacent to the column faces. Popov and Bertero (40), suggested
that all beams in energy dissipating building frames should
be designed to form plastic hinges away from the column face
to prevent beam bar yielding from penetration into the joint
core. Abdel-Fattah and Wight (17), investigated relocating
the beam flexural hinges away from the face of the column with
the use of intermediate layers of longitudinal reinforcement
and extra top and bottom steel in the beam. They noted that
with such an arrangement the joint was not highly distressed
and a better environment to develop the required bond stresses
inside the joint was provided.

Bond deterioration along beam and column bars within joints
during seismic loading is undesirable since slip of
reinforcement results in increased deformation of the frame,
loss of the stiffness and reduction in energy dissipation
capability of connections. Therefore, design codes limit the

diameter of beam and column longitudinal bars in moment resisting frames to a proportion of the column and beam depth, respectively. Hawkins, Kobayashi and Fourney (41) studied the bond deterioration in exterior connections subjected to cyclic loading. They observed that under cyclic loading, bond failed at much lower drift level than for monotonic loading. Zhu and Jirsa (42) evaluated few selected past investigations of beam-to-column connections and observed no significant bond damage at interstory drift of 3 percent. Park (43) studied the anchorage of beam bars in four interior beam-to-column connection subassemblies and showed that by including the concrete strength and the ratio of the areas of compression to tension reinforcement, a considerable relaxation in the maximum permitted diameter of beam bars passing through interior joints can be achieved.

The effect of concrete properties on the performance of beam-to-column connections was reported in two different studies. Bertero, Popov, and Fourzani (8) tested two interior beam-to-column connections constructed of light-weight concrete, and compared the results with similar specimens but constructed of normal-weight concrete. They observed that the energy dissipated by the light-weight concrete specimens was considerably smaller than that of the similar normal-weight concrete specimens. This was mainly due to the earlier slippage

of beam reinforcement through the joint. Ehsani, Mousa and Vallenilla (22) tested four exterior beam-to-column connections constructed of high-strength concrete (f_c' = 9500 psi). They concluded that the shear strength of the joint should be a function of the concrete compressive strength, and that connections constructed with high-strength concrete can exhibit ductile response, similar to those constructed with ordinary-strength concrete, only if properly detailed.

Early in the 1980s, the presence of the floor slab was introduced as a major factor that influenced the behavior of beam-to-column connections. In a real building, the slab is cast monolithically with the floor beams and interact structurally with the framing members. Durrani and Wight (10) investigated the effect of a floor slab on the behavior of interior connections by testing six beam-to-column connection subassemblies. They concluded that the joint confinement provided by the transverse beams depended upon their torsional stiffness. They also proposed a hysteretic model which realistically represented the hysteretic behavior observed during their tests. Ehsani and Wight (11) studied the behavior of connections with a floor slab by testing twelve exterior beam-to-column connection subassemblies. They observed that

all slab reinforcement yielded during negative bending, which caused the column to beam flexural strength ratio to drop below 1 and resulted in hinging of columns instead of beams.

As more data on the effect of the presence of a floor slab became available, the need to define an effective slab width to be considered in the design of connections became important. Zerbe and Durrani (16) tested seven exterior beam-to-column connections with a variable slab width. They concluded that the participation of floor slab to negative bending in exterior connections depended upon the extent of torsional damage in the transverse beams. They also recommended that in connections where torsional failure of transverse beams is anticipated, the effective slab width can be considered as the column width plus twice the depth of the transverse beams. Pantazopoulou and Moehle (44) studied data from recent tests on connections with a floor slab and developed a simple model to account for the contribution of slab to the strength and stiffness of beams under negative bending. They recommended that a slab width equal to 1.5 times the effective beam depth on each side of the beam should be considered effective before yielding of beam reinforcement. For deformation levels to be expected in a moderate earthquake, they recommended an effective slab width equal to 3 times the beam effective depth on each side of the beam.

Although the behavior of beam-to-column connections has been under investigation for a long period of time, some difficulties arise when their performance is evaluated in relation to the overall building response. Recently, testing of isolated interior or exterior connections have been criticized for not going far enough in simulating frame structures where redistribution of forces among framing members is permitted. Jirsa (45), expressed the need to test indeterminate beam-to-column connection subassemblies in order to simulate actual structures and indicated that the rationality of the design recommendations is a function of the rationality of the test specimens.

Besides some small scale structure tested on shaking tables, few studies reported tests on indeterminate beam-to-column connection subassemblies. A cooperative research program was initiated by Japan and the United States in 1977 to improve the safety of building structures subjected to earthquakes. The central activity of the program was the testing of a large-scale seven-story reinforced concrete structure at the Building Research Institute in Tsukuba-Japan (46). One of the observation from the test results was that the structure carried base shear substantially higher than the base shear calculated theoretically before the test. This increase in the expected

base shear was the result of the contribution of the slab reinforcement to beam flexural capacity and the strain hardening of the reinforcement.

Seckin (47) tested two indeterminate subassemblies, each consisting of one interior column and one exterior column framed together with a continuous beam extending beyond the interior column. Based on the test results it was concluded that the system tended to utilize its reserved capacity when load redistribution starts. It was also observed that a well confined exterior joint would result in plastic deformation in beam segments, even if the beam rebars slip through the interior joint. Kokusho et al (48) studied the effect of axial force which may develop in the beams of indeterminate structures due to restraint against free elongation. They observed an increase in the beam flexural capacity which ranged from 50 percent to 100 percent of the strength of unrestricted beams.

12

Chapter 2

EXPERIMENTAL PROGRAM

2.1 Description of Test Specimens

Eleven half-scale specimens were tested during this study. The specimens were divided into two categories. The first category consisted of six multiple-connection subassemblies, and the second category consisted of five single-connection subassemblies. The configuration and the designation of the specimens are shown in Table 2.1.

Each of the multiple-connection subassemblies represented one story of a two-bay frame isolated at the column mid-heights as shown in Fig. 2.1. This specimen configuration was based on the assumption that, under lateral loading, the points of inflection in a multistory frame occurred at mid-height of columns and remained stationary. The first specimen, specimen C, represented the basic configuration, and was composed of one interior and two exterior connections. The second specimen, specimen CTB, was identical to the first specimen except that transverse beams were added to the basic configuration. The third specimen, specimen CS1, had a floor slab in addition to

Table 2.1

SPECIMEN CONFIGURATION

Category	Specimen Designation	Specimen Type	Specimen Configuration	Specimen Description
1	C	Combined		Basic Configuration
	CTB	Combined		Transverse Beams
	CS1	Combined		Transverse Beams and Slab
	CS2	Combined		Reduced Joint Reinforcement
	CS3	Combined		Relocated Flexural Hinges
	CS4	Combined		Reduced Joint Reinf. (Repeat of CS2)
2	I	Interior		Subset of C
	E	Exterior		Subset of C
	IS1	Interior		Subset of CS1
	ES1	Exterior		Subset of CS1
	ES2	Exterior		Smaller Transverse Beams

the transverse beams. The fourth specimen, specimen CS2, was similar to specimen CS1 except that it had smaller amount of joint transverse reinforcement. The fifth specimen, specimen CS3, was identical to specimen CS2 except that the beam flexural hinging regions were relocated away from the face of the columns. The sixth specimen, specimen CS4, was a repeat of specimen CS2.

The five single-connection specimens represented interior or exterior connections isolated at the beam mid-span of the multiple-connection specimens, as shown in Fig. 2.1. Specimen I and specimen E represented the interior connection and the exterior connection of specimen C, respectively. Specimen IS1 and specimen ES1 represented the interior connection and the exterior connection of specimen CS1, respectively. Specimen ES2 was an exterior connection, which was identical to specimen ES1 except that the transverse beams were smaller. Specimen ES2 did not represent any part of any of the multiple-connection specimens.

Since the comparison of behavior between the multiple and the single connection subassemblies is a major part of this study, six of the specimens were divided into two series. First, the without slab series, and it consisted of specimens C, I, and E. Second, the with slab series, and it consisted

of specimens CS1, IS1, and ES1. Specimens C and CS1 are referred to as the continuous or the combined specimens. Specimens I and IS1 are referred to as isolated or single interior connections, and specimens E and ES1 are referred to as isolated or single exterior connections.

2.2 Specimen Configuration and Reinforcing Detail

The overall dimensions of the test specimens i.e. the total column height, the center to center of the columns, and the total width of the slab were restricted by the testing frame and were equal to 58 in., 84 in. and 56 in., respectively. Figure 2.2 shows an elevation and a plan view of a typical multiple-connection specimen with a floor slab.

Different column cross-sections were used for the interior and the exterior columns. The interior columns were 10 x 10 in. with eight #6 reinforcing rebars distributed uniformly around the column perimeter. The exterior columns were 10 x 10 in. with four #6 rebars placed at the column corners. All beams had an 8 x 12 in. cross-section which was symmetrically reinforced with two #5 rebars at the top and two #5 rebars at the bottom. The main beam rebars passed through the interior joint and were terminated with 90 degree standard hooks at the outer face of the exterior joints. The slab was 56 in. wide and 3 in. thick with eight #3 rebars uniformly distributed on

both sides of the main beam. Except in specimen ES2, all specimens had a cross-section of transverse beams which was identical to that of the main beam. In specimen ES2, however, the cross-section of transverse beams was reduced to 7.5 x 10.5 in. with two #4 rebars at the top and two #4 rebars at the bottom. A summary of the reinforcement is given in Table 2.2, and the detailing of the reinforcement and the member cross-sections are shown in Figs. 2.3, 2.4(a), and 2.4(b) respectively. Columns and beams were provided with adequate shear reinforcement to avoid any premature shear failure.

The main beam reinforcement of specimen CS3 was modified to move the flexural hinging regions a distance equal to the beam effective depth away from the faces of the columns. The top beam reinforcement was reduced to two #3 rebars and the bottom beam reinforcement was reduced to two #4 rebars. Additional two #4 U-shape reinforcing rebars were added to the top and the bottom reinforcement covering a distance of 10.3 in. away from the faces of the columns. The detail of the beam reinforcement of specimen CS3 is shown in Fig. 2.5.

2.3 Design Parameters

2.3.1 Flexural Strength

The design of test specimens was based on the well accepted

Table 2.2

MEMBER REINFORCEMENT

Specimen	Beam Top Reinf.	Beam Bottom Reinf.	Interior Column Reinf.	Exterior Column Reinf.	Slab Reinf.	Joint Hoop reinf.
C	2#5	2#5	8#6	4#6	--	3#3
CTB	2#5	2#5	8#6	4#6	--	3#3
CS1	2#5	2#5	8#6	4#6	8#3	3#3
CS2	2#5	2#5	8#6	4#6	8#3	2#3
CS3*	2#3 2#4	2#3 2#4	8#6	4#6	8#3	2#3
CS4	2#5	2#5	8#6	4#6	8#3	2#3
I	2#5	2#5	8#6	--	--	3#3
E	2#5	2#5	--	4#6	--	3#3
IS1	2#5	2#5	8#6	--	8#3	3#3
ES1	2#5	2#5	--	4#6	8#3	3#3
ES2	2#5	2#5	--	4#6	8#3	3#3

* 2#4 rebars are provided only in strong section (see Fig. 2.5).

strong column-weak beam design philosophy. The interior and the exterior columns were subjected to 40 Kips and 25 Kips axial load, respectively. These loads simulated the gravity load and were equivalent to about 23 percent of the balanced load for the interior column and about 15 percent of the balanced load for the exterior column. The P-M interaction diagrams of the columns are shown in Fig. 2.6.

In specimens without a slab, the beam top and bottom reinforcement were equal, hence the positive and the negative flexural capacities of the beam were identical. The basic specimen C, had a column to beam flexural strength ratio of 1.88 for the interior connection and 2.41 for the exterior connection. In specimens with a slab, however, the negative flexural capacity depended upon the amount of slab reinforcement assumed effective in resisting tension. In the design of specimens, reinforcement in the entire width of slab was assumed effective in calculating the flexural capacity of the beams. Based on this assumption, the column to beam flexural strength ratio for the specimen with a slab (CS1), was equal to 1.19 for the interior connection. For the exterior connection, the column to beam flexural strength ratio was 1.20 for slab in tension, and 2.08 for slab in compression. The calculated column and beam flexural capacities varied slightly among specimens due to the slight variation in the measured concrete

strength. Table 2.3 summarizes the column and beam flexural strengths, and the column to beam flexural strength ratios for all specimens using the actual material properties.

2.3.2 Shear in the Joint

The shear stress in the joints was calculated as follows:

$$v_j = \frac{V_j}{h_c b_j} \tag{2.1}$$

where V_j is the shear in the joint as defined in Fig. 2.7, h_c is the depth of the column in the loading direction and, b_j is equal to $(b_b + b_c)/2$ but less than $b_b + (b_c/2)$. Where b_b is the width of the beam, and b_c is the width of the column.

The joint shear stresses in the interior and exterior connections of all specimens, based on Eqn. 2.1, are summarized in Table 2.4. These shear stresses were calculated based on the actual material properties with the steel yield strength increased by 25 percent to account for strain hardening. The design joint shear stress in exterior connections without a floor slab was $5.54\sqrt{f_c'}$, which by including the slab reinforcement in joint shear calculation, becomes $15.04\sqrt{f_c'}$ for specimens with a slab. Similarly, the joint shear stress in interior connections was $11.08\sqrt{f_c'}$ in specimens without a slab and $20.45\sqrt{f_c'}$ if the reinforcement in the entire slab width was

Table 2.3

FLEXURAL STRENGTH OF BEAMS AND COLUMNS

| Specimen | M_b^+ | M_b^- | Interior | | Exterior | | |
			M_{col}	R	M_{col}	R^+	R^-
	(K-in)	(K-in)	(K-in)		(K-in)		
C	494.0	494.0	931.5	1.88	594.5	2.41	2.41
CTB	491.5	491.5	922.5	1.88	590.5	2.40	2.40
CS1	568.5	982.5	925.5	1.19	591.5	2.08	1.20
CS2	568.5	982.5	925.5	1.19	591.5	2.08	1.20
CS3	664.0	1031.5	938.5	1.11	599.5	1.81	1.16
CS4	583.5	1005.0	943.5	1.19	602.5	2.07	1.20
I	488.0	488.0	910.5	1.87	--	--	--
E	488.0	488.0	--	--	585.5	2.40	2.40
IS1	555.5	959.5	902.5	1.19	--	--	--
ES1	560.5	968.5	--	--	585.5	2.09	1.21
ES2	572.5	988.5	--	--	595.5	2.08	1.20

\+ Slab in Compression
\- Slab in Tension

included is joint shear calculations. The design joint shear varied slightly among the specimens due to the slight variation in the measured concrete strength. The concrete strength for each specimen at testing date and the joint shear stress factors are given in Table 2.4.

2.3.3 Joint Reinforcement

The joint transverse reinforcement in interior and exterior connections consisted of three #3 closed hoops placed 3 in. apart. In the case of specimens CS2, CS3, and CS4, only two #3 hoops were used with a center-to-center spacing of 4 inches. The transverse hoop reinforcement ratio, ρ, was 0.96 percent for three hoops and 0.64 percent for two hoops. This ratio is defined as

$$\rho = \frac{A_{sj}}{b_c(d-d')} \qquad (2.2)$$

where A_{sj} is the total hoop area, b_c is the width of the column, and $(d-d')$ is the distance between the beam top and bottom reinforcement.

2.3.4 Anchorage of Reinforcement

To control the slippage of beam and column reinforcement passing through the joint, the provided ratios of the column

Table 2.4

JOINT SHEAR STRESSES AND JOINT REINFORCEMENT

Specimen	f'_c	Interior Joint				V_{col}	Exterior Joint*			Joint Reinf.
		V_{col}	V_j	v_j	γ		V_j	v_j	γ	
	(psi)	(Kips)	(Kips)	(psi)		(Kips)	(Kips)	(psi)		(%)
C	5805	17.0	76.0	844	11.08	8.3	38.0	422	5.54	0.96
CTB	5640	16.9	76.1	845	11.25	8.5	38.1	423	5.63	0.96
CS1	5695	26.8	138.9	1543	20.45	16.9	102.2	1135	15.04	0.96
CS2	5695	26.8	138.9	1543	20.45	16.9	102.2	1135	15.04	0.64
CS3	6000	29.2	119.0	1322	17.07	17.8	80.0	889	11.48	0.64
CS4	6130	27.4	138.2	1536	19.62	17.3	101.8	1131	14.45	0.64
I	5425	16.8	76.2	846	11.49	–	–	–	–	0.96
E	5425	–	–	–	–	8.4	38.1	423	5.74	0.96
IS1	5265	26.1	139.5	1550	21.36	–	–	–	–	0.96
ES1	5425	–	–	–	–	16.7	102.4	1138	15.45	0.96
ES2	5810	–	–	–	–	17.0	102.1	1134	14.88	0.96

* Shear in Exterior Joint with Slab in Tension

$$\gamma = v_j / \sqrt{f'_c}$$

24

depth to the beam bar diameter and the beam depth to the column bar diameter were equal to 16. For the beam bars terminating in the exterior joints embedment lengths of 7.65 in. and 7 in. were provided for top and bottom beam bars, respectively. These embedment lengths are measured from the face of the hoops to the end of the bent rebar, as shown in Fig. 2.8.

2.3.5 Relocation of Beam Flexural Hinges

Two beam sections with different flexural strengths were designed in order to shift the beam inelastic action away from column faces. The first section is the strong section and it was located between the column faces and a distance equal to 10.3 in. away from the column faces. The second section is the weak section and it covered the rest of the beam. The design of the sections was such that when beam hinging occurred at the weak section, the corresponding moment at the face of the column would remain below the flexural strength of the strong section, as illustrated in Fig. 2.9. The Flexural strengths of the weak and the strong sections were based on the assumption that the entire slab reinforcement was effective in tension. The moment developed at the face of the column when the weak section reached its maximum strength was used to determine the column to beam flexural strength ratio shown in Table 2.2. Although the beam bars were not expected to

yield at the column face, the joint shear stresses, shown in Table 2.3, were calculated as if the beam reinforcement at the strong section was yielding. The 25 percent increase in the strength of the reinforcement to account for strain hardening, however, was not included in calculating the shear in the joints.

2.4 Preparation of Specimens

2.4.1 Material Properties

The test specimens in this study were designed with a 28-day concrete compressive strength of 5000 psi with a slump of 3 to 4 inches. The actual concrete strength, however, varied between 5500 psi and 6000 psi. This was obtained by testing 6 x 12 in. standard concrete cylinders. A total of 18 cylinders were cast with each multiple-connection specimen and 6 cylinders were cast with each single-connection specimen. Half of the cylinders were tested on the 28th day and the other half were tested on the day of testing the specimen. The average concrete compressive strengths at 28 days and at the day of testing of specimens are summarized in Table 2.5.

Reinforcement in each specimen consisted of Grade 60 steel. The stress-strain relationship of steel was obtained by testing

Table 2.5

STRENGTH OF CONCRETE

Specimen	Compressive Strength (psi) at		Age at Day of Test
	28 Days	Day of Test	Days
C	5170	5805	230
CTB	4940	5640	217
CS1	4925	5695	204
CS2	5020	5695	162
CS3	5710	6000	47
CS4	5670	6130	62
I	5140	5425	180
E	5140	5425	184
IS1	4845	5265	181
ES1	4745	5425	167
ES2	5340	5810	52

three randomly selected samples representing each rebar diameter. The properties of the steel at yield, strain hardening and ultimate are listed in Table 2.6.

2.4.2 Fabrication Process

The specimens were cast vertically in a reusable plywood formwork, shown in Fig. 2.10, which was cleaned and modified after each casting to accommodate the different configurations of the test specimens. Prior to assembling the reinforcing cage, strain gages were bonded on the reinforcement at appropriate locations and were covered with special coatings for protection against impact and water penetration during casting of concrete.

The concrete mix for specimens was prepared in the laboratory. All specimens were cast in two stages. Stage 1, included the bottom columns, the beams and the slab. After allowing the concrete to set for one hour, the top columns were cast as a second stage. The formwork was stripped on the fifth day, and the specimens were wrapped with wet burlap bags and plastic sheets for 15 days to complete the curing process. The specimens were then stored in the laboratory, as shown in Fig. 2.11, until the day of testing. The concrete cylinders were treated identical to their mother specimens and were cured in a similar environment.

Table 2.6

REINFORCING STEEL PROPERTIES

Rebar #	ϵ_y in/in	ϵ_{sh} in/in	f_y Ksi	f_u Ksi	E Ksi	E_{sh} Ksi
3	0.002	0.012	66	105	33000	2917
4	0.002	0.011	63	102	31500	2000
5	0.0021	0.0075	60	101	28570	1570
6	0.0025	0.009	68	107	27200	2059

2.5 Testing Procedure

2.5.1 Test Set-Up

The test set-up consisted of a steel reaction frame with a four-hinge interior loading frame capable of lateral displacement. Figure 2.12 shows a photograph of the testing frame and Fig. 2.13 shows a schematic of the loading frame. The test specimens were tested in a vertical position with the lateral displacements applied at the top of the columns through the rigid transfer beam of the four-hinge loading frame. The top ends of the columns were pin connected to the rigid transfer beam and the bottom ends of the columns were attached to the reaction frame through a link mechanism that allowed rotation as well as vertical movement but restrained the column ends from lateral displacement.

Since this study is one of the few attempts at testing indeterminate subassemblies, it may be of interest to discuss the merits as well as the limitations of this testing arrangement. Short of testing a multistory frame, the test set-up used in this study is relatively simple and convenient for studying the performance of connections in indeterminate subassemblies. It is also a suitable arrangement for studying the effect of axial restriction on the elongation of main beams in multi-bay frame subassemblies subjected to large deformation

reversals. The later facility may also be regarded as its limitation if it is believed that the floor beams in a real building are free to elongate. In that case, this set-up will more closely simulate the first floor behavior since the foundations, unlike floor beams, can not expand. It also approximates the situation where a particular story experiences relatively more inelastic deformations than that experienced by the adjacent stories. Furthermore, by terminating the top and bottom columns at inflection points, the effect of axial restraint may be exaggerated at large drift levels. On balance, however, it is believed that this testing arrangement represents a step closer to reality and can provide a better insight into the behavior of connections and frame subassemblies.

The cyclic routine was applied through a displacement controlled actuator placed at the top of the four-hinge loading frame. One inch thick steel plates were welded to the reinforcement at the column and beam free ends to provide connection between the test specimen and the test set-up. In single-connection specimens, the beam free ends were pin connected with the reaction frame as shown in Fig 2.14. Such a connection restrained the beam against any vertical movement, while rotation and horizontal translation were permitted. The column axial load was applied 24 hours prior to testing, through hydraulic jacks placed at the bottom of the columns.

2.5.2 Displacement Routine

All specimens were subjected to the same predetermined displacement routine shown in Fig. 2.15. This routine consisted of twelve cycles varying from 0.25 percent to 5 percent of the total column height with the one percent cycle repeated three times in order to detect the stiffness decay. Before reaching the peak of any cycle, the test was paused several times to collect data. These stops corresponded to significant changes in the slope of the load vs. displacement curves.

2.6 Instrumentation

2.6.1 Load-Displacement

The displacement applied at the top of the columns and its corresponding load were measured with a Linear Variable Differential Transformer (LVDT) and a load cell directly attached to the actuator. The load and displacement from the actuator were continuously plotted on an X-Y analog plotter.

2.6.2 Shear in the Columns

The distribution of the total load among the columns of the multiple-connection specimens was measured with three shear transducers placed between the top ends of the columns and the

rigid transfer beam. These shear transducers were composed of a full Wheatstone bridge attached diagonally to a steel clevis to measure shear forces only.

2.6.3 Strain Gages

An average of 90 strain gages were attached to the reinforcement of the multiple-connection specimens. These strain gages were located in the joints and their surrounding beams, columns, and slab, as shown in Fig. 2.16. The isolated interior and isolated exterior connections had strain gages placed at locations similar to these in the interior and the exterior connections of the multiple-connection specimens.

2.6.4 LVDTs

Six LVDTs were used to measure the beam elongation and the rotation in the beam flexural hinging regions. These LVDTs were placed at the top and the bottom of the main beams covering a gage length of 12 in. away from the face of the column. Two pairs were used in the interior connection and one pair was used in the exterior connection. The location of the LVDTs is shown in Fig. 2.16.

Chapter 3

RESPONSE OF INDETERMINATE SUBASSEMBLIES

In order to study the performance of connections in indeterminate frames, six multiple beam-to-column connection subassemblies were tested during this experimental investigation. The variables studied were the presence of unloaded transverse beams, the presence of a floor slab, the amount of joint transverse reinforcement, and the location of the beam flexural hinging region. In this chapter, the general performance of the test subassemblies is presented, and the effect of each of the studied variables on the performance of beam-to-column connections is discussed.

3.1 General Behavior

Different types of data collected during the tests consisted of the load vs. displacement plots, the formation and propagation of cracks, the reinforcement strain history, and the rotation and elongation of beam flexural hinging regions. These results are presented in this section in terms of the overall behavior of each specimen.

34

3.1.1 Load-Displacement Response

All specimens were subjected to the same predetermined displacement routine. The displacement was applied horizontally at the top of the columns simulating the lateral shear imposed on columns during seismic input. The maximum displacement during each cycle corresponded to an even percentage of the total column height referred to as drift level. For the purpose of consistency, the term 'drift' will replace 'displacement' throughout the rest of the report. The drift was defined as positive drift when the load was applied from the right to the left, and negative drift when the load was applied from the left to the right. The resulting load vs. drift plots of each multiple-connection subassembly are shown in Figs. 3.1(a) through 3.1(f). These plots provide a variety of information on the response of subassemblies. These include the lateral shear resistance during each cycle, stiffness degradation of the test specimen, and the energy dissipated during each cycle.

The cyclic strength of a specimen is defined as the load resisted by the specimen at the peak of a displacement cycle. The maximum strength of a specimen, however, is the maximum load carried by the specimen during the entire cyclic routine. The ratio of the cyclic strength to the maximum strength of

the test specimens is summarized in Table 3.1. Due to symmetry in all multiple-connection specimens, the strength was taken as the average of the strengths achieved at the positive peak and the negative peak of a cycle. The reference specimen, C, and the specimen with unloaded transverse beams, CTB, reached their maximum strength at the 4 percent drift cycle and were able to maintain their full strength throughout the 5 percent drift cycle. The specimen with a floor slab, CS1, and the specimen with a floor slab but with a reduced amount of joint transverse reinforcement, CS4, showed increasing resistance throughout the entire loading routine. Specimen CS2 which is identical to specimen CS4 reached its maximum strength during the 4 percent drift cycle. During the 5 percent drift cycle the specimen experienced a small drop in its strength. This drop in strength is attributed to an unforeseen shear damage in the bottom interior column resulting from a malfunction of the test set-up.

The specimen CS3, with the relocated flexural hinging regions also achieved its maximum strength during the 4 percent drift cycle. During the 5 percent drift cycle, however, the specimen was able to carry only 86 percent of its maximum load. This significant drop in the strength of specimen CS3 is due to excessive damage that occurred in the flexural hinging regions.

Table 3.1

RELATIVE CYCLIC STRENGTH OF SPECIMENS

Specimen	Cyclic strength normalized with respect to the maximum strength							
	Drift (%)							
	0.25	0.5	1	1.5	2	3	4	5
C	0.17	0.32	0.54	0.71	0.81	0.92	1.00	1.00
CTB	0.16	0.29	0.52	0.71	0.82	0.95	1.00	1.00
CS1	0.13	0.25	0.47	0.58	0.70	0.85	0.96	1.00
CS2	0.13	0.25	0.44	0.58	0.71	0.91	1.00	0.98
CS3	0.13	0.27	0.47	0.62	0.75	0.94	1.00	0.86
CS4	0.14	0.26	0.46	0.62	0.75	0.92	0.99	1.00

Stiffness is an important measure of the performance of connections. Excessive shear deformation in the joints or loss of bond in beam and column reinforcement is reflected in the degradation of stiffness. During the loading sequence, 1 percent drift cycles, i.e. cycles 3, 7 and 11, were introduced to measure the stiffness of the test specimens. The stiffness measured from these cycles is defined as the average slope of the two lines connecting the zero displacement points to the positive and negative peaks of the cycles, as shown in Fig. 3.2. This stiffness definition was adopted in this study and it will be used throughout the report. The stiffness measured in cycle 3 in all test specimens was equal to their initial stiffness. The stiffness measured in cycles 7 and 11 represent the stiffness after the specimen has experienced drifts of 2 percent and 4 percent, respectively. For the purpose of comparison, the stiffness measured in cycles 3, 7 and 11 is normalized with respect to the initial stiffness for all multiple-connection subassemblies, as shown in Table 3.2.

Two distinct behaviors were observed with respect to stiffness degradation. The multiple-connection subassemblies without a floor slab, specimens C and CTB, lost more than 50 percent of their initial stiffness after they were subjected to a drift level of 4 percent. In the multiple-connection subassemblies with a floor slab, however, the loss of stiffness

Table 3.2

STIFFNESS DEGRADATION OF SPECIMENS

Specimen	Stiffness of 1 percent drift cycles normalized with respect to initial stiffness		
	Cycle		
	3	7	11
C	1.00	0.83	0.44
CTB	1.00	0.88	0.49
CS1	1.00	0.91	0.69
CS2	1.00	0.91	0.63
CS3	1.00	0.90	0.61
CS4	1.00	0.93	0.67

was significantly lower and it varied with the extent of the overall damage of the test specimen. Specimens CS1 and CS4, which were able to maintain their strength throughout the loading sequence lost only about 30 percent of their initial stiffness, while specimens CS2 and CS3, which had severe damage in the interior column and in the flexural hinging regions, respectively, lost about 40 percent of their initial stiffness.

The energy dissipated by each specimen during a loading cycle is represented by the area enclosed within the load vs. drift curve of that cycle. Table 3.3 summarizes the amount of energy dissipated by the multiple-connection subassemblies during various drift cycles. Although the hysteresis loops of the multiple-connection specimens with a slab appear to be narrower than the hysteresis loops of the multiple-connection specimens without a floor slab, both type of specimens dissipated approximately an equal amount of energy up to a drift level of 4 percent. Beyond the drift level of 4 percent, the specimens without a floor slab dissipated less energy than the specimens with a slab because of the increased pinching in their hysteretic loops at mid-cycles which resulted from the more severe loss of stiffness.

Table 3.3

ENERGY DISSIPATION (K-in.)

Specimen	Drift (%)							
	0.25	0.5	1	1.5	2	3	4	5
C	0.0	0.6	4.7	11.8	23.2	57.5	90.3	114.5
CTB	0.2	0.6	4.0	9.2	18.2	50.4	90.3	118.5
CS1	0.1	1.0	4.7	9.2	20.0	55.7	91.4	145.6
CS2	0.2	1.0	4.6	11.6	18.6	48.4	93.9	116.4
CS3	0.2	1.2	4.9	9.7	18.2	50.8	97.5	136.5
CS4	0.2	1.2	5.3	10.9	19.6	58.1	110.5	137.3

3.1.2 Cracking Pattern

The cracking patterns provide important clues to the behavior of test subassemblies. During each test the formation and propagation of cracks was carefully observed and photographs were taken to keep a complete record of the test specimens.

Several cracking patterns were common to nearly all specimens. Flexural cracking of the beams is one example. Since the columns were designed to be stronger than the beams, flexural cracks were formed in the beams. Flexural cracks appeared in the beams as early as the second loading cycle. By the end of the third cycle, i.e. at 1 percent drift level, the flexural cracks from the two loading directions joined and extended through the entire depth of the beam. With each additional loading cycle, the cracks opened wider and depending upon the type of specimen, a few additional flexural cracks formed along the length of the beam. Figures 3.3(a) and 3.3(b) show flexural hinges in the main beam of multiple-connection subassemblies C and CS1, respectively. The flexural hinge in specimens without a floor slab generally extended over a distance equal to 1.25 the effective beam depth away from the face of the column. In specimens with a floor slab, however, the flexural hinge extended over a length equal to 0.75 the effective beam depth away from the face of the column.

Specimen CS3 was detailed to move the flexural hinges a distance equal to the beam effective depth away from the face of the column. Flexural cracks in the beams started at the intended location during the second loading cycle. As the test progressed, these cracks formed an inclined grid located away from the column face as shown in Figs. 3.4(a) and 3.4(b). Flexural cracks at the beam-column interface did not develop throughout the entire loading routine. This indicates that relocating the beam flexural hinges protected the joints from surrounding inelastic action. During the negative loading direction of cycle 10 (4 percent drift), the bottom beam reinforcement of the right exterior connection of specimen CS3 buckled causing the bottom cover of concrete to spall off, as shown in Fig. 3.5. And when the specimen was subjected to the 5 percent drift cycle, a beam shear failure, shown in Fig. 3.6, occurred in that same connection. Buckling of beam reinforcement and complete failure in the beam was only observed in specimen CS3.

The columns in all specimens were designed to withstand anticipated shear forces without any shear damage. Hairline shear cracks were observed in the columns of specimens with a floor slab during the 3 percent loading cycle. These cracks did not develop any further during the entire loading routine. In case of specimen CS2, however, the exterior bottom columns

were not properly connected to the test set-up, which caused the entire shear applied to the top columns to be resisted by the interior bottom column only. This caused the interior bottom column to develop severe shear cracks, as shown in Fig. 3.7, which may have altered the intended behavior of the test specimen. Therefore, a new specimen, specimen CS4, was built and tested in order to study the effect of the amount of joint transverse reinforcement properly.

Transverse cracks in the slab of all multiple-connection subassemblies were observed at the column face during the third loading cycle. In addition to the major crack at the column face, several other cracks developed which were parallel to the column face and extended across the entire width of the slab as shown in Fig. 3.8. In specimen CS3 the transverse cracks in the slab were similar to other specimens except that the major crack was located at a distance equal to the beam effective depth away from the column face, as shown in Fig. 3.9.

Despite a large column to beam flexural strength ratio of 2.41, for exterior connections without a floor slab, and 1.20 for exterior connections with a floor slab, the exterior columns of all multiple-connection specimens suffered severe flexural cracks at the outer faces of the columns, as shown in Figs

3.10(a) and 3.10(b). These cracks which started at a drift level of 1.5 percent and became significant by the end of the loading routine, resulted from the elongation of beam flexural hinges which was restrained by the exterior columns in multiple-connection subassemblies.

Shear cracks in the joints could only be observed in specimen C, which did not have transverse beams. These cracks consisted of major diagonal cracks connecting the opposite corners of the interior joint and several hairline cracks parallel to the major cracks, as shown in Fig. 3.11. In exterior connections due to the low joint shear stress level of $5.54\sqrt{f_c'}$, only very few minor shear cracks were observed in the joints.

Torsional cracks in the transverse beams of the exterior connections were common to all specimens with a floor slab. These cracks were initiated during the fourth loading cycle (1.5 percent drift) as several small cracks inclined approximately at 45 degrees on the back face of the transverse beams. By the end of the fifth cycle, a major crack had developed that spiraled around the transverse beam and joined the flexural cracks at the face of the column as shown in Fig. 3.12. Torsional cracks in the transverse beams of the interior connections were mostly insignificant and formed much later during the test.

3.1.3 Reinforcement Strain History

The strain in reinforcement was measured with electrical resistance strain gages. The strain data was used primarily to determine cracking of concrete and yielding of reinforcement. The strain data was also used to detect slippage of beam bars passing through interior joints, pull out of beams bars terminated in exterior joints, and slippage of column bars passing through interior and exterior joints.

Shear stress in the joint can only be assessed from strain measurements in the joint hoop reinforcement. In the case of joints without transverse beams, shear cracks could be readily observed. In the case of joints with transverse beams, however, sudden change in strain in the joint reinforcement indicates initiation of shear cracks in the joint. Figure 3.13 shows a typical variation in strain of the joint hoop reinforcement. The sudden increase in strain between points A and B indicates a transfer of stress from concrete to steel when the concrete cracked. From strain measurements, it is observed that concrete in the joints of all specimens cracked as early as the third loading cycle.

The level of strain in the joint reinforcement and hence the shear deformation of the joint varied with the type of connection and the configuration of the test subassembly.

Strain variation in the joint reinforcement of interior and exterior connections of specimen C, without a floor slab, is shown in Fig. 3.14. In exterior connection which had a joint shear stress level of $5.54\sqrt{f_c'}$, strain in the joint reinforcement reached a maximum value of 40 percent of the yield strain. In the interior connection which had a joint shear stress level of $11.08\sqrt{f_c'}$, the strain in the joint reinforcement exceeded the yield strain. The addition of transverse beams in specimen CTB substantially reduced the strain in the joint reinforcement of both interior and exterior connections, indicating that the transverse beams helped in confining the joint and also assisted in resisting the joint shear stress.

The presence of a floor slab in specimen CS1 increased the joint shear which resulted in yielding of the joint reinforcement in both interior and exterior connections during the 3 percent drift loading cycle, as shown in Fig. 3.15. The strain level in the joint reinforcement of specimens CS2 and CS4 was almost identical to that of specimen CS1. In specimen CS3, which had a joint shear stress level almost equal to that of specimen CS1, the strain level in the joint reinforcement remained below yielding, indicating that shifting the inelastic action away from the face of the joint provided an excellent protection against joint shear.

Strain gages were attached to slab reinforcement across the entire width of the slab to determine the slab width effective in resisting bending. The behavior of slab reinforcement was common to all multiple-connection subassemblies with a floor slab. In general, the slab longitudinal reinforcement close to the main beam experienced high strains during early cycles, while the slab reinforcement farther away from the main beam experienced relatively lower strain. Figure 3.16 shows a typical behavior of slab reinforcement close to the main beam and Fig. 3.17 shows the lower strains in slab reinforcement farther away from the main beam. At a drift level of 3 percent all slab reinforcement yielded except for the rebar farthest away from the beam which approached the yielding strain. This indicates that in all multiple-connection specimens the entire slab width was effective in resisting bending.

Strain measurements along the main beam reinforcement are used to determine yield penetration through the joints. Except for specimen CS3, which had flexural hinges relocated away from the column face, yielding of both top and bottom beam bars penetrated through interior and exterior joints. In case of specimen CS3, yield penetration through the joints occurred only in the beam top reinforcement, as shown in Fig. 3.18.

Strain measurements along the main beam reinforcement are also used to detect any slippage of beam bars through the interior joint resulting from loss of anchorage. Beam bars passing through an interior joint are under tension on one side of the joint and under compression on the other side of the joint. This is only possible if bars experience no loss of bond in the joint. Figure 3.19 shows a typical strain history of the beam bar of specimen C, without a floor slab, at the face of the column. It is noted that the bar exhibited compressive strain during negative bending indicating no loss of bond across the joint. Similar behavior was observed in the beam bars passing through the interior joint of specimen CTB. In case of specimens with a floor slab, however, the performance of the beam reinforcement varied according to the location of the rebar. The beam bottom rebars remained in tension even though the moment sense at the section requires the rebar to be in compression, as shown in Fig. 3.20. This suggests deterioration of bond and slippage of rebar through the joint. The beam top rebar also remained in tension while the moment sense requires the bar to be in compression, as shown in Fig. 3.21. This, however, is due to the presence of slab which shifted the neutral axis above the beam top reinforcement and is not the result of slippage of rebar.

In exterior connections, beam rebars terminating in the joint did not experience any loss of bond or rebar pull out in any of the test subassemblies. Figure 3.22 shows a typical strain history of a beam rebar at the face of the column. The rebar sustained tension without any loss of anchorage. The strain history also indicates that the rebar is under tension even when the beam is subjected to positive bending. This is again due to the participation of the slab in compression which raised the neutral axis above the beam top reinforcement.

The slippage of column bars resulting from loss of bond in the joint core can be seen from the strain in the column bars immediately above and below the joint. When subassemblies are subjected to lateral load, the column bars are expected to be in tension on one side of the joint and in compression on the other side of the joint. If these bars had a perfect bond within the joint, the strain would change its sense from tension to compression somewhere within the joint. The observed strain data for the multiple-connection specimens C, CS1, CS2, and CS4 indicates that the bars of the interior column in these specimens remained in tension irrespective of the direction of loading. A typical strain variation for a bar of an interior column at the location indicated is shown in Fig. 3.23. In multiple-connection specimens CTB and CS3, where the joints were protected by the presence of transverse beams and by

moving the beam flexural hinges away from the joint face, respectively, the slippage of column bars was minimum as indicated by the strain history shown in Fig. 3.24.

In exterior columns, the restraining effect provided by the columns against beam elongation changed the deformed shape of the column from that of double-curvature into a single-curvature. Therefore, the outer column bars were always under high tension on both sides of the joint, as shown in Fig. 3.25, while the inner column bars were always under either compression or low tension, as shown in Fig. 3.26. Due to this type of deformation slippage of column bars through the joint core was limited.

3.1.4 Rotation and Elongation of Beam Flexural Hinging Regions

The rotation in the beam flexural hinging region of both interior and exterior connections was measured with displacement transducers mounted at 1.5 in. above and below the beam faces. These transducers covered a gage length of 12 in. from the face of the column. The rotation in the beam flexural hinging regions was calculated as the difference in the readings of transducers above and below the beam divided by the distance between the centerlines of the two transducers. Figures 3.27(a) and 3.27(b) show the rotation history in the

interior and the exterior connections of specimens C and CS1, respectively. It is noted that the presence of a floor slab significantly reduced the rotation of the flexural hinges for both interior and exterior connections of the multiple-connection subassemblies.

The elongation of the main beams results mostly from the yielding of the longitudinal bars in the flexural hinging region. Figure 3.28 shows elongation of the beams measured over the flexural hinging regions of interior and exterior connections of specimen C and CS1. It is noted that the total elongation in both specimens is almost identical. This indicates that unlike results obtained from tests on isolated connections (16), the presence of the floor slab did not reduce the beam elongation as the entire subassembly is restrained against beam elongation by the exterior columns. The effect of such a restriction on the overall behavior of the connections will be discussed in detail in the next chapter.

3.2 Effect of Transverse Beams

Specimens C and CTB were identical except that specimen CTB had 56 in. long transverse beams added to all three connections. These transverse beams were not loaded directly or indirectly during the loading routine. From the hysteretic behavior of both specimens, shown in Figs. 3.1(a) and 3.1(b),

it is clear that the presence of the transverse beam did not significantly affect the overall performance of the test subassembly. Both specimens reached the same peak load which occurred at a lateral drift of 4 percent and remained constant until the end of the test at 5 percent drift. The energy dissipation capacity of both specimens represented by the area enclosed within the hysteresis loops was also identical. The loss of stiffness, however, was slightly improved when the transverse beams were added to the basic configuration. Although both specimens displayed an almost identical initial stiffness, specimen C lost about 55 percent of its initial stiffness by the end of the loading routine, while specimen CTB lost about 50 percent of its initial stiffness. Since both of these specimens had the same level of joint shear stress and the same amount of joint transverse reinforcement, the slight improvement in the loss of stiffness is attributable to the confinement of the joints by the transverse beams.

The effect of the presence of transverse beams on confining the joints could be further demonstrated by comparing the strain in the joint transverse reinforcement of specimens C and CTB. Figure 3.29 shows the strain variation of the interior and the exterior joints of both specimens. Specimen C, which had a joint shear stress level of $5.54\sqrt{f_c'}$ for the exterior connection and $11.08\sqrt{f_c'}$ for the interior connection experienced

yielding of joint reinforcement only in the interior connection and beyond a drift level of 3 percent. The specimen CTB, with joint shear stress level similar to that of specimen C, experienced substantially reduced strain in the joint reinforcement of both the interior and the exterior connections. This is in conformity with the observations made from tests on individual connections (9,16) which indicated that unloaded transverse beams provide additional area of concrete that assisted the joints in resisting lateral shear.

Other aspects of behavior including cracking of beams, columns and loss of bond of beam and column rebars were also not significantly affected by the presence of transverse beams. This seems to contradict with previous conclusions made from tests on isolated connections (16,39), which indicated major improvement in the performance of connections when transverse beams were present. In multiple-connection test specimens, however, the joints are partially confined by the continuity of the system. Shear deformation in the joints is also restricted as the main beams are not free to elongate. Therefore, the connections became less sensitive to the external joint confinement provided by the transverse beams.

3.3 Effect of the Floor Slab

The effect of the presence of the floor slab on the behavior of beam-to-column connections in multiple-connection systems can be studied by comparing the behavior of specimens C and CS1. Specimen CS1 had main beam and columns identical to those of specimen C, and also had 56 in. long transverse beams in all three connections and a 56 in. wide floor slab cast monolithically with the beams. Specimen CTB, which had transverse beams without a floor slab is an intermediate step between specimen C and CS1, thus it is included in this discussion.

The presence of the floor slab in specimen CS1 resulted in a substantial increase in the lateral load resistance of the test subassembly. This is indicated by the envelopes of the load vs. drift curves of all three specimens, shown in Fig. 3.30. Unlike the specimens without a floor slab, the load carrying capacity of specimen CS1 increased continuously until the last loading cycle. At 5 percent drift, the strength of the specimen CS1 was approximately 40 percent greater than the strength of specimens C and CTB.

The presence of transverse beams and the floor slab also had a significant effect on the loss of stiffness of the multiple-connection subassemblies. Figure 3.31 shows the loss

of stiffness of the three specimens at various drift levels. Up to a drift level of one percent, the specimens maintained their initial stiffness. However, beyond the 1 percent drift level the loss of stiffness varied with the type of specimen. At 4 percent drift, specimens C and CTB, which did not have a floor slab, had lost more than half of their initial stiffness while in the specimen with a floor slab, CS1, the stiffness loss was approximately one third of the initial stiffness.

Figure 3.32 indicates that the energy dissipated by all three specimens was approximately the same up to a drift of 4 percent, despite the significant difference in their strength. Beyond the 4 percent drift level, however, the specimen CS1 was able to dissipate more energy than the two specimens without a slab. This additional dissipation of energy is attributed to torsional cracks in the transverse beams at the exterior connections which became significant at 4 percent drift.

The effect of the presence of a floor slab on the behavior of connections can be further studied by considering the strain in the joint transverse reinforcement of specimens C, CTB and CS1. Figure 3.33 shows the variation of such strain in the interior as well as exterior connections of the continuous subassemblies. The strain in the joint reinforcement of the specimen CS1, with a floor slab, was significantly higher than

the strain in specimens C and CTB for both interior and exterior connections. This is the result of two factors. First, as indicated by several researchers (14,16) the contribution of the floor slab to the beam negative bending increased the moment at the column face and, consequently, the shear applied to the joint increased. Such an increase is related to the effective slab width contributing to the negative flexural capacity of the beam. For specimen CS1, the test results indicated that the entire slab width was effective during the beam negative bending, which increased the joint shear stress level from $5.54\sqrt{f_c'}$ to $15.04\sqrt{f_c'}$ for the exterior connection, and from $11.08\sqrt{f_c'}$ to $20.45\sqrt{f_c'}$ for the interior connection. Second, the T-beam action when the beam is subjected to positive bending (slab in compression) increased the width of the concrete compression block. In this case, the neutral axis would typically be located above the beam top reinforcement (25,28). This arrangement affected the geometry of the diagonal concrete compression strut mechanism that resists the joint shear.

Figure 3.34 shows a comparison of the concrete compression strut of an interior connection without and with a floor slab. The presence of the floor slab reduces the depth of the beam compression block on the positive moment side of the joint and also reduces the width of the column compression blocks above

and below the joint by increasing the moment in the columns. Thus, the entire size of the diagonal concrete strut is reduced, which would result in a weaker joint. Therefore, the presence of a floor slab not only increased the joint shear input but also weakened the mechanism relied upon for joint shear resistance.

3.4 Effect of the Amount of Joint Hoop Reinforcement

The effect of the amount of joint transverse reinforcement on the behavior of beam-to-column connections is discussed using test results from specimens CS1, CS2, and CS4. The three specimens were identical except for the amount of joint transverse reinforcement. In specimen CS1 the ratio of the joint transverse reinforcement for the interior and the exterior connections was equal to 0.96 percent, provided in the form of three #3 closed hoops. In specimens CS2 and CS4, only two #3 closed hoops were placed in the interior and the exterior joints which provided a joint transverse reinforcement ratio of 0.64 percent. Specimen CS4 was a duplicate of specimen CS2.

The effect of smaller percentage of transverse hoop reinforcement can be best observed from the hysteresis curves of specimen CS1, CS2, and CS4, shown in Figs 3.1(c), 3.1(e), and 3.1(f). These curves did not indicate any significant

difference in the load carrying capacity, the stiffness characteristics, and the energy dissipation of the three specimens up to drift level of 4 percent. During the last loading cycle, however, specimen CS2 was not capable of increasing its load carrying capacity which was due to the excessive shear damage in the bottom interior column.

The similarity in the hysteresis curves of the specimens indicates that a reduction in the amount of joint transverse reinforcement did not affect the overall behavior of connections in multiple-connection systems. This fact can be further substantiated by comparing strain level in the joint hoop reinforcement of the multiple-connection specimens CS1 and CS4. Despite the reduction in the amount of joint transverse reinforcement, specimen CS4 experienced strain in the joint reinforcement similar to that observed in specimen CS1, as shown in Fig. 3.35. Other behavior aspects of specimens CS1 and CS4, including the cracking pattern in the beams, columns, slab, and the bond and anchorage characteristics of the reinforcement, were also not affected by the reduction in the amount of joint transverse reinforcement. This indicates that in indeterminate connections the amount of joint transverse reinforcement is not as critical to the joint performance as perceived by tests on isolated connections as the joint is confined by the continuity of the system. This may help relax

the requirement for joint transverse reinforcement developed based on observations made from tests on isolated connections which lack the effect of continuity.

3.5 Effect of the Location of Flexural Hinges

Specimen CS3 was added to the test program to study the effect of relocating the beam flexural hinges away from the column faces on the performance of beam-to-column connections in continuous systems. Relocating flexural hinges has been investigated in the past by testing isolated interior or exterior connections (49,50). These tests indicated that relocating flexural hinges is a practical design alternative which protects the joint from its surrounding plastic action. This can eliminate strength and stiffness deterioration of the connection and reduce the amount of transverse reinforcement required to confine the joint.

Similar observations to those made from testing isolated connections were made from testing a continuous system with relocated beam flexural hinges, specimen CS3. However, the effect of continuity indicated that relocation of beam flexural hinges could have certain side effects if not properly detailed. In the case of isolated connections, the inflection points in the beams were always fixed at the beam pinned ends. This arrangement provides a shear span to beam depth ratio that

does not change during the loading routine even if the test specimen includes a floor slab. In the case of a continuous system with a floor slab, however, the location of the inflection points varies according to the ratio of the positive moment to the negative moment in the beam. Therefore, at large drift levels, when the contribution of the floor slab to the beam negative flexural capacity becomes significant, the inflection point would be located closer to the positive moment side of the beam. This results in a significant reduction in the shear span to beam depth ratio which increases the rotation demand during a certain applied drift level, and also increases the shear in the beam. This increase in the rotation demand and the beam shear caused the beam bars of the exterior connection in specimen CS3 to buckle during the 4 percent drift level cycle, and resulted in a beam shear failure of the same connection during the 5 percent drift cycle.

The beneficial effect of relocating the beam flexural hinging regions away from the face of the column can be observed by comparing the strain level in the joint reinforcement of specimens CS3 and CS4. Although both specimens had an equal amount of joint transverse reinforcement and the calculated joint shear stress levels were nearly the same, relocating the beam hinging regions reduced the shear demand on the interior and the exterior beam-column joints. This is evidenced by the

smaller strain level in the joint transverse reinforcement of specimen CS3 in comparison with specimen CS4, as shown in Fig. 3.36. As the plastic action in the beam is removed away from the face of the column, an improved environment that assists the joint in resisting the shear would be expected. Figure 3.37 shows the free body diagram of an interior joint with the beam flexural hinges relocated away from the face of the column. Although the applied moment at the face of the column is greater than the moment at the location of the flexural hinges, the elastic behavior in beam sections adjacent to columns results in deeper compression blocks on both sides of the joint. These boundary conditions provide excellent confinement to the joint concrete compression strut mechanism and also make a larger volume of concrete available to resist the compression, thus, improving the overall shear strength of the joint.

Relocation of the beam flexural hinges away from the face of the column reduced the participation of the floor slab to the beam negative flexural capacity. This can be demonstrated by comparing the strain variation across the slab width in specimens CS1 and CS3, shown in Fig. 3.38. For clarity, the strain distribution at different drift levels are shown in separate plots. It is apparent that the slab rebar farthest away from the main beams in the interior and the exterior connections of specimen CS3 did not contribute significantly

to the beam negative flexural capacity as it remained below the yield strain level during the entire testing routine. In the case of specimen CS1, however, the rebar farthest away from the main beams yielded at 4 percent drift level, indicating a full slab participation in resisting the negative moment. This is due to the reduction in the shear span to slab width ratio caused by shifting the plastic hinges away from the column face which, as indicated by Ammerman and French (51), would reduce the slab participation to the beam negative flexural capacity.

3.6 Bond and Anchorage

3.6.1 Beam Bars

Although the beam bar diameter to column depth ratio provided in the interior connections of all multiple-connection specimens (except CS3) was 16 compared to a value of 20 recommended by ACI-ASCE Committee 352 (35), the slippage of beam reinforcement passing through interior joints was minimal. In specimens without a floor slab, C and CTB, no loss of bond was observed during the entire loading routine as indicated in Fig. 3.19. This type of bond performance in both specimens indicates that the low shear stress level in the joints minimized the crack openings and eliminated fragmentation of the joint concrete core which improved the bond conditions.

In specimens CS1, CS2, and CS4, the beam top and bottom reinforcement showed a different bond behavior. The beam top reinforcement remained in tension during both loading directions as shown in Fig. 3.21. This is due to the fact that the presence of the floor slab provided a wide compression block when the section is under positive bending (slab in compression), which raised the neutral axis above the top reinforcement causing beam top reinforcement to be in tension on both sides of the joints. Under such conditions, slippage of beam top rebars is not expected. In the case of the beam bottom reinforcement loss of bond was reported early during the test, as indicated by the strain history shown in Fig. 3.20. This is the result of the slab participation to the beam negative flexural capacity which increased the tensile force at the top of the beam thus increasing the compressive stresses in the bottom steel. As indicated by Park (43), this increased the demand for bond stress requirements and caused the bottom beam bars to slip through the joint.

In order to relocate the beam flexural hinging regions away from the face of the column the #5 beam rebars in specimen CS3 were replaced by #3 and #4 rebars. This arrangement which increased the column depth to beam bar diameter ratio together

with the minimal joint shear damage improved the bond behavior. Specimen CS3, therefore, showed no slippage of beam top or bottom reinforcement during the entire loading routine.

In exterior joints of multiple-connection specimens, the beam top and bottom reinforcement terminated inside the joints did not show any sign of loss of bond or beam bar pull out. This is despite the fact that the provided development length was equal to 85 percent of the development length suggested by the current recommendations (35).

3.6.2 Column Bars

The anchorage of column reinforcement passing through interior joints largely depended on the extent of damage in the joint core and in the beam flexural hinging regions surrounding the joints. The observed strain data for specimens C, CS1, CS2, and CS4 indicated that the column bars remained in tension irrespective of the direction of loading as shown in Fig. 3.23. In specimens CTB and CS3, where the joints were protected by the unloaded transverse beams and by moving the beam plastic action away from the joint face, respectively, the slippage of column bars was minimal as indicated by the strain history shown in Fig. 3.24. Although all specimens had a column bar diameter to beam depth ratio of 16 compared to

a recommended value of 20, specimens with smaller joint shear damage showed better bond characteristics of column bars passing through interior joints.

At exterior joints, no slippage of column rebars was observed in any of the multiple-connection specimens. This is due to the restraining effect applied by the exterior columns against beam elongation. Such an effect forced the column rebars on the outer face of the columns to remain in high tension above and below the joint as shown in Fig. 25. The column rebars on the inner face of the column, on the other hand, remained in compression or low tension above and below the joint, as shown in Fig. 3.26.

66

Chapter 4

EFFECT OF CONTINUITY ON CONNECTION BEHAVIOR

This chapter provides a discussion of the behavior of connections observed from tests on multiple-connection subassemblies versus tests on single-connection subassemblies. The multiple-connection subassemblies used for this discussion are specimen C which is the basic configuration and specimen CS1 which have additional transverse beams and a floor slab. The single-connection subassemblies used for this discussion are specimens I and E which are the interior and the exterior connection subsets of specimen C, and specimens IS1 and ES1 which are the interior and the exterior connection subsets of specimen CS1.

4.1 Elongation of Beam

One of the factors which influenced the behavior of connections in continuous subassemblies is related to expansion of the flexural hinging regions followed by elongation of the main beams which results from yielding of longitudinal beam reinforcement. In single-connection test subassemblies, where

the main beams are free to elongate, the effect of the elongation of the main beam on the behavior of connections can not be detected. In multiple-connection test subassemblies, however, the elongation of the main beams is partially restrained by the columns. Such a restraint against free elongation has been observed to increase the beam flexural capacity (48) which would affect the behavior of connections as well as the overall response of the test subassembly. A comparison of the measured total elongation of the main beams in single-connection subassemblies with that of the multiple-connection subassembly, for specimens without a floor slab and with a floor slab, is shown in Figs. 4.1(a) and 4.1(b); respectively. This elongation was measured over a gage length equal to 12 in. away from the column faces for both interior and exterior connections. The effect of restraint by exterior columns to the elongation of main beams in the continuous subassemblies is obvious from the smaller growth of specimens C and CS1.

The beam elongation effect can be further observed from the cracking pattern of columns in exterior connections. Despite a large column to beam flexural strength ratio of 2.41 for the exterior connection without a floor slab and 1.20 for the exterior connection with a floor slab, extensive flexural cracks developed on the outer face of the exterior columns of

the multiple-connection specimens C and CS1, as shown in Figs. 3.10(a) and 3.10(b). These cracks, which started at a drift level of 1.5 percent were accompanied by high strain in the column outer longitudinal rebars as shown in Figs. 4.2(a) and 4.2(b). Such cracks did not develop in the column of the isolated exterior connections, specimens E and ES1, because of the free elongation of the main beam.

4.2 Rotation of Beam Hinging Regions

The rotation of the flexural hinging regions was measured with two LVDTs placed 1.5 in. above and below the beam. The LVDTs covered a gage length of 12 in. away from the face of the column. Figures 4.3(a) and 4.3(b) provide a comparison of the rotation of the beam flexural hinges in continuous systems versus single-connection subassemblies. The measured rotation at the peaks of cycles was smaller in case of the connections in continuous systems for both without a floor slab connections and with a floor slab connections. This reduction in rotation of the hinging region is a logical result of the beam axial compression which developed in the multiple-connection specimens due to restriction against beam elongation.

4.3 Distribution of Applied Lateral Load

The distribution of the total lateral load among the three columns of the multiple-connection subassemblies C and CS1 followed a similar pattern. At drift levels of less than one percent, the load was almost equally distributed among the three columns. As the drift level increased, the load carried by the first column in the direction of loading increased while the load carried by the last column decreased. The load carried by the center column, however, increased continuously during the entire loading routine. Figures 4.4(a) and 4.4(b) show the distribution of the lateral load among the three columns of both specimens C and CS1, respectively. This distribution can be best explained by considering the equilibrium of individual columns as shown in Fig. 4.5. As the deformation level increases and plastic hinges form in the beams, axial force develops in the main beams due to restraining effect of the exterior columns to the elongation of beams. By including the presence of the axial force, N, the shear in the columns above the joints becomes

$$V_L = \frac{M_b^-}{H} - \frac{N}{2} \qquad (4.1)$$

$$V_c = \frac{M_b^- + M_b^+}{H} \qquad (4.2)$$

$$V_R = \frac{M_b^+}{H} + \frac{N}{2} \qquad (4.3)$$

where V_L, V_c and V_R are the shear forces in the left, center, and the right columns, respectively; M_b^+ is the positive moment in the beam (slab in compression), M_b^- is the negative moment in the beam (slab in tension), and H is the total column height. The axial force in the main beams, which increased with the drift level, caused the shear in the right column to increase and the shear in the left column to decrease. The shear in the center column is not affected as the beam axial force on the two sides of the column balance each other.

The magnitude of the axial compression in the main beams could not be measured directly during the test. However, its value can be determined indirectly from the equilibrium equations (Eqn. 4.1 - Eqn. 4.3). By subtracting Eqn. 4.1 from Eqn. 4.3,

$$N = V_R - V_L + \frac{M_b^- - M_b^+}{H} \qquad (4.4)$$

In specimen C, the beams are symmetrically reinforced, thus, the positive and the negative moments in the main beams would be equal. The factor $(M_b^- - M_b^+)/H$ in Eqn. 4.4 will, therefore, be equal to zero. Based on the measured values of V_L and V_R, the magnitude of axial compression in the main beams of specimen C can, thus, be calculated as

$$N = V_R - V_L \qquad\qquad (4.5)$$

The axial compression in the main beams of specimen C obtained by using Eqn. 4.5 is plotted against the applied drift in Fig. 4.6. Up to a drift level of 0.5 percent, the beam reinforcement remained within the elastic range, thus no axial compression developed in the beams. As the beam reinforcement began to yield, the axial compression in the main beams reached 3.5 Kips at one percent drift. At 3 percent drift, the axial compression in the beams reached a value of approximately 15 Kips which is not insignificant.

For specimen CS1, which had a floor slab, the positive and the negative moments in the main beams will not be equal because of the contribution of the floor slab to the beam negative moment. Due to the indeterminacy of the test subassembly, the

magnitude of these moments can only be determined if shear was measured at the columns both above and below the joints. Constraints of the test set-up allowed measurements of shear in the columns only above the joints. However, knowing the theoretical positive and negative flexural capacities of the beam with a slab, the upper and lower bounds for the axial force, N, can be estimated. If it were to be assumed that the slab did not contribute toward the flexural strength of the beam, i.e. $M_b^- = M_b^+$, then the calculated value of the axial force would be minimum and will simply be the difference between the lateral shear in the two exterior columns, as indicated in Eqn. 4.5. However, if the entire slab width contributed towards the flexural strength of the beam, the theoretical value of the factor $(M_b^- - M_b^+)/H$ can be calculated using the theoretical positive and negative flexural strengths of the beam. Using the flexural strengths of the beam given in Table 2.3 the value of the factor $(M_b^- - M_b^+)/H$ will be equal to 7 Kips and the corresponding axial force would represent the maximum possible value.

The bounds of N calculated using the above procedure are shown in Fig. 4.7. The actual width of slab that contributes towards the flexural capacity of the beam will be somewhere

between no participation to full participation of the slab and, accordingly, the axial force will lie between the bounds indicated. Therefore, comparing the upper and lower bounds with the value of N obtained from specimen C, it is noticed that the magnitude of axial force developed in the specimen with a floor slab, CS1, is not very much different from that developed in the specimen without a slab.

At 3 percent drift, the axial compression in the main beams of specimens C and CS1 was approximately 15 Kips. With this level of axial compression, the flexural capacity of the beams would increase by about 15 percent which would result in a reduction of the column to beam flexural strength ratio from 1.88 to 1.64 for the interior connection without a floor slab, and from 2.41 to 2.09 for the exterior connection without a floor slab. For connections with a floor slab, the reduction in the column to beam flexural strength ratio is from 1.19 to 1.04 for the interior connection, and from 1.20 to 1.05 for the exterior connection. This can be particularly critical at exterior connections where the axial compression in the main beams also increases the moment in the exterior columns causing it to crack earlier than expected. As illustrated in Fig. 4.8, the maximum moment, M_c, in the exterior column is given by

$$M_c = \frac{M_b}{2} + \frac{NH}{4} \qquad\qquad (4.6)$$

where M_b is the moment in the beam, N is the beam axial force, and H is the total column height. The moment in the exterior columns is thus increased by $(NH/4)$ in addition to the increase resulting from the increased flexural capacity of the beam due to the presence of axial compression. This implies that for a given drift level, the exterior columns in continuous systems may suffer more damage and at much earlier stage, due to restraint against beam elongation, than what is observed from tests on isolated connections where the beams are allowed to elongate freely. These observations can be demonstrated by analyzing a multiple-connection subassembly with flexural hinging regions modelled as a truss mechanism (52).

4.4 Contribution of Floor Slab to Beam Flexural Capacity

The contribution of the floor slab to the beam negative flexural capacity can be assessed from the cracking pattern in the slab and the variation of strain in the slab reinforcement. Flexural cracking in the slab normal to the main beam axis started in all connections at 1 percent lateral drift. As the cyclic loading progressed several cracks

developed in the slab of the interior and the exterior
connections. In the multiple-connection specimen CS1, these
cracks, which were parallel to the face of the column, extended
across the entire width of the slab, as shown in Fig. 3.8.
In the case of isolated interior and exterior connections IS1
and ES1, the flexural cracks in the slab followed a V-shaped
pattern pointing towards the columns, as shown in Figs. 4.9(a)
and 4.9(b). These cracks did not extend across the entire
slab width even after the specimens were subjected to 4 percent
drift.

The strain variation across the slab width of connections
tested as a continuous subassembly was different from that
observed in the slab of isolated connections. The strain
distribution across the slab width of specimens CS1, IS1 and
ES1 at 2, 3, and 4 percent drift levels is given in Fig. 4.10.
The distribution shows a rapid decay in the strain variation
across the slab width of the single connection specimens
compared to a more uniform distribution of strain in the slab
reinforcement of the multiple-connection specimen CS1. This
strain distribution, which is in conformity with the flexural
cracking pattern, indicates that a larger slab width contributed
to the negative flexural capacity of beams in the continuous
system than what is indicated by single connection tests.

This conclusion is attributed mainly to the fact that in single connection tests the specimens are usually isolated from the beam mid-spans and pin connected with the test set-up. This type of connection has two different consequences that affect the behavior of connections. First, pin connecting the beam free end to the test set-up fixes the point of inflection at that specific location. In continuous structures, however, the location of the points of inflection may vary according to the ratio of the positive and the negative moments in the beam as shown in Fig. 4.11. And because the positive moment (slab in compression) is normally smaller than the negative moment (slab in tension) the points of inflection would be located closer to the positive moment side of the beam. Therefore, on the slab in tension side of the beam there would be an increase in the slab panel length to width ratio, which as suggested by Ammerman and French (51) would increase the contribution of the slab to the beam flexural capacity.

Second, pin connecting the beam with the test set-up, which is intended to simulate continuity in the beam, causes a discontinuity in the slab. As a result, when the column is subjected to lateral drift in a direction which would result in tension in the slab, the column and the transverse beams rotate as a rigid body trying to lift the free end of the slab

upward while the main beam is pulling the center of the slab downward applying a point load at the center of the slab, as shown in Fig. 4.12. This would result in bending stresses in the transverse direction of the slab which in turn causes the slab principal flexural cracks to follow a V-shaped pattern pointing toward the column and thus reduces the contribution of the floor slab to the beam flexural capacity.

4.5 Hysteretic Behavior

The load-drift plots, also referred to as hysteresis loops, provide information on strength, stiffness, and the energy dissipation capacity of the specimens. The hysteresis plots of the multiple-connection specimens C and CS1, and their subset single-connection specimens are shown in Figs. 4.13(a) and 4.13(b), respectively.

4.5.1 Strength

The effect of continuity on the strength of connections can be seen by comparing the lateral load resistance of the multiple-connection specimens C and CS1, with the total lateral load resisted by the individual connections. As shown in Figs. 4.14(a) and 4.14(b), the strength of connections does not appear to be affected by the continuity of the subassembly up

to a drift level of 1 percent. At higher drift levels, however, the multiple-connection subassemblies displayed a significantly higher strength which at a drift level of 4 percent was approximately 20 percent greater than the total strength of the individual connections without a floor slab, and in the order of 25 percent greater than the total strength of the individual connections with a floor slab. This higher lateral load resistance of the multiple-connection subassemblies is attributed to the increase in the flexural capacity of the beams resulting from the restraining effect against axial elongation. And in the case of the connections with a floor slab, the higher lateral load resistance is partly due to a larger contribution by the slab to the negative flexural strength of the beams in continuous systems.

4.5.2 Stiffness

Stiffness degradation of the test subassemblies was measured by including in the loading routine cycles 3, 7, and 11 with displacement amplitude equivalent to one percent drift. The loss of stiffness in the multiple-connection specimens appears to be less severe than the loss of stiffness observed in interior or exterior connections tested individually. As shown in Fig. 4.15(a), the multiple-connection specimen without

a floor slab lost about half of its stiffness by the end of the eleventh cycle at 4 percent drift, while the single-connection specimens lost almost three quarters of their original stiffness. For connections with a floor slab, the multiple-connection specimen lost only about one third of its original stiffness while the individual interior and exterior connections lost approximately 50 to 70 percent of their original stiffness by the end of the loading routine as indicated in Fig. 4.15(b).

4.5.3 Energy Dissipation

The energy dissipation as measured by the area enclosed within the hysteresis loops of the specimens was not affected by the continuity of the test subassembly. Figures 4.16(a) and 4.16(b) show that the hysteretic energy dissipated by specimens C and CS1 was approximately equal to the total energy dissipated by their subset connections tested individually.

4.6 Shear in the Joint

The joint shear stress in the interior and the exterior connections without a floor slab was $11.08\sqrt{f'_c}$ and $5.54\sqrt{f'_c}$, respectively. By including the slab reinforcement in the joint shear calculations, the joint shear stress becomes $20.45\sqrt{f'_c}$

for the interior connections and $15.04\sqrt{f_c'}$ for the exterior

connections. A joint transverse reinforcement ratio of 0.96

percent, in the form of three #3 closed stirrups placed at 3

in. spacing, was provided in both the interior as well as the

exterior connections with and without a floor slab. Since the

connections without a floor slab did not have transverse beams,

the joint shear damage could be inspected visually. Diagonal

shear cracks developed in the interior joints of both single

and multiple-connection specimens during the fourth loading

cycle. The shear cracks in the interior connection of the

multiple-connection specimen, which are shown in Fig. 3.11,

however, developed faster and were more severe than the shear

cracks in the single interior connection shown in Fig. 4.17.

The shear cracks in the exterior joints of the single and

multiple-connection specimens were minimal, as shown in Fig.

4.18, and developed at a much later stage in the displacement

routine.

A comparison of strain in the joint reinforcement of the

interior and exterior connections of the single and the

multiple-connection subassemblies without a floor slab is shown

in Fig. 4.19(a). The strain in the joint of the single interior

connection, specimen I, remained below the yield level while

the strain in the interior joint of the multiple-connection

specimen exceeded the yield strain indicating a higher shear deformation in the interior joint of the continuous subassembly. The strain level in the exterior joint reinforcement of both the single and the multiple-connection specimens remained below the yield level due to the low joint shear stress level $(5.54\sqrt{f'_c})$. The joint reinforcement in the exterior connection of the multiple-connection specimen, however, experienced a relatively higher strain than that experienced by the joint reinforcement of the single exterior connection, specimen E, especially at drift level greater than 2 percent.

For connections with a floor slab, the joint shear damage can only be assessed from the strain measurements in the joint transverse reinforcement. Similar to connections without a floor slab, the joint reinforcement in single connections remained below the yield level, as shown in Fig 4.19(b). In the case of the multiple-connection specimen CS1, the strain in the joint reinforcement of both interior and exterior connections exceeded the yield level. The continuity of the subassembly, therefore, appears to have resulted in a higher joint shear in both the interior and the exterior connections, regardless of the presence of the floor slab.

The increased shear in the joints of the multiple-connection subassemblies can be explained by examining the effect of axial compression in the main beams on shear in the joints. From the equilibrium of forces acting on the joint, as shown in Fig. 4.20, if the axial force in the main beams is ignored, the shear in the interior joint is given by

$$V_j = T_1 + C_2 - V_{col} \tag{4.7}$$

and the shear in the exterior joint is given by

$$V_j = T - V_{col} \tag{4.8}$$

However, when the axial force is present, the beam is acting more like a beam-column and the compressive force, C, is no longer equal to the tensile force, T. From the equilibrium of forces acting on the joint, the compressive force is given by

$$C = T + N \tag{4.9}$$

With axial compression present in the beams, the shear in the

84

interior column of the multiple-connection subassemblies becomes

$$V_{col} = \frac{M_{nb}^{'+} + M_{nb}^{'-}}{H} \qquad (4.10)$$

where $M_{nb}^{'+}$ and $M_{nb}^{'-}$ are the beam positive and negative flexural capacities including the effect of axial compression. Substituting Eqns. 4.9 and 4.10 in Eqn. 4.7, the shear in the interior joint becomes

$$V_j = T_1 + T_2 + N - \frac{M_{nb}^{'+} + M_{nb}^{'-}}{H} \qquad (4.11)$$

Similarly for exterior connections, the lateral shear in the columns above and below the joint after including the effect of axial force in the main beams is

$$V_{col} = \frac{M_{nb}^{'}}{H} - \frac{N}{2} \qquad (4.12)$$

$$V_{col}^{'} = \frac{M_{nb}^{'}}{H} + \frac{N}{2} \qquad (4.13)$$

Considering the equilibrium of horizontal forces at mid-height of the joint, the horizontal shear in the exterior connection is then

$$V_j = T - V_{col} \tag{4.14}$$

$$V_j' = C - V_{col}' \tag{4.15}$$

Substituting the values of C, V_{col} and V_{col}' from Eqns. 4.9, 4.12 and 4.13 in Eqns. 4.14 and 4.15, the shear in the exterior joint becomes

$$V_j = T - \frac{M_{nb}'}{H} + \frac{N}{2} \tag{4.16}$$

$$V_j' = T + N - \frac{M_{nb}'}{H} - \frac{N}{2} \tag{4.17}$$

which simplifies to

$$V_j = V_j' = T + \frac{N}{2} - \frac{M_{nb}'}{H} \tag{4.18}$$

Based on Eqns. 4.11 and 4.18, the observed axial compression in the main beams of 15 Kips at 3 percent drift level would increase the shear in the interior and exterior joints of the multiple-connection specimens by almost 15 percent and 8 percent, respectively. The higher strain observed in the joint reinforcement of the multiple-connection subassemblies confirms this increase in the joint shear. Thus, in situations

where beams could be restrained against elongation, ignoring the presence of axial compression could result in underestimation of the joint shear.

4.7 Anchorage of Beam Bars

Strain measurements along the main beam reinforcement can be used in detecting slippage of bars passing through interior joints due to loss of bond. Figure 4.21 shows the strain history of the bottom beam bar of specimen I at the face of the column. It is noted that the force in the bar changed its sense from tension to compression or vice versa when the applied displacement was reversed, thus indicating no loss of bond along the joint. This behavior is similar to that observed in the beam bars of specimen C, shown in Fig. 3.19. The beam top reinforcement of both specimens experienced similar behavior.

In the isolated specimen IS1 which has a floor slab, the behavior of the beam top and bottom reinforcement were different. The strain history of the beam top reinforcement, shown in Fig. 4.22, indicates that the bar remained in tension even though the moment sense requires the bar to be in compression. This is due to the participation of the slab concrete in compression which raised the neutral axis of the

beam section above the beam top rebars. In the case of the beam bottom reinforcement, the strain history shown in Fig. 4.23 indicates that minimal loss of bond occurred as the slope of the curves change slightly when the bars are under compression. The performance of the beam top and bottom reinforcement of specimen IS1 is similar to that of the interior connection of specimen CS1. This can be observed by comparing Figs. 4.22 and 4.23 with Figs. 3.21 and 3.20, respectively.

In exterior connections, beam bars are terminated at the joint back face with a 90 degree standard hook and an embedment length equal to 85 percent of the value recommended by ACI-ASCE Committee 352 (35). No loss of anchorage or pull out of beam bars was observed in both isolated exterior connection specimens E and ES1. This observation is very much similar to that made from the response of the beam bars terminated in the exterior connections of the multiple-connection specimens.

It can, therefore, be concluded that the bond and anchorage performance of the beam reinforcement passing through interior joints or terminated inside exterior joints was not affected by the continuity in the test subassembly as both the isolated and continuous connections showed similar beam bar behavior.

4.8 Anchorage of Column Bars

The slippage of column bars resulting from loss of bond in the joint core can be seen from the strain in the column bars immediately above and below the joint. The observed strain data for the multiple-connection specimens C and CS1, indicates that the bars of the interior column remained in tension irrespective of the direction of loading. Typical strain variation for column bars of interior columns of specimen C at the location indicated is shown in Fig. 3.23. The slippage of column bars was also observed in the isolated interior connection specimens I and IS1 as the column bars indicated tension though the moment sense requires the bar to be in compression. However, as shown in Fig. 4.24, tensile strain level is smaller than that in multiple-connection specimen C. This indicates that the slippage of column bars in isolated interior connections was more controlled compared to slippage in the interior connections of continuous systems. This type of behavior implies that the anchorage of column bars is a more serious problem in multiple-connection subassemblies than in isolated connections due to the greater flexural demand imposed on the columns and the more severe shear damage in the joints.

4.9 Design Implications

The current procedure for the design of connections (35) is based primarily on the behavior of connections observed in single-connection tests. As indicated by testing of multiple-connection subassemblies, any restraint to elongation of the main beams could significantly affect the joint shear stress, column to beam flexural strength ratio, lateral load distribution among the columns, and the shear and moment imposed on the exterior columns. As discussed earlier, if the elongation of the main beams resulting from expansion of the plastic hinging regions is expected to be partially restrained, which can possibly happen in a highly indeterminate frame building, then it might be appropriate to account for the presence of axial compression in the main beams in designing beam-to-column connections.

In a real situation, the restriction to the elongation of the main beams may not be as severe as that imposed by the test set-up of this experimental investigation. However, the observations made from these tests may still be valuable in making a conservative estimate of axial compression that may possibly develop in the main beams of a moment-resisting frame. The axial compression in the main beams of the continuous

subassemblies was observed to begin developing as the beam main reinforcement reached the yielding strain and continued to increase until the reinforcement on the outer face of the exterior columns yielded. The maximum value of axial compression in the beams can thus be estimated from the equilibrium of moments at the exterior connection, shown in Fig. 4.8, by assuming the column to reach its yield moment. Eqn. 4.6 can then be rewritten as

$$M_{yc} = \frac{M'_{nb}}{2} + \frac{N_{max}H}{4} \qquad (4.19)$$

where M_{yc} is the yield moment capacity of the exterior column, M'_{nb} is the beam positive flexural capacity including the effect of the axial compression, and N_{max} is the maximum value of axial compressive force in the main beam. Since the ultimate moment capacity of the column is more readily computed and the difference between the yield capacity and the ultimate moment capacity is usually not substantial, the M_{yc} value in Eqn. 4.19 can be substituted with the column ultimate flexural capacity, M_{nc}. Rearranging Eqn. 4.19, the maximum value of the beam axial force can be calculated from the beam and the exterior column flexural capacity as

$$N_{max} = \frac{4}{H}\left(M_{nc} - \frac{M_{nb}'}{2}\right)$$ (4.20)

Equation 4.20 indicates that the value of the beam axial force would be larger if a smaller value of the beam flexural capacity is used. This would occur when the beam is subjected to positive bending (slab in compression). The presence of the floor slab could, therefore, be neglected as its effect on the beam positive flexural capacity is insignificant. It was also shown earlier that the magnitude of the beam axial force is not affected by the presence of the floor slab as both specimens, C and CS1, developed almost identical values of N , as indicated in Fig 4.7.

Substituting the column to beam flexural strength ratio for an exterior connection

$$R = \frac{2M_{nc}}{M_{nb}'}$$ (4.21)

M_{nc} can be eliminated from Eqn. 4.20 and the axial force can be expressed more meaningfully as a function of the column to beam flexural strength ratio and the positive flexural capacity of the beam as

$$N_{max} = \frac{2M_{nb}'(R-1)}{H}$$ (4.22)

In calculating the axial force by using Eqn. 4.22, the effect of axial force on the flexural capacity of the beam can be initially ignored. The maximum value of the axial force can then be easily determined in two or three iterations. Applying this procedure to the test subassemblies, Eqn. 4.22 yields a maximum axial compression in the beam of 22 Kips which agrees well with the maximum value of the beam axial force of approximately 25 Kips obtained from the test results as shown in Fig. 4.6 and 4.7.

The observations and discussions presented in this chapter are based on the premise that unlike those in isolated connection tests where the beams are free to elongate, the main beams in an indeterminate subassembly may not be completely free to grow and the indeterminate subassembly is thus likely to develop some axial compression. Consequently, the results and conclusions drawn from this discussion would apply to the situation where axial restriction to the elongation of main beams is anticipated.

Chapter 5

EFFECTIVE SLAB WIDTH

5.1 General

Since the first recommendations for the design of beam-column joints in 1976 (34), and subsequent revision in 1985 (35), the question of the effect of the presence of a floor slab on the behavior of beam-column joints and how to include the slab in the design of joints has not been completely resolved. The current procedure for the design of connections has been criticized for not addressing this important issue. Numerous studies (12,13,18,23,24,25,28,49,53,54,55) have underscored the significance of the presence of a slab on the behavior of beam-to-column connections. Among other things, the presence of a slab has been observed to affect strength, stiffness, and shear in the joints. Perhaps the most critical of all in terms of the overall performance of the buildings is the effect on the column to beam flexural strength ratio. Under lateral loading, the slab which acts as an integral part of the main beam increases both the positive and the negative flexural capacity of the beams. The contribution of slab to

the positive flexural capacity of the beams in term of equivalent effective slab width, as recommended by ACI 318-83 Building Code (37,38), is well accepted and is commonly used in gravity load design of buildings. However, the contribution of slab to the negative flexural capacity of beams, i.e. when slab is in tension, whether in term of an effective slab width or otherwise has not yet been settled. The primary reasons for not having any specific recommendations on the effective width of slab include (a) lack of adequate and conclusive test data, (b) difficulty in comparing results from tests of specimens having varied configurations and tested under different loading conditions, and most importantly, (c) the lack of information on correlating the response of connections tested in the laboratory to that expected in a real building.

5.2 Theoretical Models

The participation of the slab in beam-column-slab connection tests has been generally reported in the form of strain distribution in slab reinforcement across the width. This strain distribution has been mathematically modelled and good agreement has been obtained between the theoretical results and the observed participation of the slab in single-connection tests. Pantazopoulou, Moehle, and shahrooz (56) developed a theoretical model which is based on a strain distribution

across the slab width which varies as a function of $\sin^2\alpha$ to estimate the effective slab width; where α is the acute angle formed by the rigid link assumed to develop between the beam at a distance equal to the beam effective depth away from the face of the column and the transverse beams at end of slab rebar locations as shown in Fig. 5.1. This function represents a rapid decay in strain of slab reinforcement in the transverse direction which is in good agreement with strain distribution observed from tests on isolated connections. Based on this model, they proposed an effective slab width on each side of the beam equal to 1.5 times the beam depth for up to yielding of beam reinforcement, increasing to approximately three times the beam depth for deformations expected during severe earthquake loading.

Cheung, Paulay, and Park (57,58) developed a model to identify the slab and beam structural behavior and possibly quantify the slab contribution. This model is based on the assumption that when tensile forces, T_x, are generated in the slab reinforcement parallel to the beam, shear forces, T_s, and a moment M at the slab-main beam interface must develop to maintain equilibrium, as shown in Fig. 5.2(a). Consequently, orthogonal tensile forces T_y are necessary to sustain the moment M, as shown in Fig. 5.2(b). This suggests a mechanism of force transfer within the slab panel consisting of a fan-type

compression field which, in order to be developed, only slab bars anchored in a suitable region, such as shown shaded in Fig. 5.3, are assumed effective. This mechanism of force distribution justifies the V-shape flexural cracks observed in the slab of the isolated connections tested in this and in many other programs.

Such theoretical models certainly explain the observed response on isolated beam-column-slab connection subassemblies. However, in continuous subassemblies, where the slab is not acting as an isolated panel, the applicability of such an approach may not be appropriate. Ammerman and Wolfgram-French (51) addressed the effect of boundary conditions and continuity on modeling the slab contribution to the beam negative flexural capacity. According to them, the presence of an end beam at the location of the line of infection in isolated connections is best approximation to continuous structure. This is mainly because of the restriction of the transverse-curvature mechanism, shown in Fig. 5.4, which would cause the longitudinal-curvature to be uniform across the entire slab width and, thus, eliminate the V-shape flexural cracks observed in slabs of isolated connections. Unlike the previous two models, this study indicated that the slab participation to the beam flexural capacity can be influenced

by the continuity in the system. Therefore, the observed participation of slab in continuous subassemblies provides a better benchmark for calibrating the theoretical models.

5.3 Experimental Data

Based on observations of strain distribution in slab reinforcement across the slab width few researchers have made specific recommendations on the effective slab width. Paulay and Park (49) suggested that slab contribution to the load input into the joint should be estimated by assuming an effective slab width on each side of the beam as four times the thickness of the slab for interior connections and twice the thickness of the slab for exterior connections. Based on tests on exterior connections in which transverse beams exceeded their cracking torsional capacity, Durrani and Zerbe (55) suggested an effective slab width equal to the width of the column plus twice the depth of the transverse beams.

Other experimental investigations (12,13,18,24,25,28, 53,54) which tested connections with a slab reported a wide range af slab participation to the beam negative flexural capacity. The reason that no specific effective slab width could be extracted directly from these studies is the different configurations and different loading conditions used in these studies. However, all of these studies share the following

common conclusions: (a) the presence of slab increased the beam negative flexural capacity, which if neglected could result in hinging of columns instead of beams and caused increased shear damage in the joints, and (b) the extent of slab participation to the beam flexural capacity is directly related to the torsional capacity of transverse beams.

A summary of recommended effective slab widths and typical distribution of strain across the slab width as reported by various researchers is shown in Figs. 5.5(a) and 5.5(b). The broken lines in these figures represent the width of slab used in the test specimens, and the solid lines represent the effective slab width i.e. the width within which the slab reinforcement yielded in tension during negative bending of the beams. The effective slab width has generally been expressed in terms of the slab thickness, depth of the main beam, or the depth of transverse beams. For the purpose of comparison the slab widths shown in Figs. 5.5(a) and 5.5(b) are expressed in terms of the main beam total depth.

Durrani and Wight (53) and Ehsani and Wight (54) tested interior and exterior connections with a relatively small slab width of approximately one beam depth on each side of the beam. After a few cycles the entire slab width was effectively contributing to the beam negative flexural capacity. Suzuki

et al (13) and Kitayama et al (25) tested interior and exterior connections with available slab width equals to four times the total beam depth on each side of the beam. Their effective slab width at 4 percent lateral drift varied between 2.5 and 3 times the total beam depth on either side of the beam. Joglekar et al (18) and Murray (12) also tested interior and exterior connections with available slab width equals to 3.5 times the beam depth on each side of the beam. Unlike other studies, the distribution of slab reinforcement in these specimens was more representative of a real building and was thus concentrated in the middle strip away from the main beam. The entire width of slab was observed to be effective at a drift level of 2.5 percent. Fujii et al (24) tested exterior connections with a lightly reinforced slab of width equal to three times the beam depth on either side of the beam. At 2 percent relative drift, the observed effective slab width was close to twice the total beam depth on each side of the beam. In recent tests of interior connections by Wolfgram-French and Boroojerdi (28), the entire slab width which was equal to 5 times the total beam depth on each side of the beam was found to be effective at a drift level of 4 percent.

5.4 Effective Slab Width

The participation of the slab to the beam negative bending has been typically observed to increase with increase in the drift level. In moment resisting frames, a lateral drift level of three percent is generally assumed to be a realistic upper limit. The strain measurements across the slab width in the continuous test subassembly CS1 adjacent to both interior and exterior connections indicate that the slab rebar farthest away from the main beam approached yielding at this drift level as shown in Fig. 4.10. Consequently, the width of the slab in specimen CS1 may be considered as the effective slab width which is equivalent to twice the total main beam depth on each side of the beam. This effective slab width also represent an accepted interpolation of the effective slab widths shown in Figs. 5.5(a) and 5.5(b) which varied between one to five beam depths on each side of the beam for interior connections and between one to 3.5 beam depths on each side of the beam for exterior connections.

5.5 Effect of the Size of Transverse Beams

In exterior connections the effective slab width is related to the extent of torsional damage in the transverse beams. After the transverse beams develop torsional cracks due to tension in the slab reinforcement, the resulting reduced

torsional stiffness releases the strain in the slab reinforcement farther away from the main beam. Zerbe and Durrani (16) indicated that when the induced torsional moment in the transverse beams reaches their torsional capacity the transverse beams become flexible and they can no longer support the slab. Under these conditions they recommended the effective slab width to be limited to a distance equals to one transverse beam depth on each side of the main beam.

In the case of specimen CS1, a comparison of the induced torsional moment in the transverse beams of the exterior connection with their cracking and nominal strength calculated based on the Hsu's theory (59) is shown in Fig. 5.6. It is apparent from this figure that the induced torsional moment in the transverse beams remained lower than their nominal torsional capacity. Also, comparing the induced torsional moment with the nominal torsional capacity calculated based on ACI-318 (37,38), Fig. 5.6 indicates that the torsional moment induced in the transverse beams remained below their torsional capacity. Therefore, in conformity to the previous recommendation, if the moment induced in transverse beams is smaller than their nominal torsional capacity, an effective slab width equals to twice the beam depth on each side of the main beam can develop.

To study the effect of the torsional stiffness of transverse beams on slab participation, an isolated exterior connection, specimen ES2, with a slab was also tested. The main beam, the column and the slab of specimen ES2 were identical to those of specimen ES1. The transverse beams of specimen ES2, however, had a cracking and nominal torsional capacities equal to 80 percent and 75 percent, respectively, of those of specimen ES1, while the initial and cracking torsional stiffness of the transverse beams in specimen ES2 were approximately 70 percent of those of the transverse beams of specimen ES1.

The overall behavior of specimen ES2 was similar to that of specimen ES1 except for the strain distribution across the slab width. Figure 5.7 shows that the strain level in the slab reinforcement of specimen ES1 was higher than the strain in the slab reinforcement of specimen ES2 indicating a larger slab participation to the beam negative flexural capacity in specimen ES1. This is regardless of the fact that the ratio of the torsional moment induced in the transverse beams to their torsional capacity was approximately the same in both specimens, as shown in Fig. 5.8. Therefore, it can be concluded that a reduction in initial torsional stiffness of transverse beams would result in reduction of slab participation to the beam flexural capacity.

5.6 Design Recommendations

Based on the results of this study and review of observations made by other investigators, the following procedure is suggested to account for the presence of a floor slab in the design of beam-to-column connections.

1. Reinforcement in a slab width equal to twice the total beam depth on each side of the beam should be considered effective in calculating the negative flexural capacity of the beams. The column to beam flexural strength ratio and the shear in the columns should, accordingly, be based on the increased capacity of the beams. In the case of exterior connections, if the torsional moment induced in the transverse beams by tension in the slab reinforcement within the effective slab width exceeds their torsional strength, the effective slab width for the design of exterior connections should be reduced to one beam depth on each side of the beam.

2. When calculating shear in the joint, the slab reinforcement within the effective slab width should be considered together with the beam top reinforcement as indicated in the free body diagram shown in Fig. 5.9. Although the slab reinforcement does not pass through the joint, the compressive force in concrete equilibrating

tension in the top steel is directly applied to the joint. The calculated shear in the joint will thus be higher than that given by the current recommendations.

Appendix A includes two examples which demonstrate the application of the suggested procedure to include the slab in the design of interior and exterior beam-to-column connections.

Chapter 6

SUMMARY AND CONCLUSIONS

6.1 Summary

Six two-bay frame subassemblies each consisting of two exterior connections and one interior connection and five isolated connection subassemblies were tested under earthquake-type loading to study the behavior of beam-to-column connections in indeterminate subassemblies. The present understanding of the behavior of beam-to-column connections is based on the response of connections tested as isolated connections. The current procedures for designing connections, therefore, reflect the inadequacies inherent in isolated connection tests. As these test results have shown, the indeterminacy of the test subassembly can significantly change the response of connections.

The main objective of this investigation was to study the performance of connections in indeterminate subassemblies and to correlate the behavior with that observed in isolated connection tests. The variables investigated in this study were: (1) the amount of joint transverse reinforcement, (2)

the location of beam flexural hinging regions relative to the face of columns (3) the presence of transverse beams, and (4) the presence of transverse beams with a floor slab,

The experimental program consisted of tests on a total of eleven half-scale beam-to-column connection subassemblies. Six of the subassemblies were multiple-connection subassemblies with each consisting of two exterior connections and one interior connection in the form of a single story of a two-bay frame isolated at column mid-heights. The first specimen (C), consisted of three columns framed together with one continuous beam. The second specimen (CTB), was identical to the first specimen except that transverse beams were added to the basic configuration. The third specimen (CS1), had additional transverse beams and a floor slab. The fourth specimen (CS2), was similar to specimen CS1 except that it had smaller amount of joint transverse reinforcement. The fifth specimen (CS3), was identical to specimen CS2 except that the beam flexural hinging regions were relocated a certain distance away from the face of the columns. The sixth specimen (CS4), was a repeat of specimen CS2.

The other five specimens consisted of two isolated interior connections and three isolated exterior connections. Specimen I and specimen E represented the interior connection and the exterior connection of specimen C, respectively. Specimen IS1

and specimen ES1 represented the interior connection and the exterior connection of specimen CS1, respectively. Specimen ES2 was an exterior connection, which was identical to specimen ES1 except that the transverse beams were smaller.

Each specimen was subjected to twelve displacement cycles of increasing amplitude which varied between 0.25 percent and 5 percent of the total column height. The specimens were tested in a vertical position with the cyclic displacement applied laterally at the top of the columns. Each specimen was appropriately instrumented to measure various aspects of behavior.

6.2 Conclusions

Based on the results obtained from this experimental investigation, the following conclusions are drawn:

1. The behavior of connections in isolated connection subassemblies was observed to be significantly different than the behavior of connections in indeterminate connection subassemblies. This difference in behavior resulted primarily from the elongation of main beams at large deformation reversals. When such elongation was partially restricted in indeterminate subassemblies, significant axial compression developed in the beams which affected the response of connections as follows:

a) Interior and exterior connections in indeterminate subassemblies experienced higher joint shear than that experienced by the joints in isolated connections.

b) Because of the presence of axial compression, the flexural capacity of main beams in indeterminate subassemblies increased which reduced the effective column to beam flexural strength ratio.

c) The accumulated effect of elongation of main beams was particularly severe at exterior columns which experienced significantly higher moments.

These observations suggest that the design of connections needs to be reviewed in global perspective of the structural response.

2. The lateral load resistance capacity of the indeterminate subassemblies was approximately 20 percent higher than the capacity based on the strength of isolated connections. This is attributed mainly to the increased flexural capacity of the main beams due to the presence of axial compression. The lateral load resistance of indeterminate subassemblies increased by 40 percent when a floor slab was added.

3. A larger width of slab contributed to the negative flexural capacity of the beams in indeterminate subassemblies compared to that in isolated connections.

4. The continuity of the test subassembly did not affect the overall energy dissipation capacity for both with and without floor slab cases.

5. The stiffness degradation in indeterminate subassemblies was more controlled and gradual compared to that of the isolated connections. The stiffness degradation in indeterminate subassemblies further improved when a floor slab was present.

6. The beneficial effect of the presence of transverse beams was also observed in connections of indeterminate subassemblies. In the presence of the floor slab, the confinement provided by the transverse beams was reduced and the joints suffered more shear damage.

7. Although the restriction to elongation of beams in indeterminate subassemblies created more adverse effects, it benefitted the interior connections by limiting the crack openings in the hinging regions at the faces of the joint.

8. Relocating the beam flexural hinges away from the face of the column in indeterminate subassembly protected the joints by increasing the volume of concrete in the joint diagonal compression strut, thus improving the overall joint shear strength. However, relocating the hinges

reduced the shear span to beam depth ratio which increased the shear demand on the beams which could cause early beam shear failure if not properly detailed.

9. The presence of a floor slab in interior connections decreased the slippage of beam top reinforcement and increased the slippage of beam bottom reinforcement passing through the joint. This suggests that the anchorage requirement for beam top and bottom reinforcement need not necessarily be equally restrictive when a floor slab is present.

10. Based on strain measurements across the slab in indeterminate subassemblies, a slab width equal to twice the main beam depth on each side of the beam was found most effective in resisting bending. The use of this slab width is suggested for calculations of beam negative flexural capacity and shear in the joints. The effective slab width at exterior connections reduced to one beam depth on each side of the beam when transverse beams cracked in torsion.

REFERENCES

112

REFERENCES

1. Hanson, N.W., and Connor, H.W., "Seismic Resistance of Reinforced Concrete Beam-Column Joints," Journal of the Structural Division, ASCE, Vol. 93, No. ST5, October 1967, pp. 533-560.

2. Wight, J.K., and Sozen, M.A., "Strength Decay of RC Columns Under Shear Reversals," Journal of the Structural Division, ASCE, Vol. 101, No. ST5, May 1975, pp. 1053-1065.

3. Gosain, N.K., Brown, R.M., and Jirsa, J.O., "Shear Requirements for Load Reversals on RC Members," Journal of the Structural Division, ASCE, Vol. 103, No. ST7, July 1977, pp. 1461-1476.

4. Uzumeri, S.M., "Strength and Ductility of Cast-in-Place Beam-Column Joints," Reinforced Concrete Structures in Seismic Zones, ACI Publication SP-53, Detroit 1977, pp. 293-350.

5. Scribner, C.F., and Wight, J.K., "Delaying Shear Strength Decay in Reinforced Concrete Flexural Members Under Large Load Reversal," Report No. UMEE 78R2, Department of Civil Engineering, The University of Michigan, Ann Arbor, May 1978.

6. Paulay, T., Park, R., and Priestley, J.N., "Reinforced Concrete Beam-Column Joints Under Seismic Actions," ACI Journal, November 1978, pp. 585-593.

7. Viwathanatepa, S. Popov, E.P., and Bertero, V.V., "Seismic Behavior of Reinforced Concrete Interim Beam-Column Subassemblages," Report No. UCB/EERC-79/14, The University of California, Berkeley, June 1979.

8. Bertero, V.V., Popov, E.P., and Forzani, B., "Seismic Behavior of Lightweight Concrete Beam-Column Subassemblages," ACI Journal, January-February 1980, pp. 44-52.

9. Meinheit, D.F., and Jirsa, J.O., "Shear Strength of R/C Beam-Column Connections," Journal of the Structural Division, ASCE, Vol. 107, No. ST11, November 1981, pp. 2227-2244.

10. Durrani, A.J., and Wight, J.K., "Experimental and Analytical Study of Internal Beam to Column Connections Subjected to Reversed Cyclic Loading," Report No. UMEE 82R3, Department of Civil Engineering, The University of Michigan, Ann Arbor, July 1982.

11. Ehsani, M.R., and Wight, J.K., "Behavior of External Reinforced Concrete Beam to Column Connections Subjected to Earthquake Type Loading," Report No. UMEE 82R5, Department of Civil Engineering, The University of Michigan, Ann Arbor, July 1982.

12. Murray, P.A., "A Study of Beam-Column Joints Under Seismic Loads: Component Test Versus Building Response," MS Thesis, Department of Civil Engineering, The University of Texas at Austin, August 1982.

13. Suzuki, N., Otani, S., and Aoyama, H., "The Effective Width of Slabs in Reinforced Concrete Structures," Transaction of the Japan Concrete Institute, Vol. 5, 1983, pp. 309-316.

14. Leon, R.T., "The Effect of Floor Member Size on the Behavior of Reinforced Concrete Beam-Concrete Joints," Proceedings, 8th World Conference on Earthquake Engineering, San Francisco, July 1984, pp. 445-452.

15. Kanada, K., Kondo, G., Fujii, S., and Morita, S., "Relation Between Beam Bar Anchorage and Shear Resistance at Exterior Beam-Column Joints," Transaction of the Japan Concrete Institute, Vol. 6, 1984, pp. 433-440.

16. Zerbe, H.E., and Durrani, A.J., "Effect of a Slab on the Behavior of Exterior Beam to Column Connections," Report No. 30, Department of Civil Engineering, Rice University, Houston, Texas, March 1985.

17. Abdel-Fattah, B.A., and Wight, J.K., "Experimental Study of Moving Beam Plastic Hinging Zones for Earthquake Resistant Design of R/C Buildings," Report No. UMCE 85-11, Department of Civil Engineering, The University of Michigan, December 1985.

18. Joglekar, M., Murray, P., Jirsa, J., and Klingner, R., "Full Scale Tests of Beam-Column Joints," Earthquake Effects on Reinforced Concrete Structures, U.S.-Japan Research, ACI Publication SP-84, Detroit 1985, pp. 271-304.

19. Kanada, K., Fujii, S., and Morita, S., "Effect of Joint Shear Reinforcement on Behaviors of Exterior Beam-Column Joints under Reversed Cyclic Loadings," Transaction of the Japan Concrete Institute, Vol. 7, 1985, pp. 559-566.

20. Otani, S., Kitayama, K., and Aoyama, H., "Beam Bar Bond Requirements for Interior Beam-Column Connections," Proceedings of the International Symposium on Fundamental Theory of Reinforced and Prestressed Concrete, Nanjing Institute of Technology, China, September, 1986.

21. Bastos, J.N., Jirsa, J.O., and Klingner, R.E., "The Role of Subassemblage Tests in Modeling Connections of Full-Scale Structures," Proceedings of the 8th European Conference on Earthquake Engineering, Vol. 4, Lisbon 1986, pp. 7.4/65-72.

22. Ehsani, M.R., Mousa, A.E., and Vallenilla, C.R., "Comparison of Inelastic Behavior of Reinforced Ordinary- and High-Strength Concrete Frames," ACI Structural Journal, March-April 1987, pp. 161-169.

23. Cheung, P., Paulay, T., and Park, R., "A Reinforced Concrete Beam-Column Joint of a Prototype One-Way Frame with Floor Slab Designed for Earthquake Resistance," Research Report 87-6, Department of Civil Engineering, University of Canterbury, Christchurch, New Zealand, July 1987.

24. Fujii, S., and Morita, S., "Behavior of Exterior Reinforced Concrete Beam-Column-Slab Subassemblages under Bi-Directional Loading," Paper Prepared for the U.S.-N.Z.-Japan-China Seminar on the Design of R.C. Beam-Column Joints for Earthquake Resistance, University of Canterbury, Christchurch, New-Zealand, August, 1987.

116

25. Kitayama, K., Otani, S., and Aoyama, H., "Behavior of Reinforced Concrete Beam-Column Connections with Slabs," Paper Prepared for the U.S.-N.Z.-Japan-China Seminar on the Design of R.C. Beam-Column Joints for Earthquake Resistance, University of Canterbury, Christchurch, New-Zealand, August, 1987.

26. Hawkins, N.M., Lin, I., and Ueda, T., "Anchorage of Reinforcing Bars for Seismic Forces," ACI Structural Journal, September-October 1987, pp. 407-418.

27. Kurose, Y., Guimaraes, G.N., Liu, Z., Kreger, M.E., and Jirsa, J.O., "Study of Reinforced Concrete Beam-Column Joints Under Uniaxial and Biaxial Loading," PMFSEL Report No. 88-2, Department of Civil Engineering, The University of Texas at Austin, December 1988.

28. Wolfgram-French, C., and Boroojerdi, A., "Contribution of R/C Floor Slab in Resisting Lateral Loads," Journal of Structural Engineering, ASCE, Vol. 115, No. 1, January 1989, pp. 1-18.

29. Miranda, E., and Bertero, V.V., "The Mexico Earthquake of September 19, 1985 - Performance of Low-Rise Buildings in Mexico City," Earthquake Spectra, Vol. 5, No. 1, February 1989, pp. 121-143.

30. "The Behavior of Reinforced Concrete Buildings Subjected to the Chilean Earthquakes of May 1960," Advanced Engineering Bulletin, No. 6, Portland Cement Association, Skokie, Illinois,

31. Fintel, M. "Behavior of Structures in the Caracas Earthquake," Civil Engineering, ASCE, February, 1968, pp. 42-46.

32. Nielsen , N. N., and Nakagawa, K., "The Tokachi-Oki Earthquake, Japan, May 1968," IISEE Earthquake Report No. 2, Tokyo, June 1968.

33. Lew, H. S., Leyendecker, E. V., and Dekkeys, R. D., "Engineering Aspects of the 1971 San Fernando Earthquake," National Bureau of Standards, Building Science Series 40, Dec. 1971.

34. ACI-ASCE Committee 352, "Recommendations for Design of Beam-Column Joints in Monolithic Reinforced Concrete Structures," ACI Journal, Vol. 73, No. 7, July 1976, pp. 375-393.

35. ACI-ASCE Committee 352, "Recommendations for Design of Beam-Column Joints in Monolithic Reinforced Concrete Structures," ACI Journal, Vol. 82, No. 3, May-June 1985, pp. 266-283.

36. NZS 3101: 1982, "Code of Practice for the Design of Concrete Structures," Standards Association of New Zealand, Wellington, 1982.

37. ACI Committee 318, "Building Code Requirements for Reinforced Concrete (318-83)," American Concrete Institute, Detroit 1983.

38. ACI Committee 318, "Commentary on Building Code Requirements for Reinforced Concrete (ACI 318-83)," American Concrete Institute, Detroit 1983.

39. Zhang, L., and Jirsa, J.O., "A Study of Shear Behavior of Reinforced Concrete Beam-Column Joints," PMFSEL Report No. 82-1, Department of Civil Engineering, The University of Texas at Austin, February 1982.

40. Popov, E.P., and Bertero, V.V., "Hysteresis Behavior of Ductile Moment Resisting Reinforced Concrete Frame Components," Report No. EERC 75/16, The University of California, Berkeley, April 1975.

41. Hawkins, N.M., Kobayashi, A.S., and Fourney, M.E., "Reversed Cyclic Loading Bond Deterioration Tests," Structures and Mechanics Report No. SM 57-5, Department of Civil Engineering, University of Washington, Seattle, November, 1975.

42. Zhu, S., and Jirsa, J.O., "A Study of Bond Deterioration in Reinforced Concrete Beam-Column Joints," PMSFEL Report No. 83-1, Department of Civil Engineering, The University of Texas at Austin, July 1983.

118

43. Park, R., "Anchorage of Beam Longitudinal Bars in Beam-Interior Column Joints," Paper Prepared for the 4th. U.S.-N.Z.-Japan-China Seminar on the Design of R.C. Beam-Column Joints for Earthquake Resistance, Hawaii, May 24-26, 1989.

44. Pantazopoulou, S.J., and Moehle, J.P., "The Effect of Slabs on the Flexural Behavior of Beams," Report No. UCB/EERC-87/17, The University of California, Berkeley, October, 1987.

45. Jirsa, J.O., "Beam-Column Joints: Irrational Solutions to a Rational Problem," Significant Developments in Engineering Practice and Research, ACI Publication SP-72, Detroit 1981, pp. 177-198.

46. United States/Japan Joint Technical Coordinating Committee, "Interim Summary Report of Tests of 7-Story RC Building," Journal of Structural Engineering, ASCE, Vol. 110, No. 10, October 1984, pp. 2393-2411.

47. Seckin, M., "Post Yield Interaction of Members in a Moment-Resisting Reinforced Concrete Frame," Proceedings of the 8th European Conference on Earthquake Engineering, Vol. 4, Lisbon 1986, pp. 7.3/41-48.

48. Kokusho, S., Hayashi, S., Wada, A., and Sakata, H., "Elastic and Plastic Behavior of Reinforced Concrete Beam in Consideration of Axial Restriction Effect of Deformation," Report of the Research Laboratory of Engineering Materials, Tokyo Institute of Technology, No. 13, 1988, Nagatsuta, Yokohama 227, Japan, pp. 253-270

49. Paulay, T., and Park, R., "Joints in Reinforced Concrete Frames Designed for Earthquake Resistance," Research Report 84-9, Department of Civil Engineering, University of Canterbury, Christchurch, New Zealand, June 1984.

50. Abdel-Fattah, B., and Wight, J.K., "Study of Moving Beam Plastic Hinging Zones for Earthquake-Resistant Design of R/C Buildings," ACI Structural Journal, V. 84, No. 1, January-February 1987, pp. 31-39.

51. Ammerman O. V., and Wolfgram-French, C., "R/C Beam-Column-Slab Subassemblages Subjected to Lateral Loads," Journal of Structural Engineering, ASCE, Vol. 115, No. 6, June 1989, pp. 1289-1308.

52. Yalcin, U., Zerbe, H.E., and Durrani, A.J., "Seismic Resistance of Connections with Beams Restrained Against Free Elongation," Proceedings, 4th U.S. National Conference on Earthquake Engineering, Palm Spring, California, May 20-24, 1990

53. Durrani, A.J., and Wight, J.K., "Earthquake Resistance of Reinforced Concrete Interior Connections Including a Floor Slab," ACI Structural Journal, September-October 1987, pp. 400-406.

54. Ehsani, M.R., and Wight, J.K., "Effect of Transverse Beams and Slab on the Behavior of Reinforced Concrete Beam-to-Column Connections," ACI Journal, March-April 1985, pp. 188-195.

55. Durrani, A.J., and Zerbe, H.E., "Seismic Resistance of R/C Exterior Connections with Floor Slab," Journal of Structural Engineering, ASCE, Vol. 113, No. 8, August 1987, pp. 1850-1864.

56. Pantazopoulou, S.J., Moehle, J.P., and Shahrooz, B.M., "Simple Analytical Model for T-Beam in Flexure," Journal of Structural Engineering, ASCE, Vol. 114, No. 7, July 1988, pp. 1507-1523.

57. Paulay, T., "Mechanisms and Magnitudes of Slab Participation in Two-Way Frames," Paper Prepared for the 4th. U.S.-N.Z.-Japan-China Seminar on the Design of R.C. Beam-Column Joints for Earthquake Resistance, Hawaii, May 24-26, 1989.

58. Cheung, P., Paulay, T., and Park, R., "Interior and Exterior Reinforced Concrete Beam-Column Joint of a Prototype Two-Way Frame with Floor Slab Designed for Earthquake Resistance," Research Report 89-2, Department of Civil Engineering, University of Canterbury, Christchurch, New Zealand, March 1989.

59. Hsu, Thomas T.C., "Torsion of Reinforced Concrete," Van Nostrand Reinhold (Publisher), 1984.

120

F I G U R E S

Prototype Structure

Exterior Connection

Multiple Connection

Interior Connection
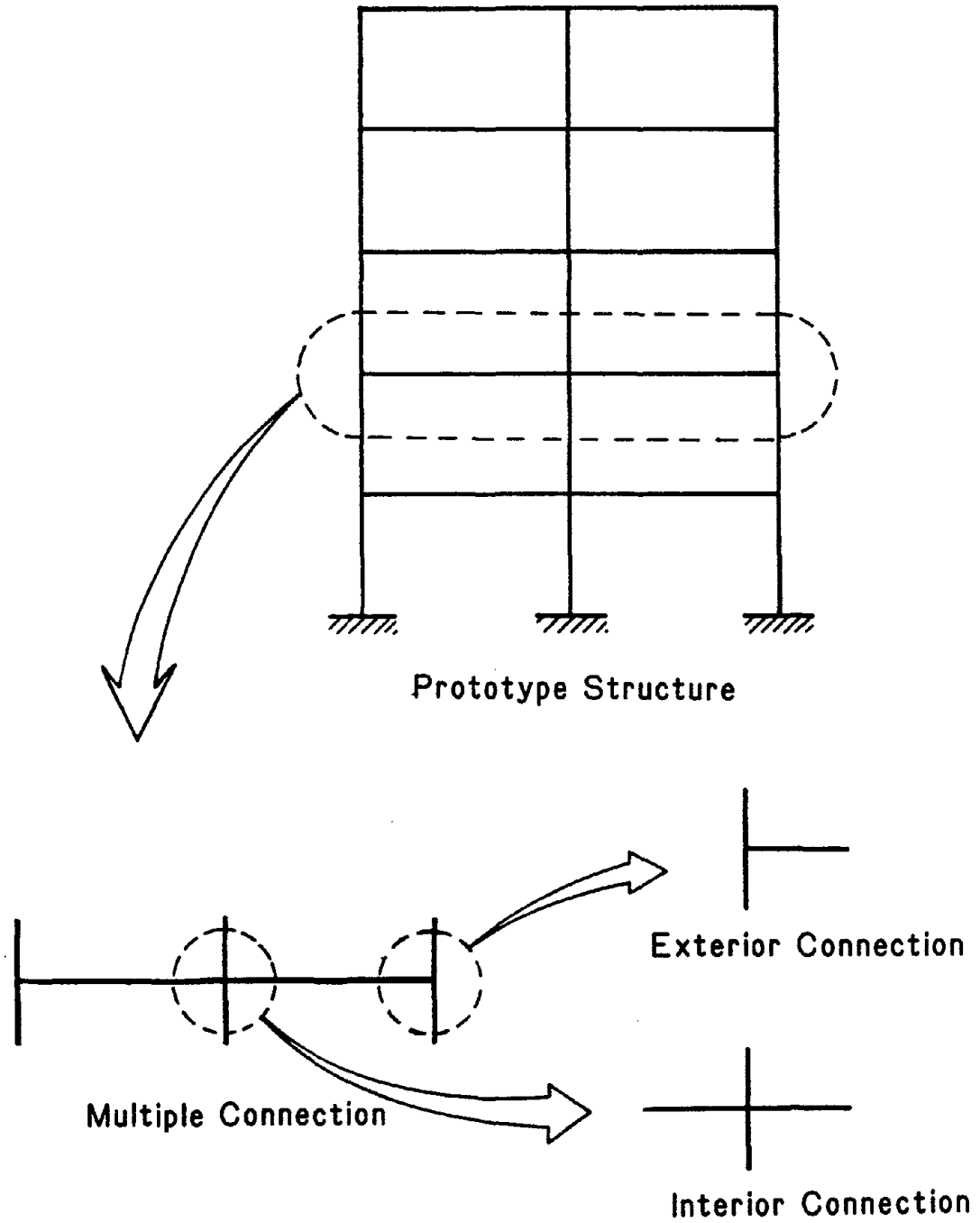
Fig. 2.1 Prototype Frame and Test Subassemblies
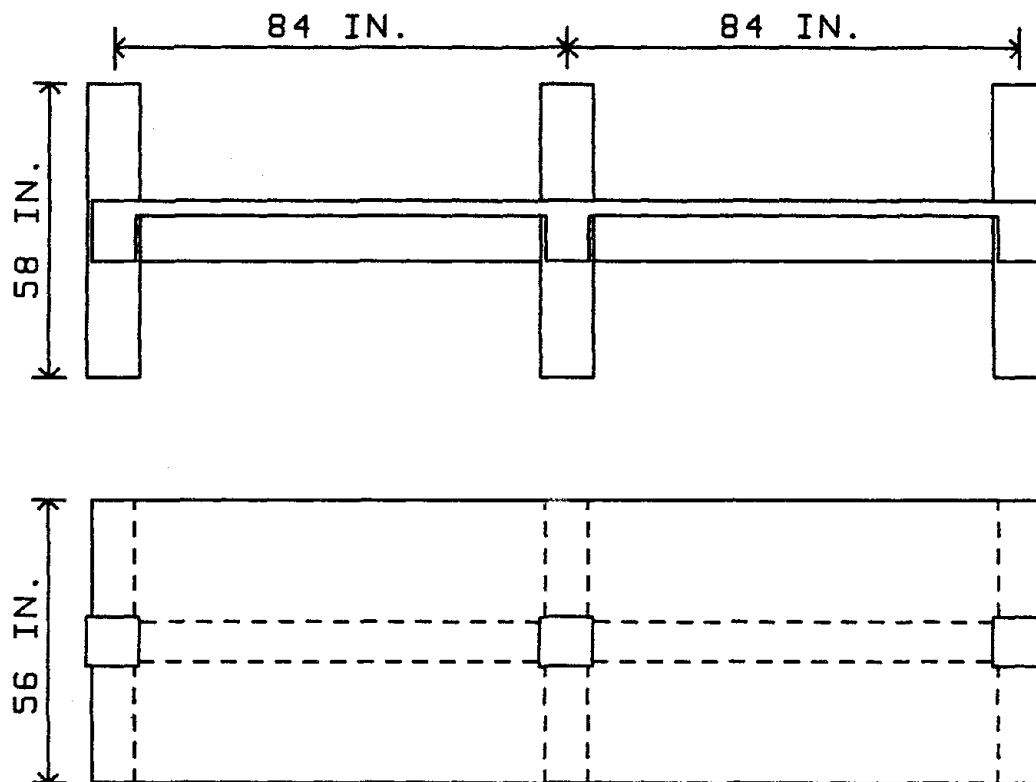
Fig. 2.2 Specimen Configuration
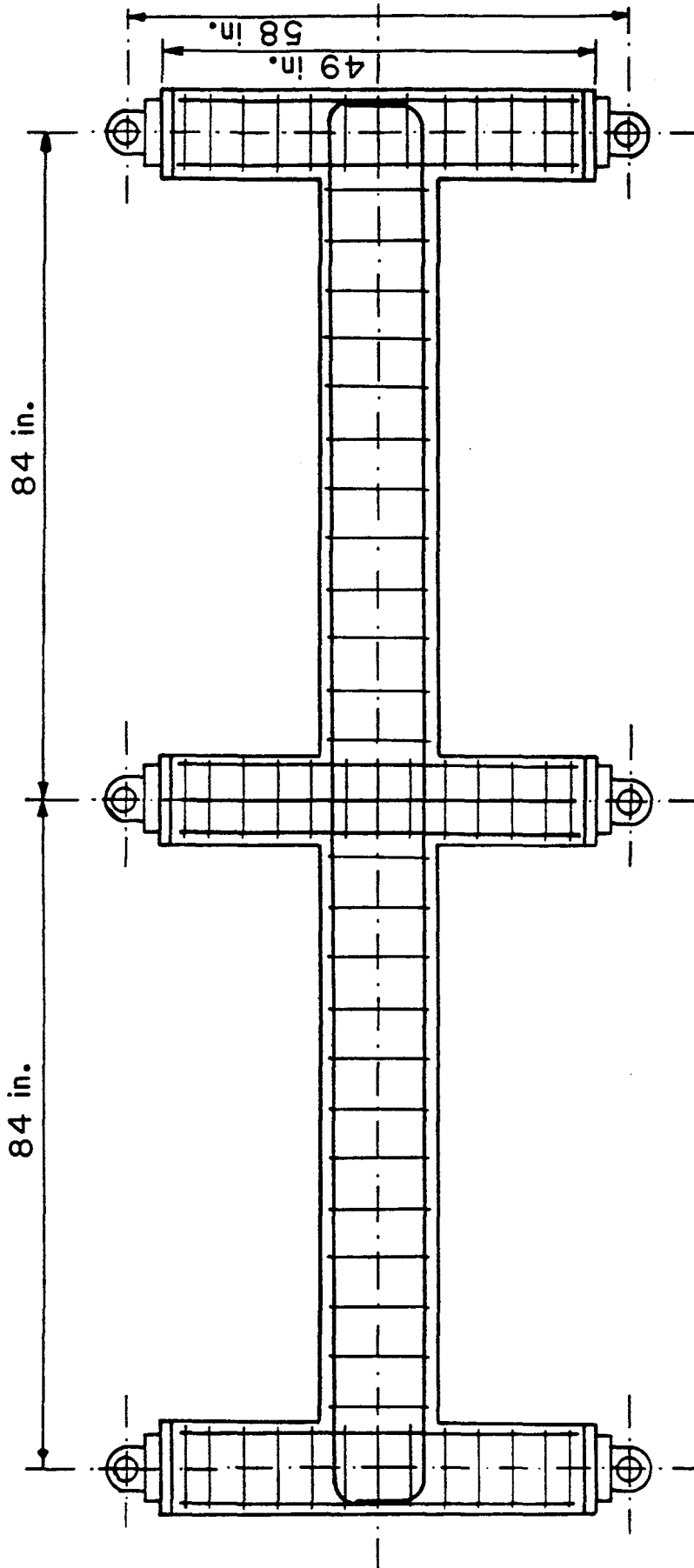
Fig. 2.3 Typical Reinforcement Detail of the test Subassembly

126

Note: 1" clear cover in all sections

Main Beam

Beam with a Slab

Exterior Column
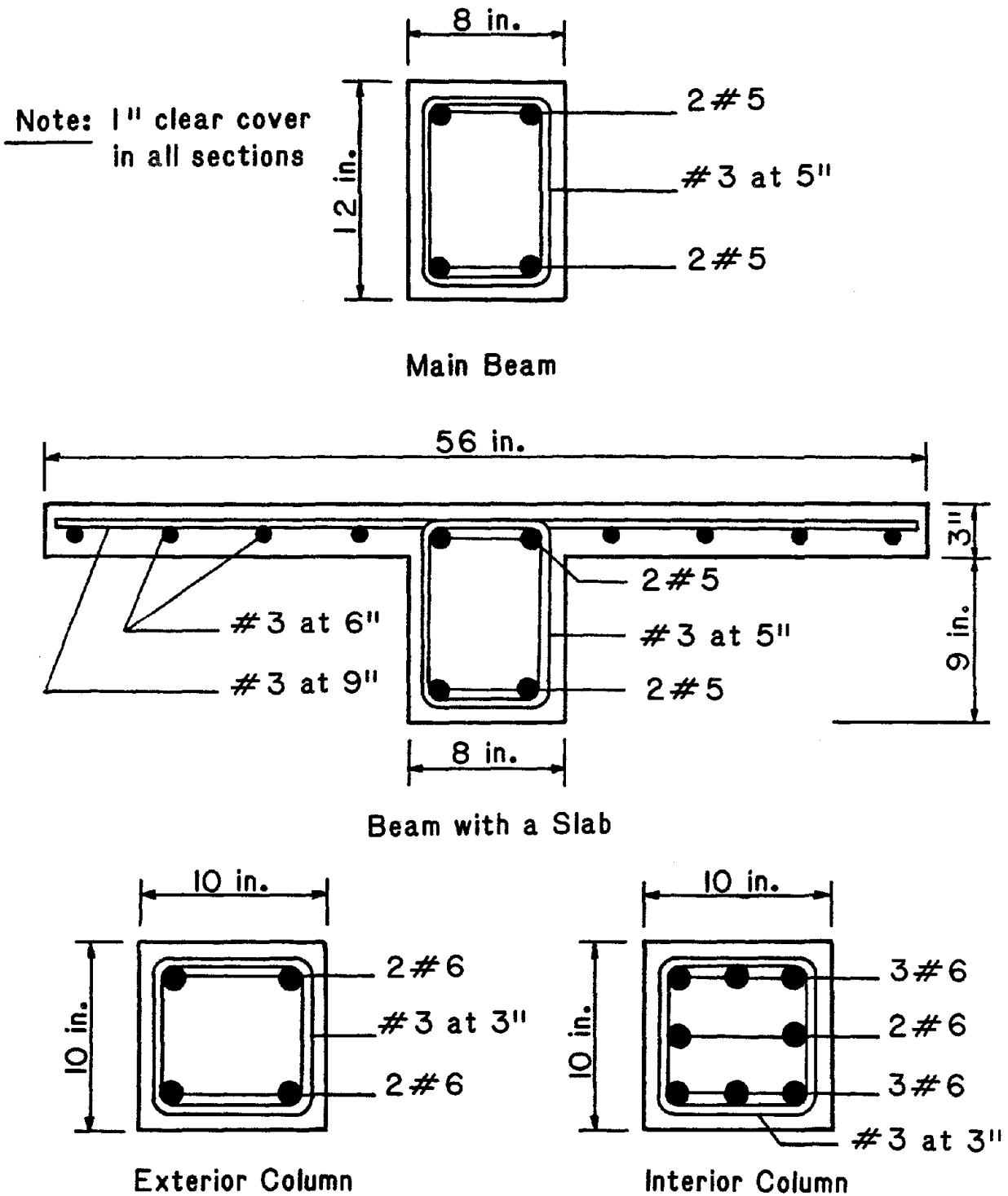
Interior Column

Fig. 2.4(a)   Cross-Sections of Main Beams and Columns
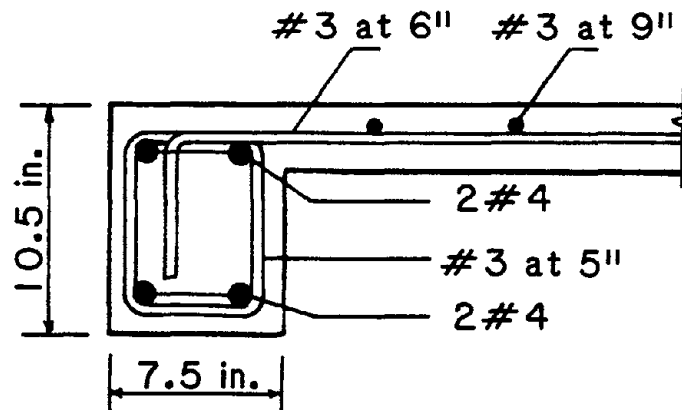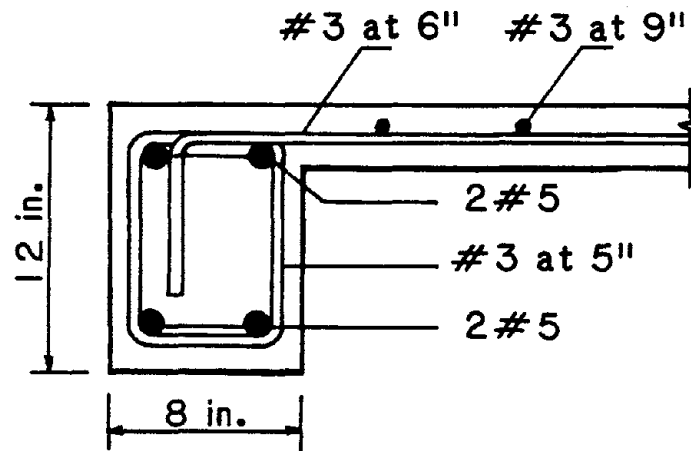
Fig. 2.4(b) Cross-Sections of Transverse Beams

128

Section: A—A

8 in.

12 in.

2#3

#3 at 5"

2#4

Section: B—B

8 in.

12 in.

2#3
2#4

#3 at 5"

4#4
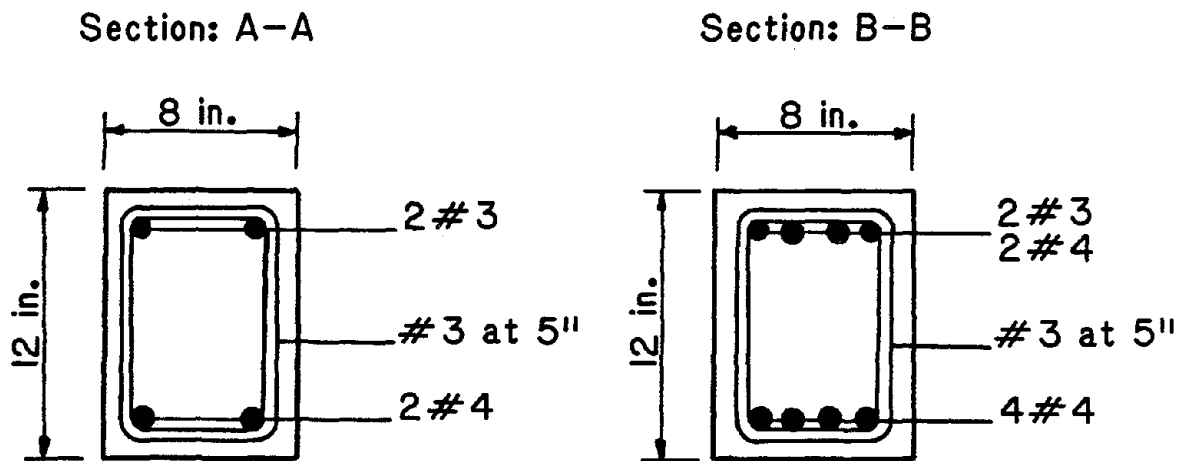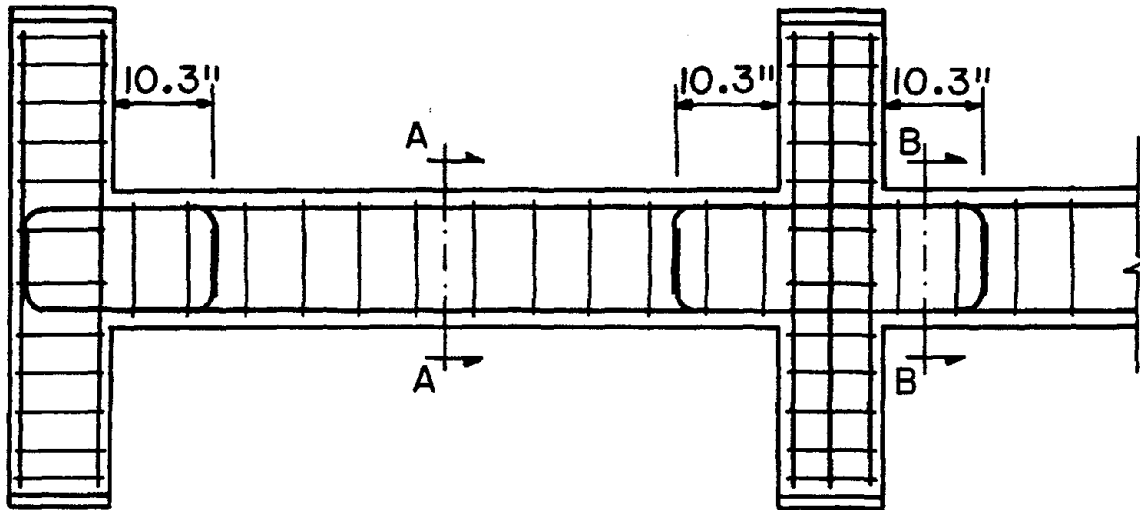
Fig. 2.5 Reinforcement Detail for Relocating Flexural Hinge
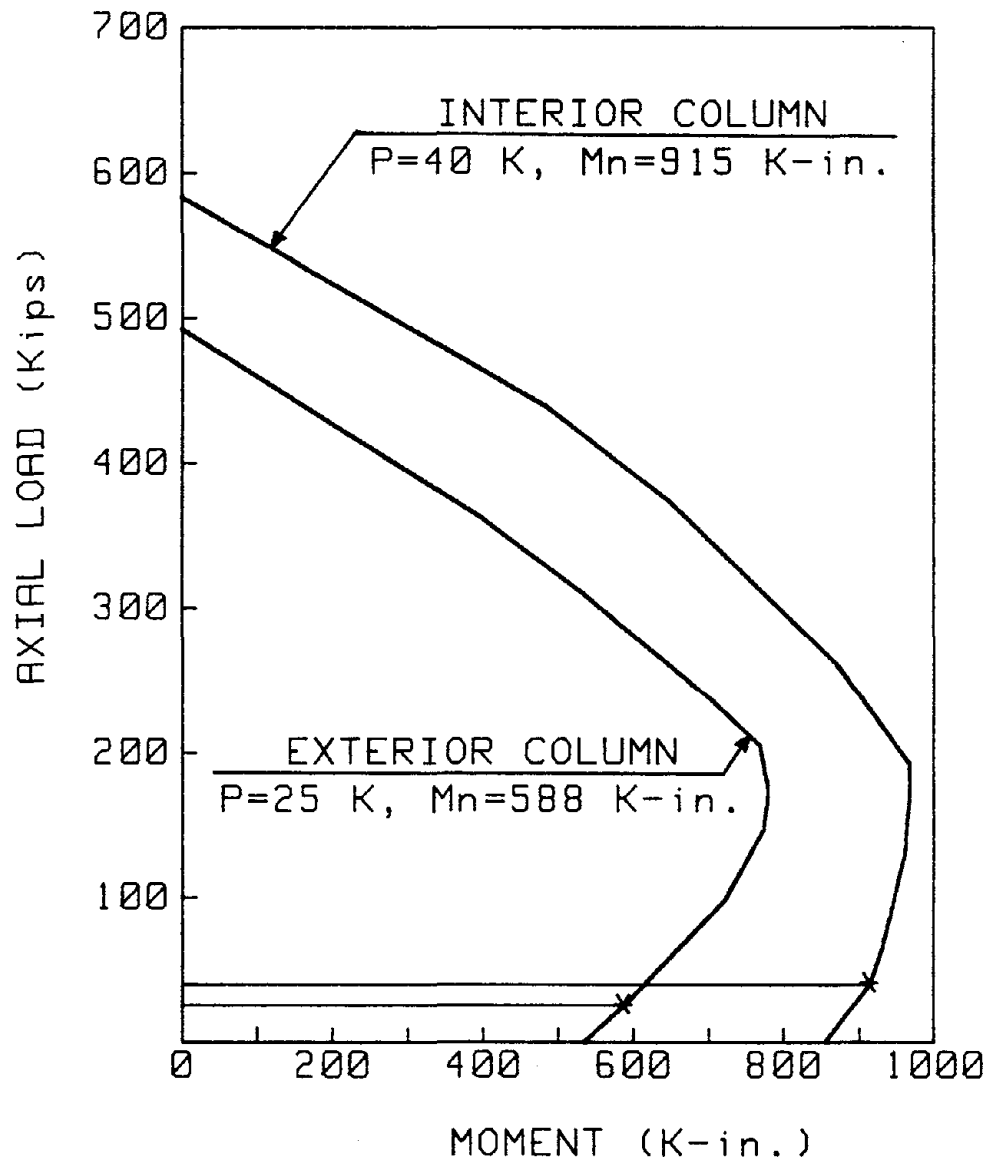
Fig. 2.6 Column Axial Load-Moment Interaction Diagrams

130
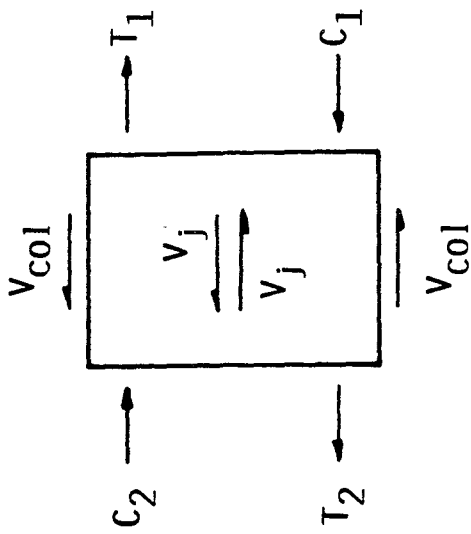
INTERIOR JOINT

$V_j = T_1 + C_2 - V_{col}$

$T_1 = A'_s (1.25) f_y$

$C_2 = T_2 = A_s (1.25) f_y$

EXTERIOR JOINT
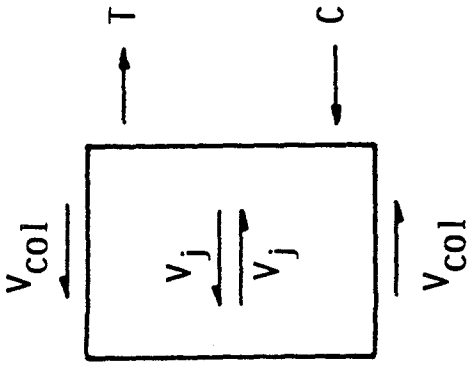
$V_j = T - V_{col}$

$T = A'_s (1.25) f_y$

Fig. 2.7 Shear in the Joints
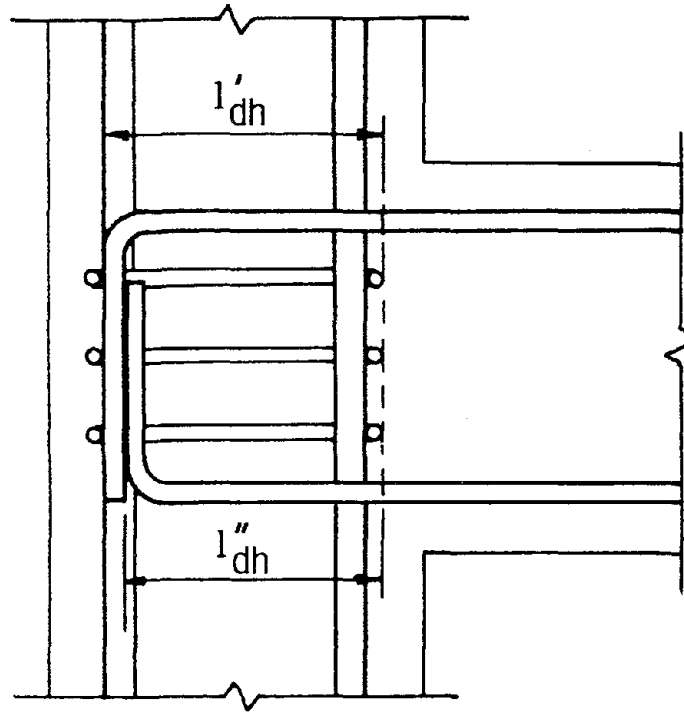
l'_{dh} = Development Length for Beam Top Reinforcement

l''_{dh} = Development Length for Beam Bottom Reinforcement

Fig. 2.8 Development Length in Exterior Joint

STRONG
SECTION

WEAK SECTION

STRONG
SECTION

10.3"

10.3"

74"

1032
1030

795 kip-in

Negative Flexural Capacity

Maximum Applied Moment

428 kip-in

Positive Flexural Capacity

664
723
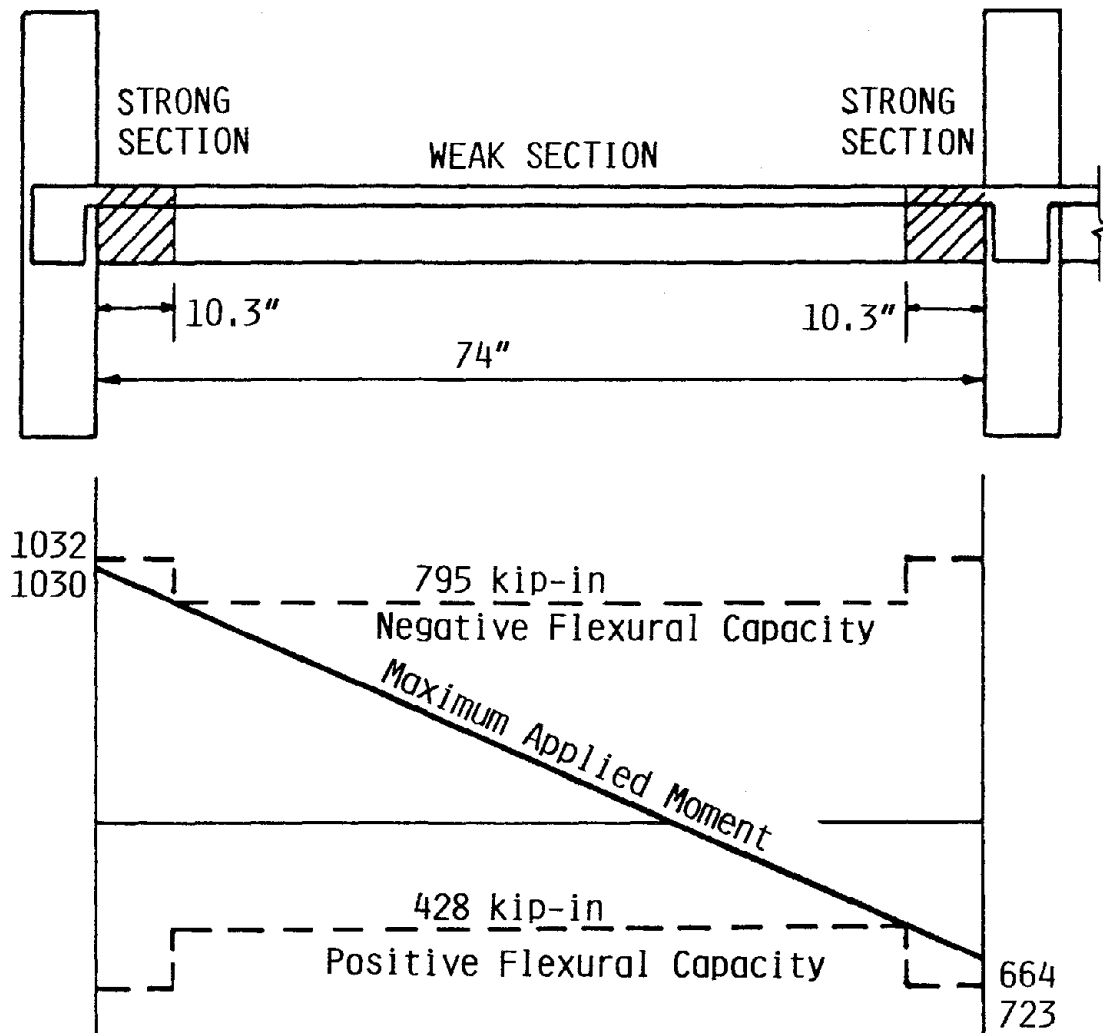
Fig. 2.9 Applied Moment vs. Beam Strength of Specimen CS3
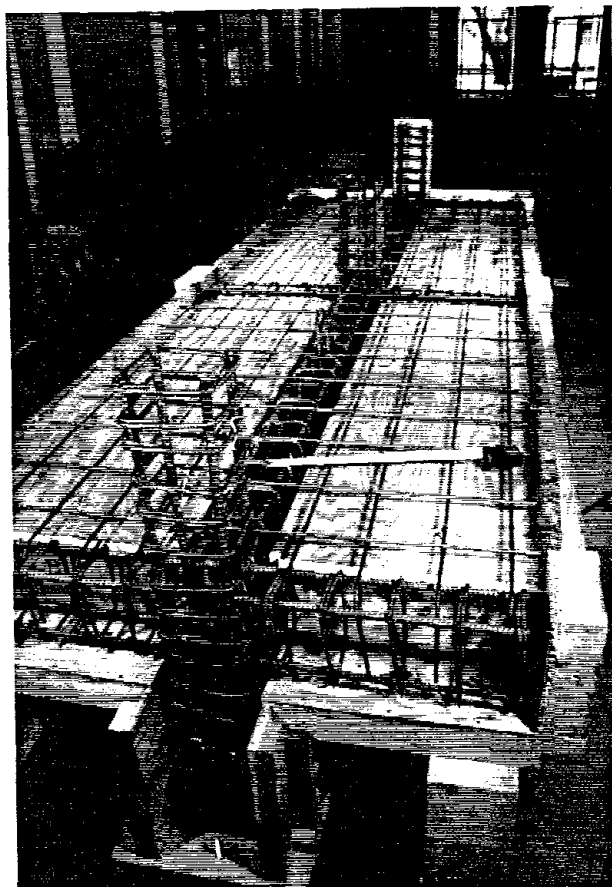
Fig. 2.10   Specimen CS1 Before Casting

134
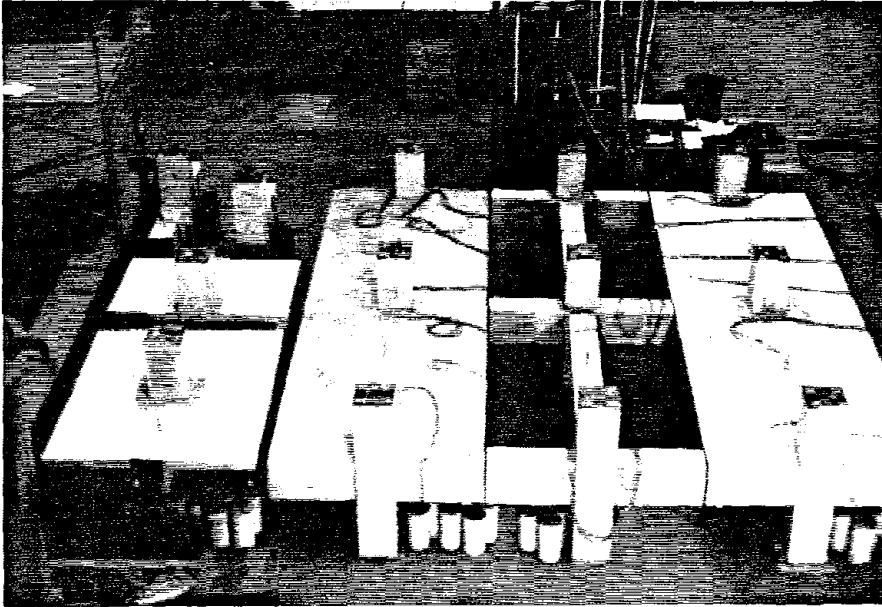
Fig. 2.11 Specimens Stored in the Laboratory
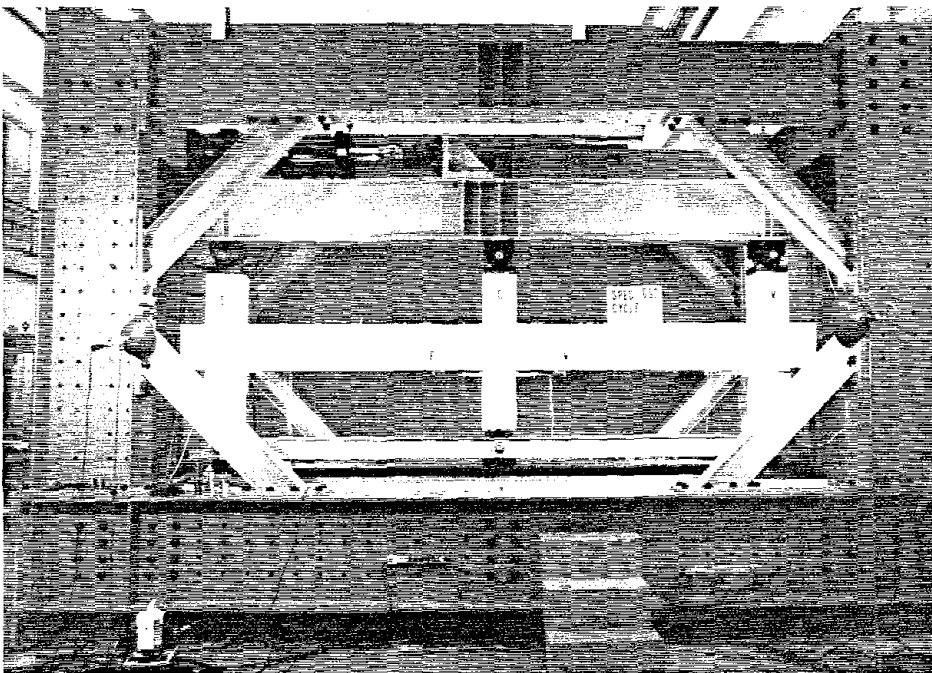
Fig. 2.12 Test Set-Up
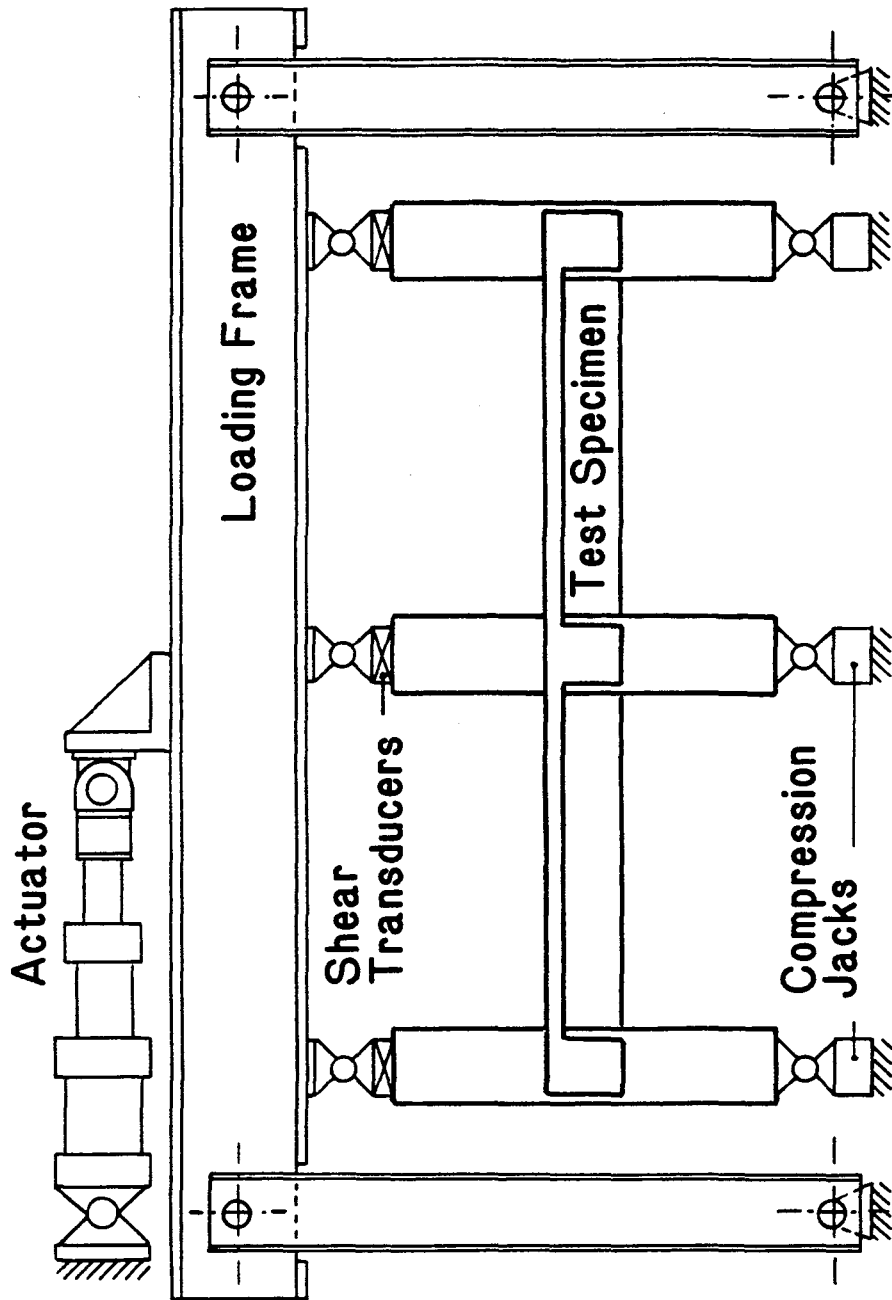
Fig. 2.13 Schematic of Loading Arrangement
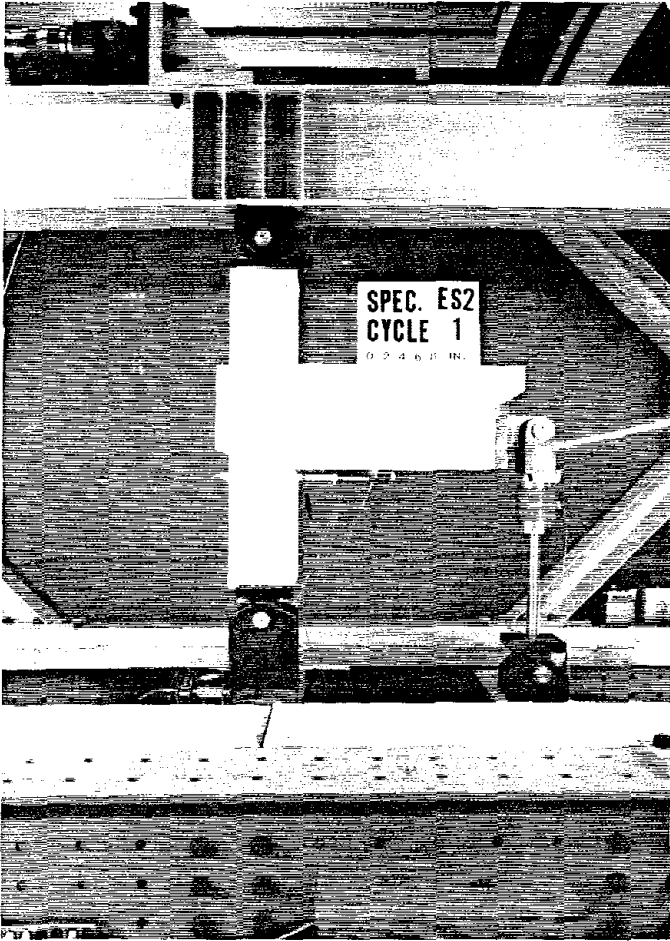
Fig. 2.14   Beam-End Connection Assembly
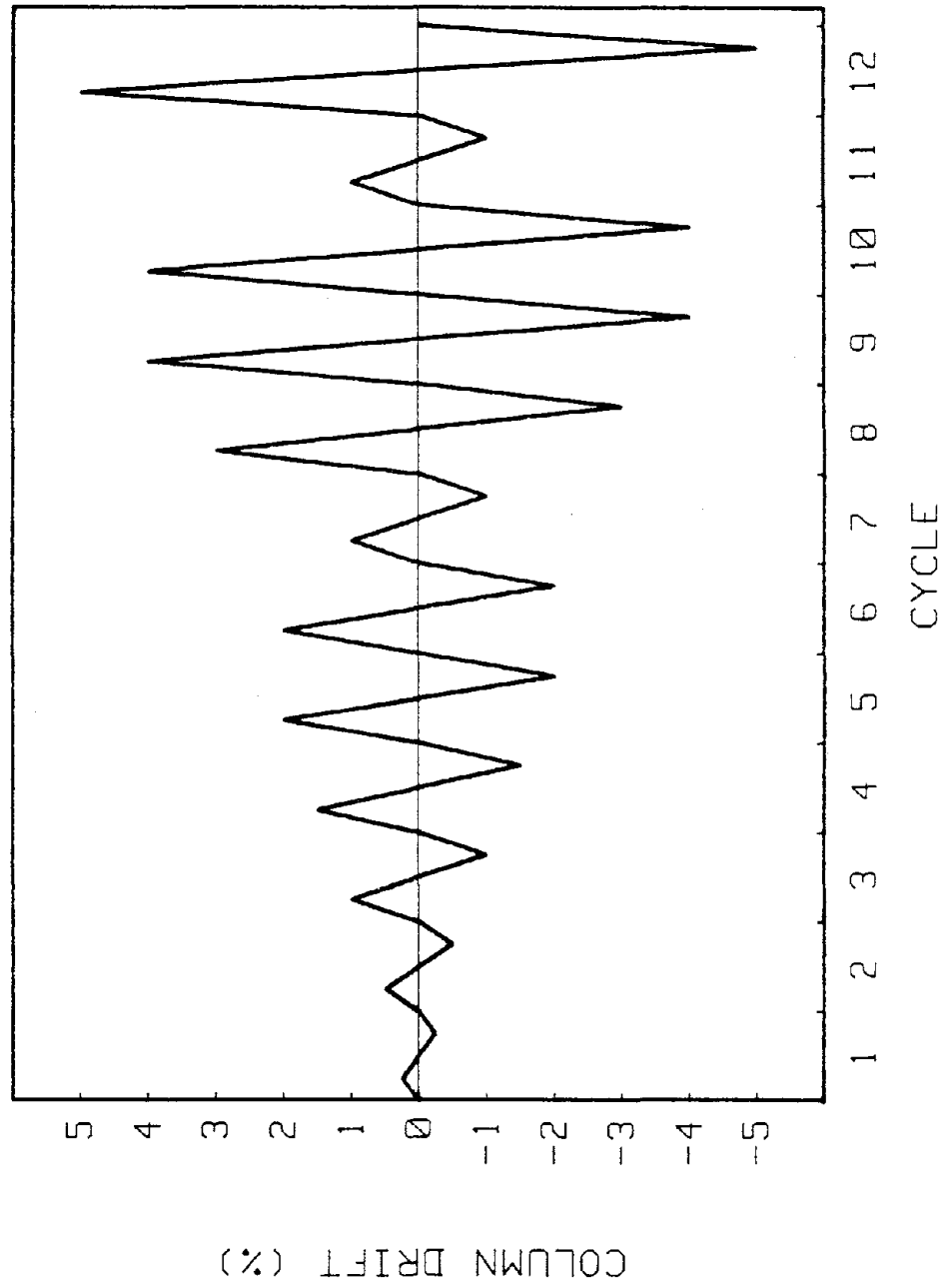
Fig. 2.15 Cyclic Displacement Routine
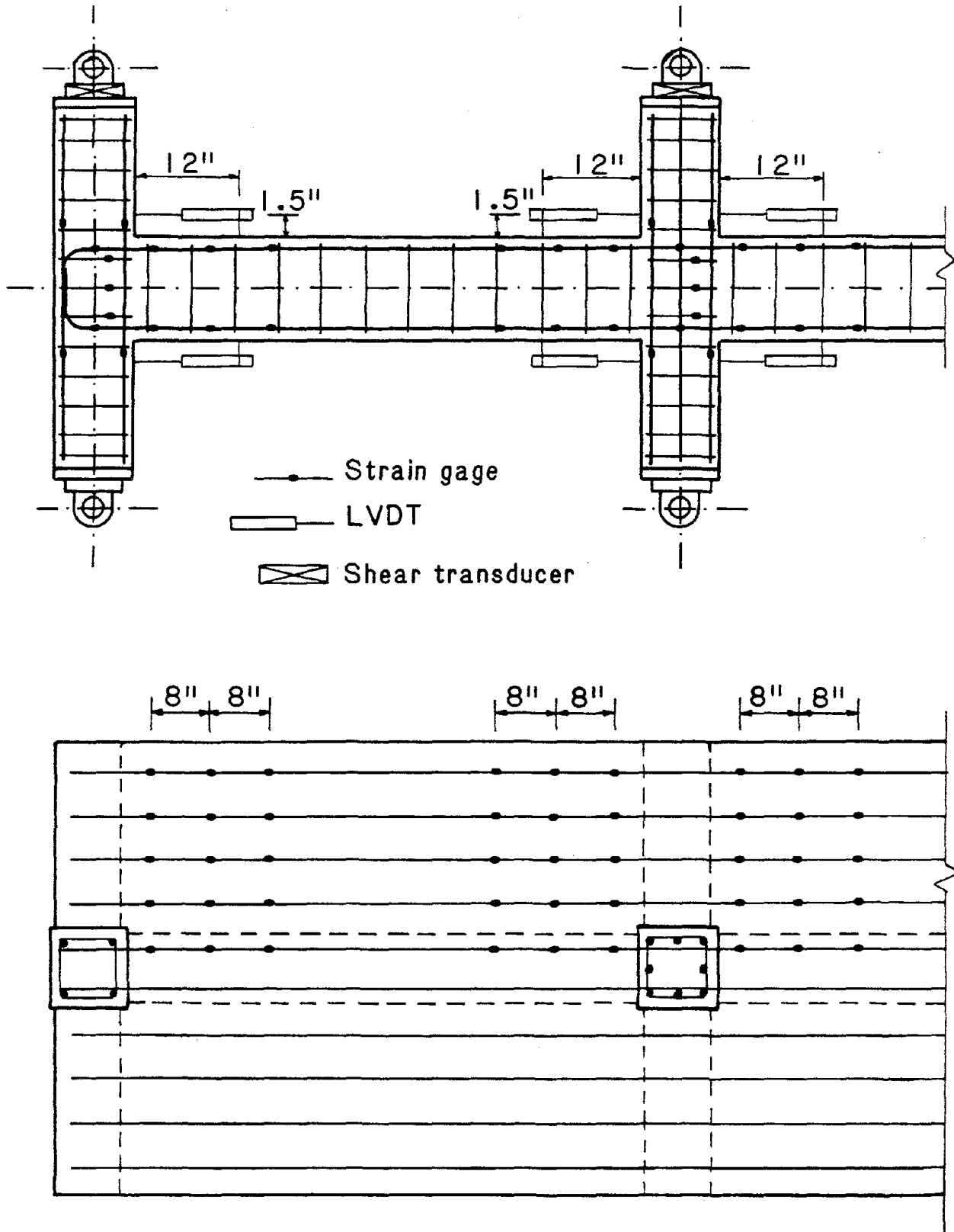
Fig. 2.16   Instrumentation Detail
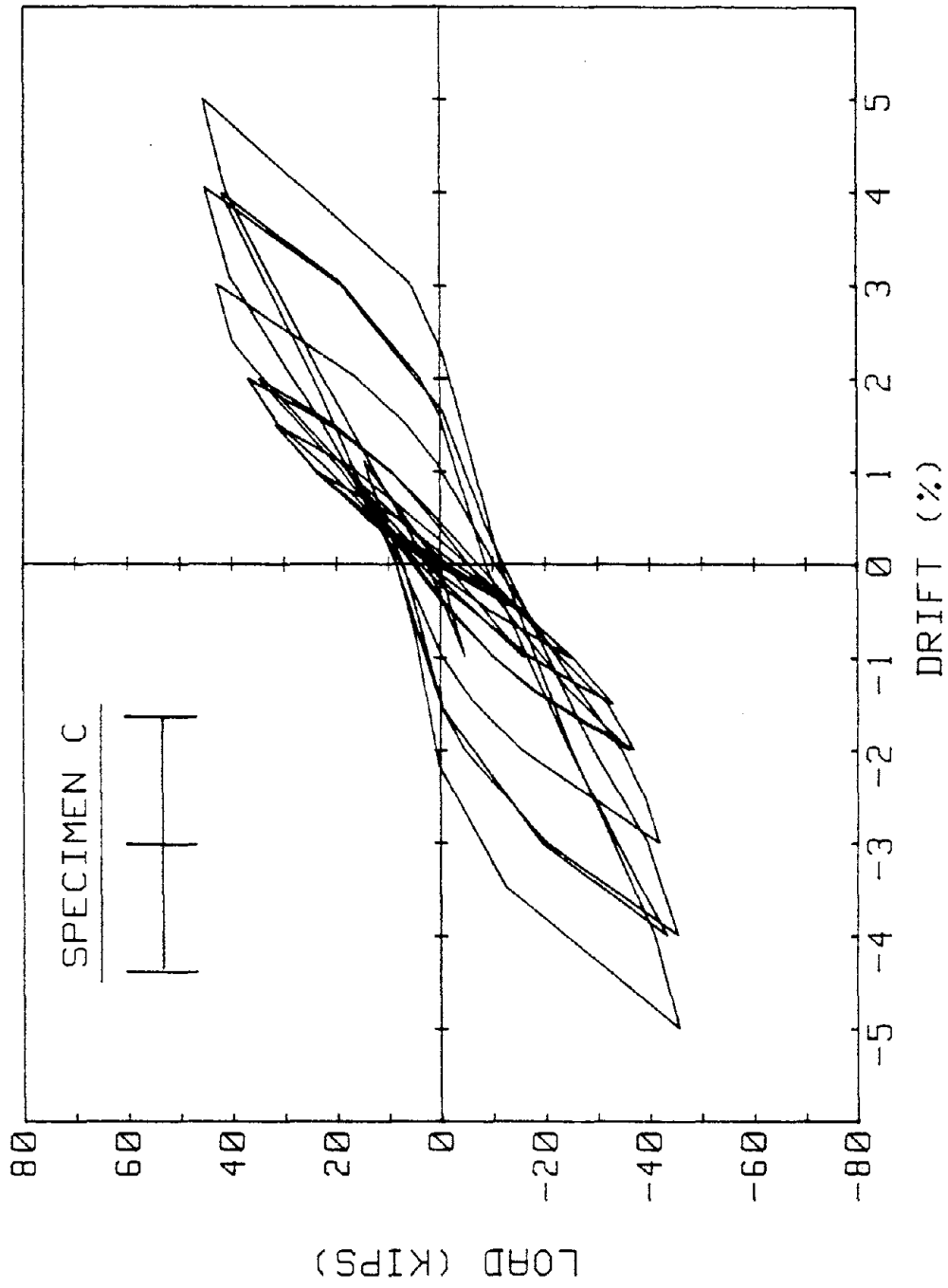
Fig. 3.1(a) Load vs. Drift Plots of Specimen C
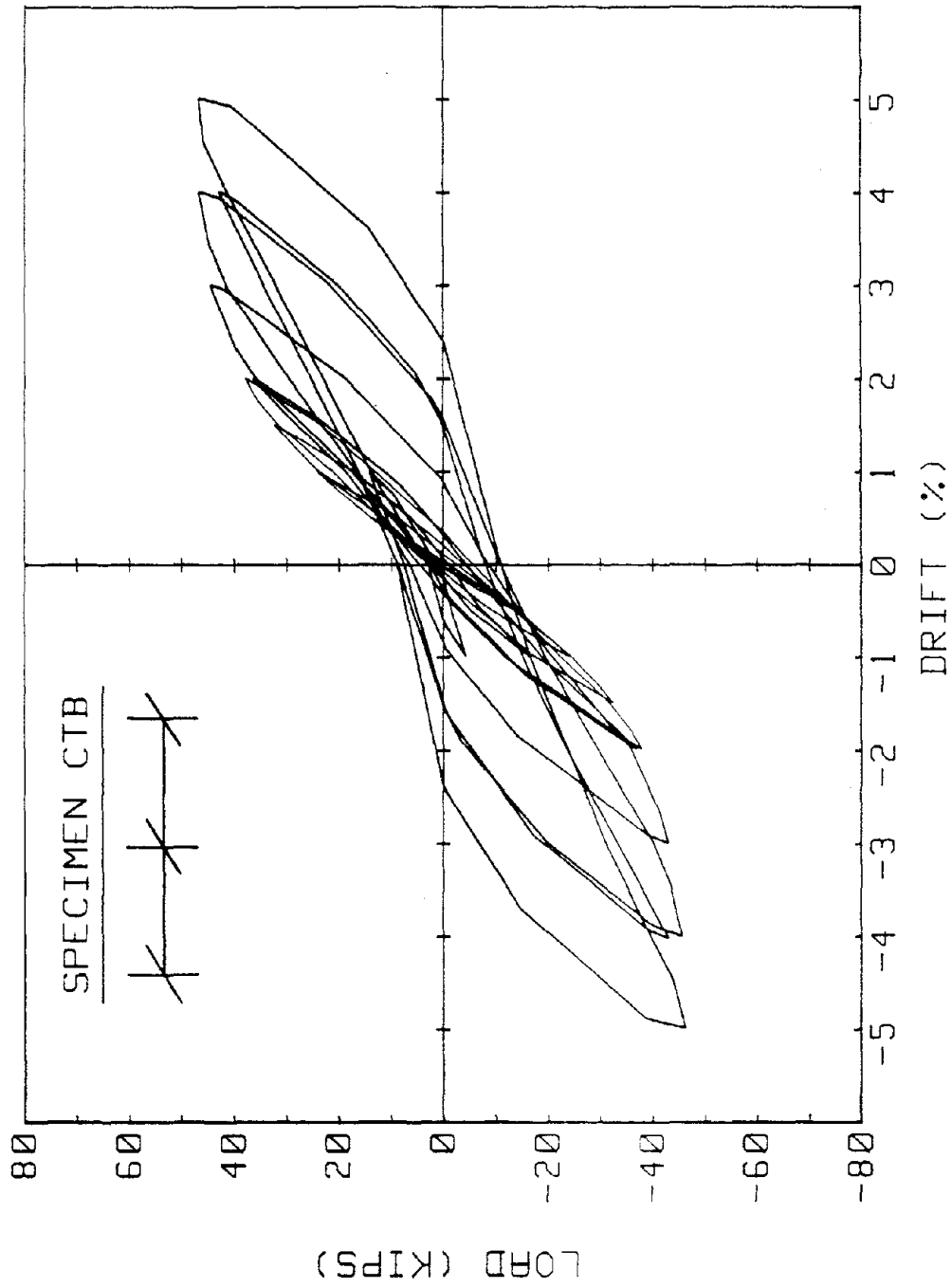
Fig. 3.1(b) Load vs. Drift Plots of Specimen CTB
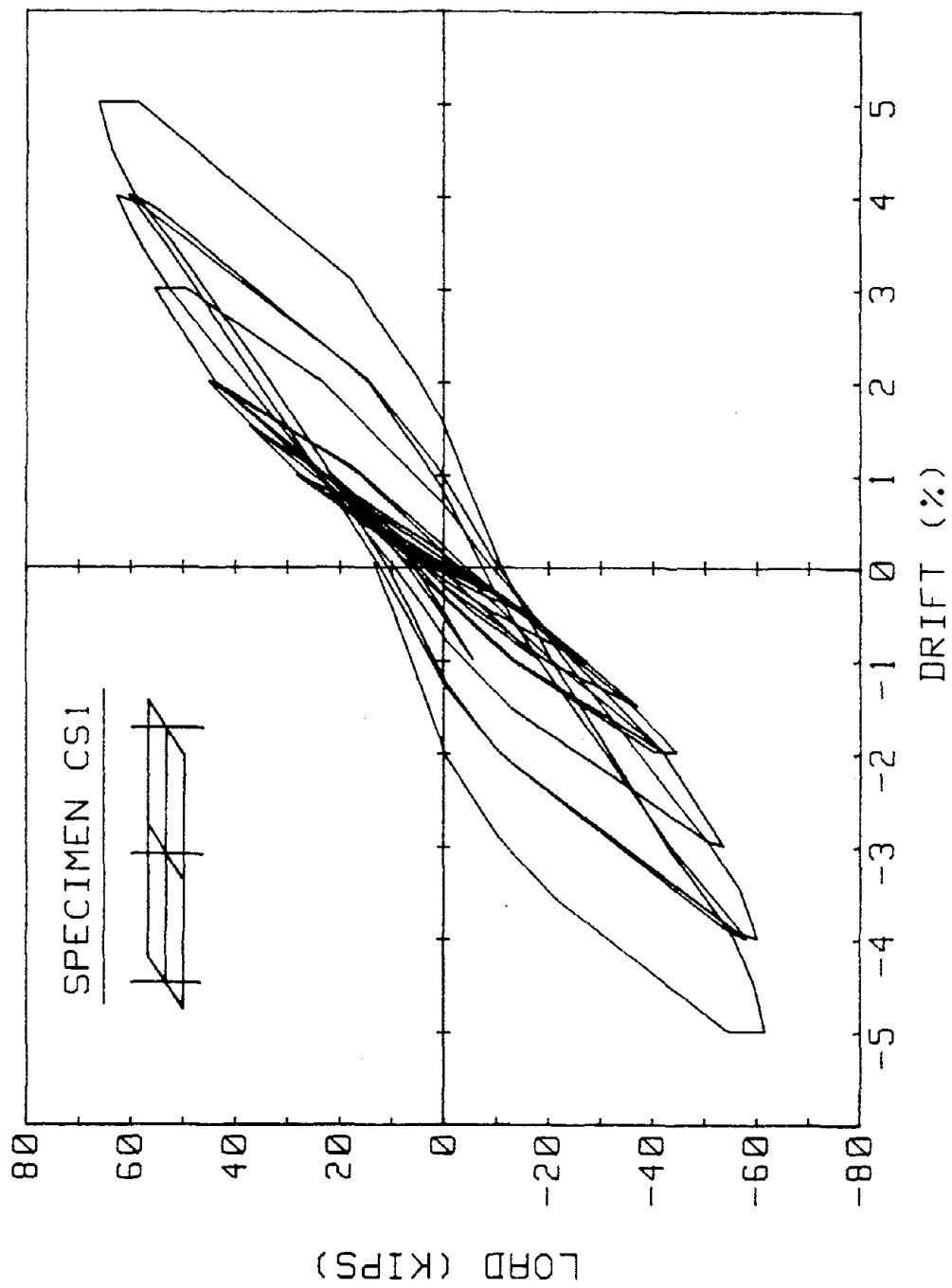
Fig. 3.1(c) Load vs. Drift Plots of Specimen CS1
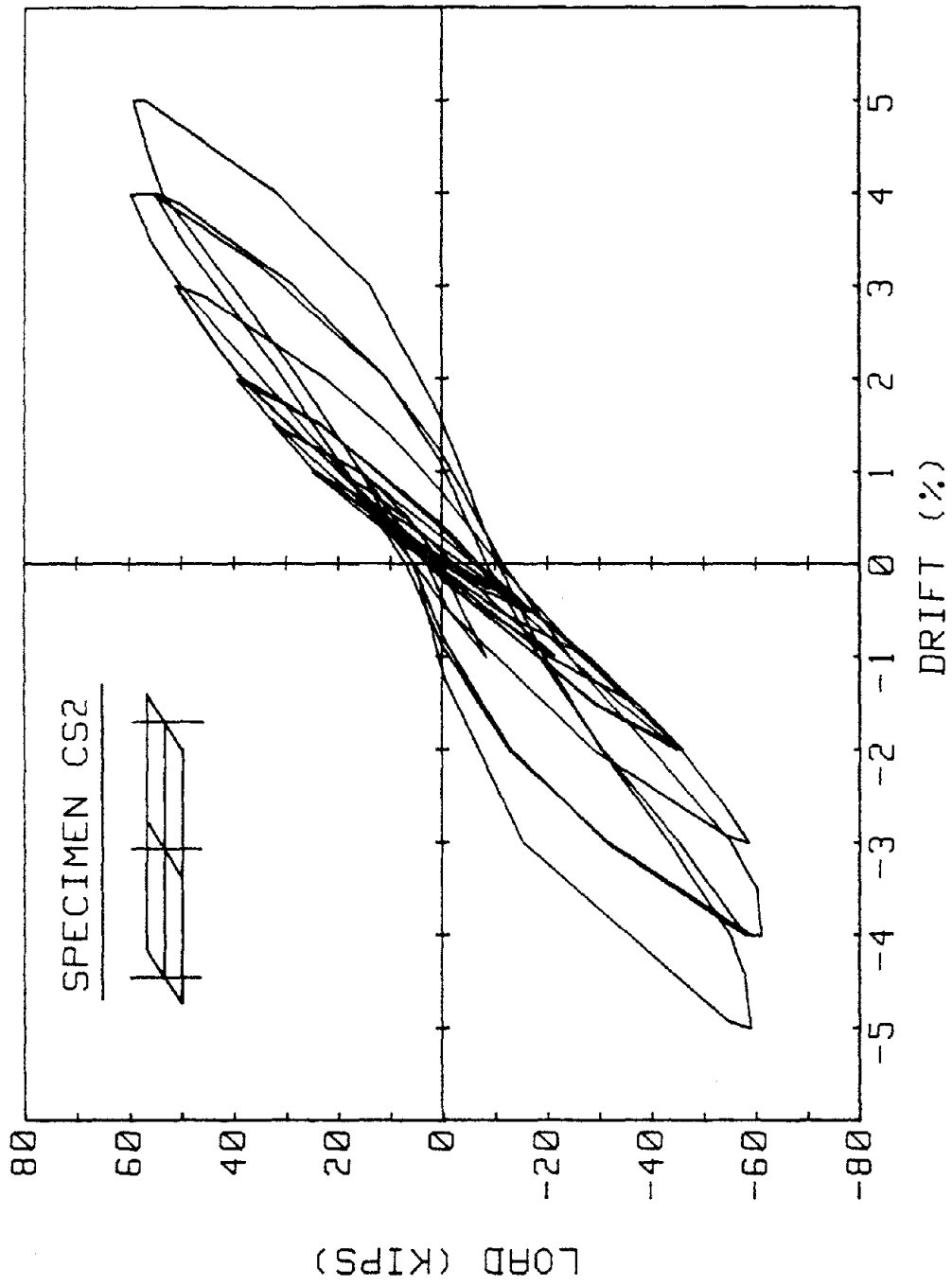
Fig. 3.1(d) Load vs. Drift Plots of Specimen CS2
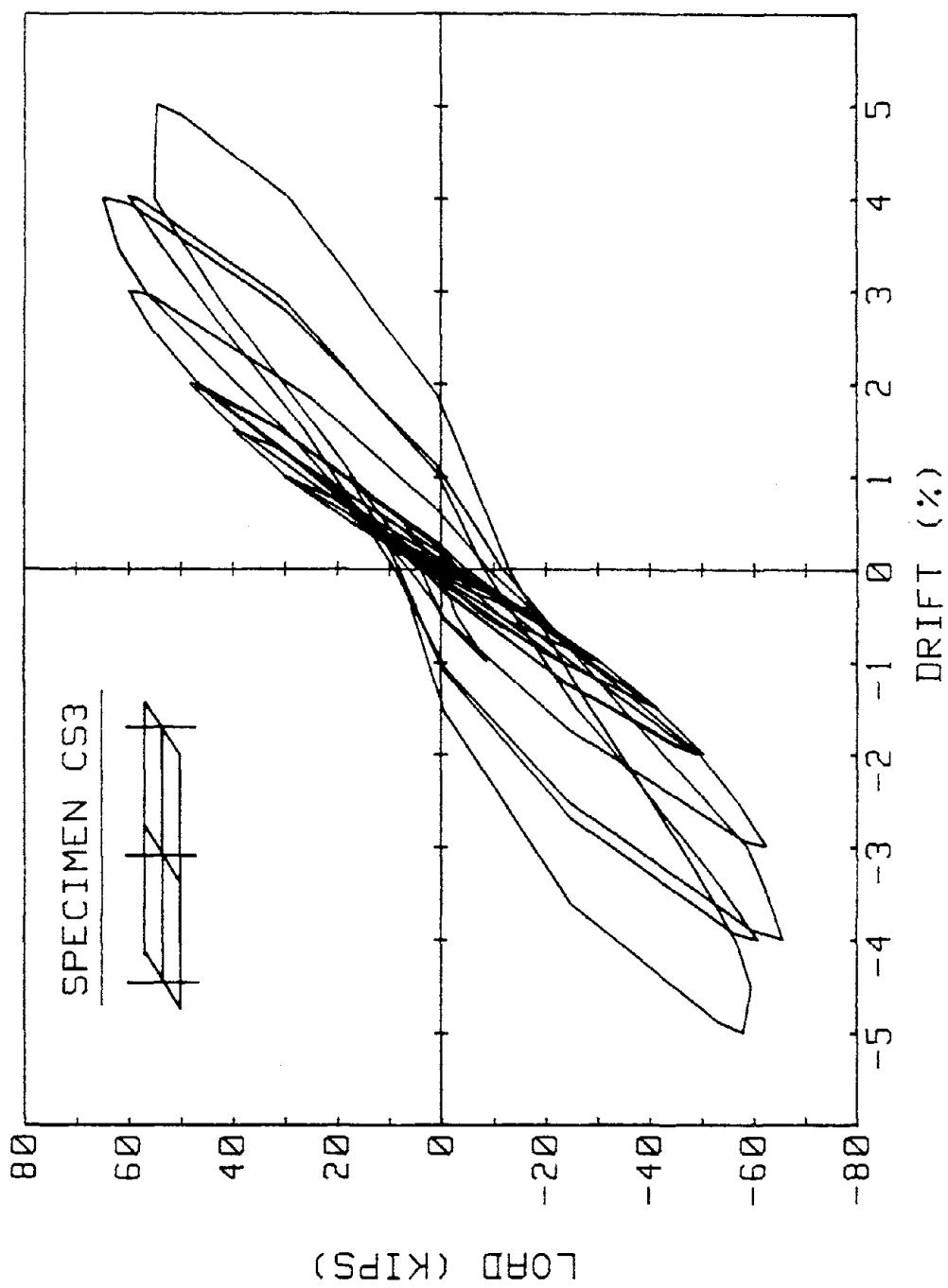
Fig. 3.1(e) Load vs. Drift Plots of Specimen CS3
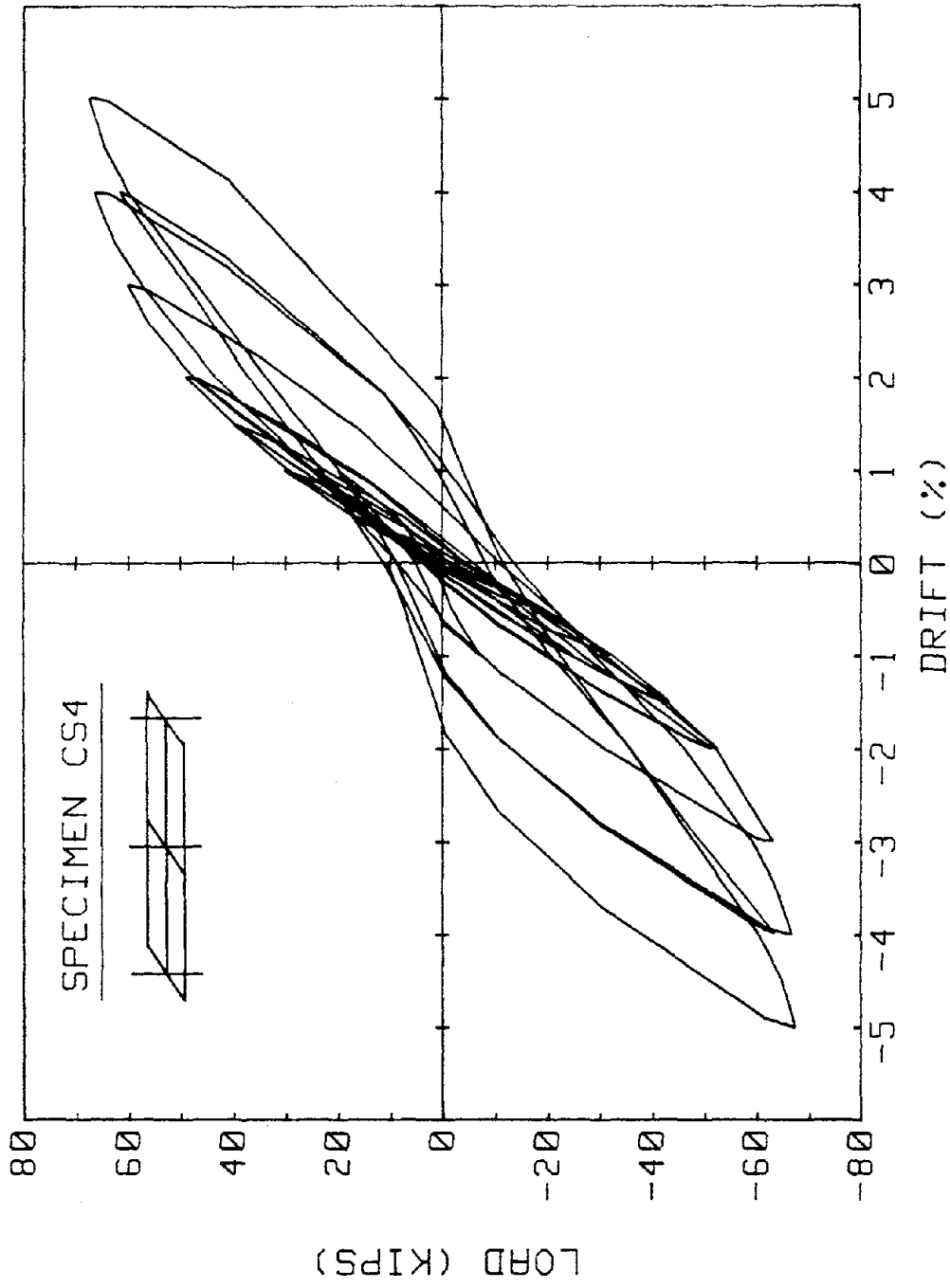
Fig. 3.1(f) Load vs. Drift Plots of Specimen CS4
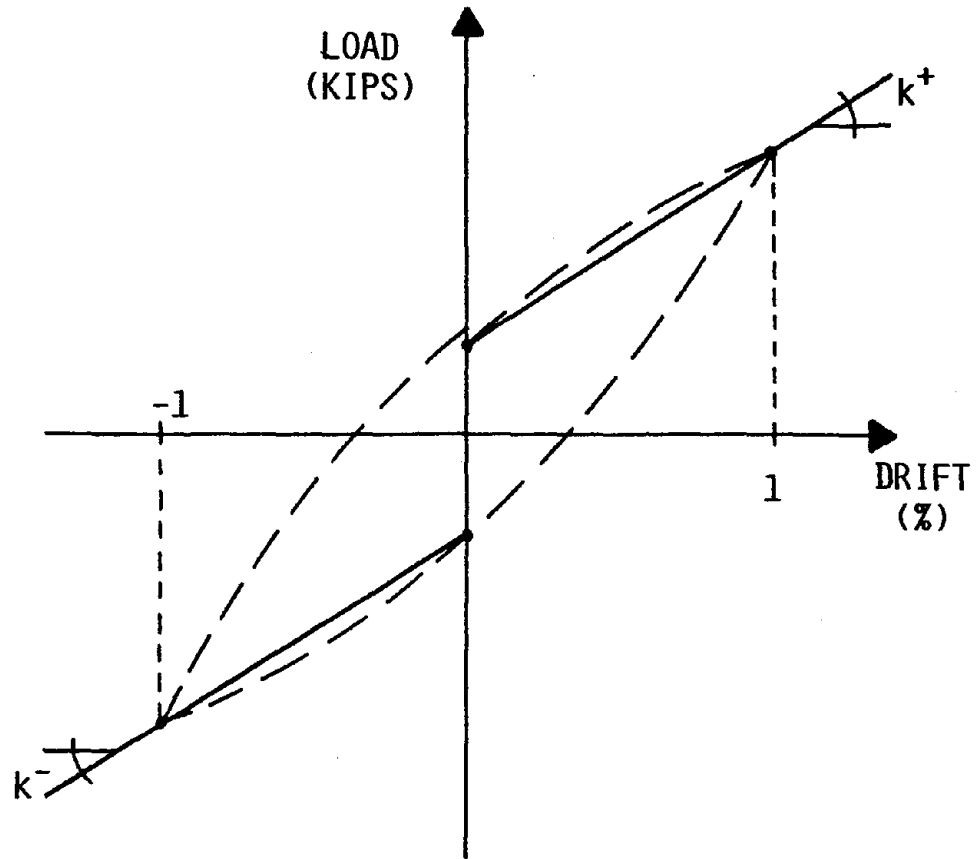
Fig. 3.2 Stiffness Definition of Specimens
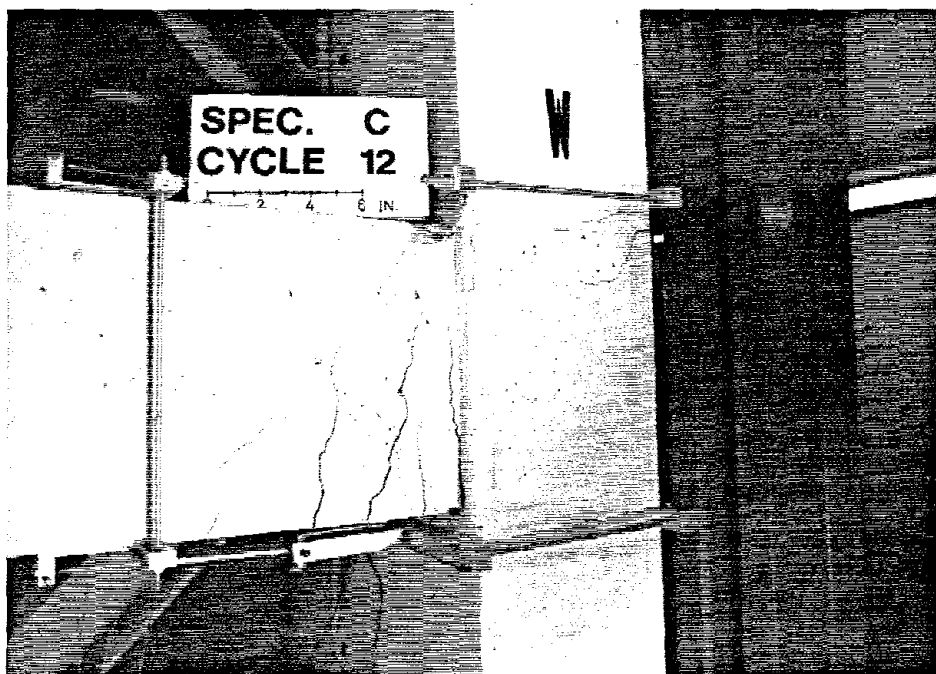
Fig. 3.3(a)   Flexural Cracks in Specimen C
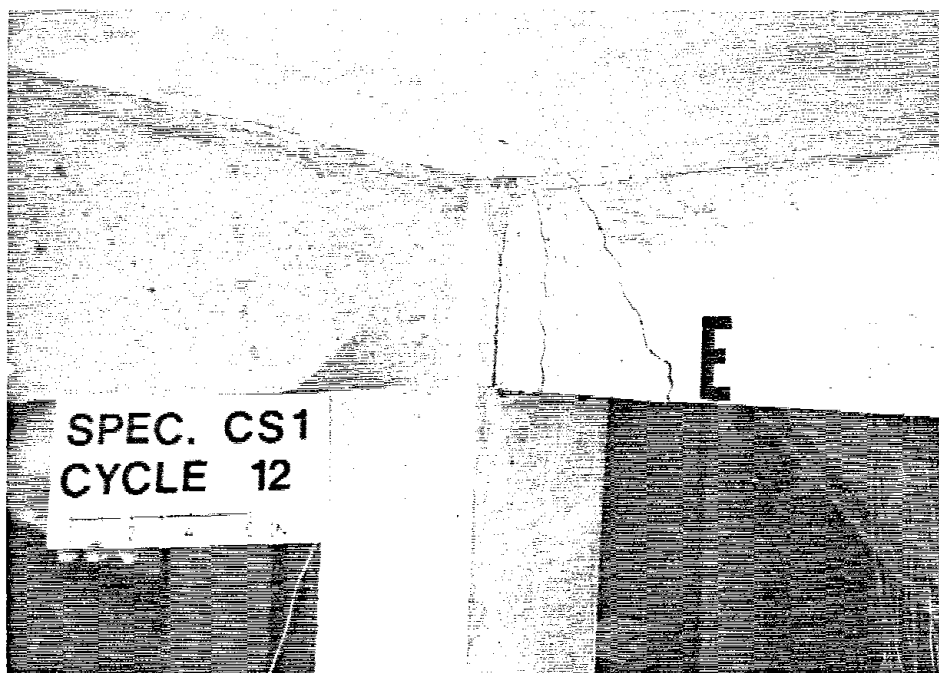
Fig. 3.3(b)   Flexural Cracks in Specimen CS1
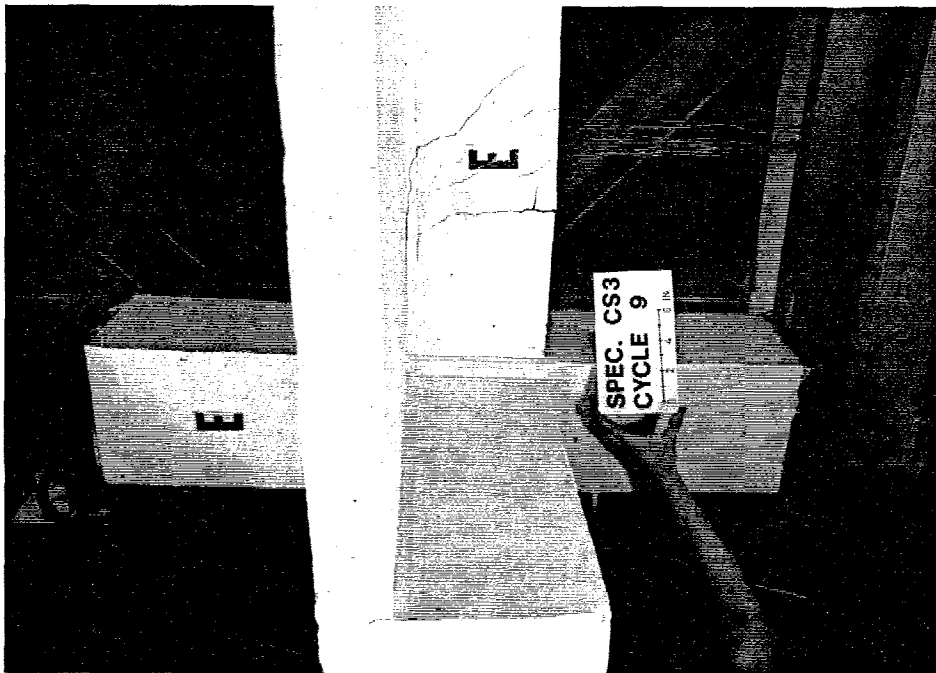
Fig. 3.4(a) Flexural Cracks in Specimen
CS3 (Left Connection)
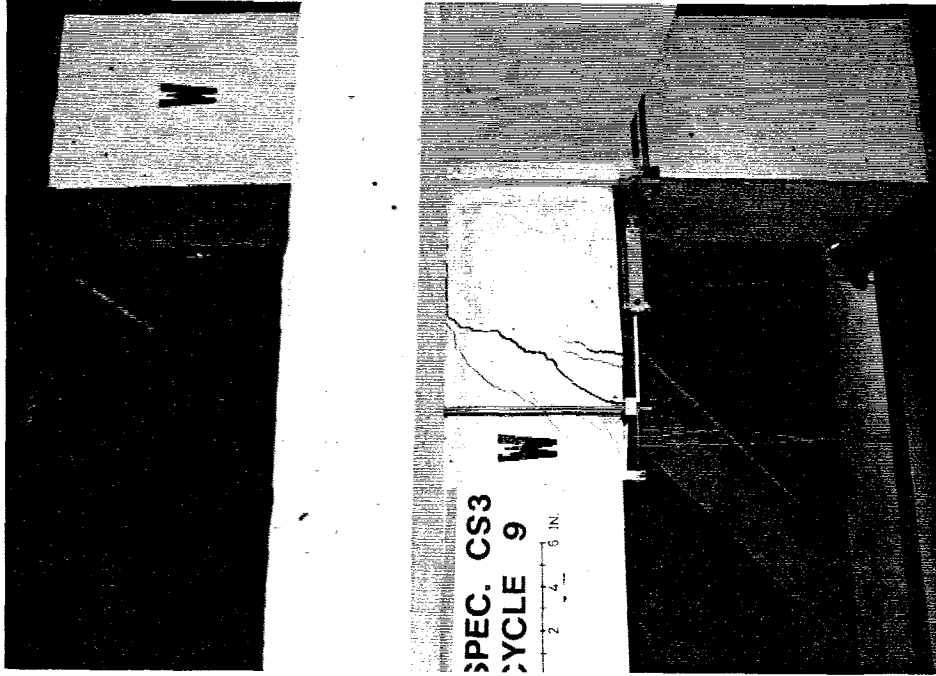
Fig. 3.4(b) Flexural Cracks in Specimen
CS3 (Right Connection)
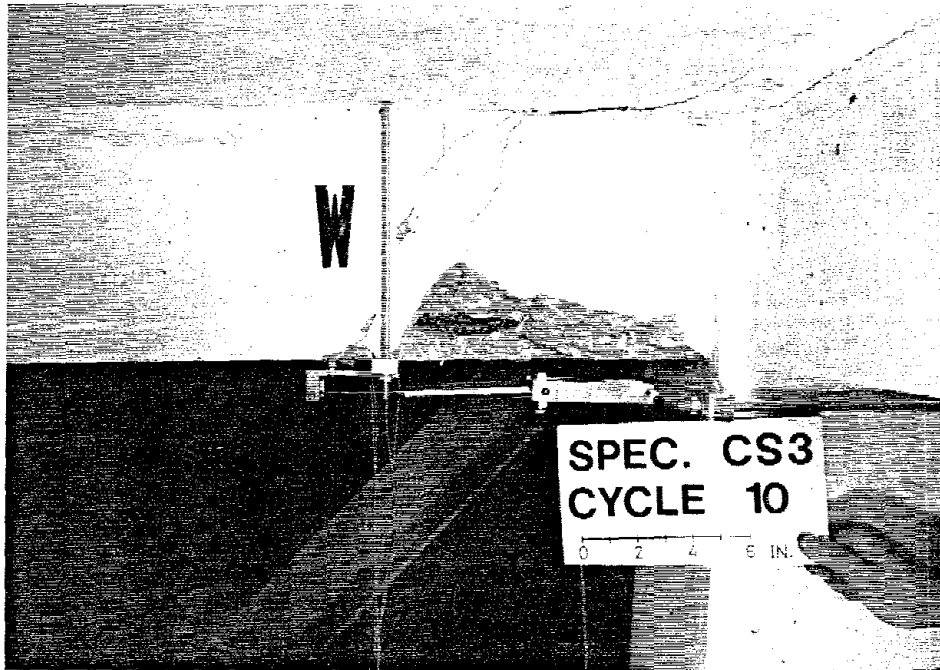
Fig. 3.5 Buckling of Beam Reinforcement in Specimen CS3
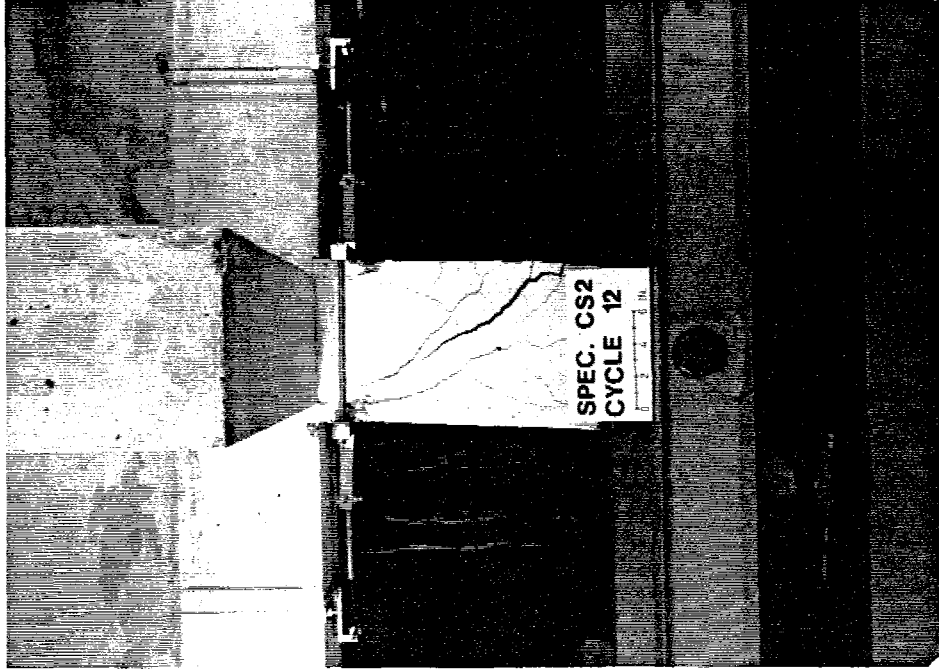
Fig. 3.7 Failure of Specimen CS2 (Center Connection)
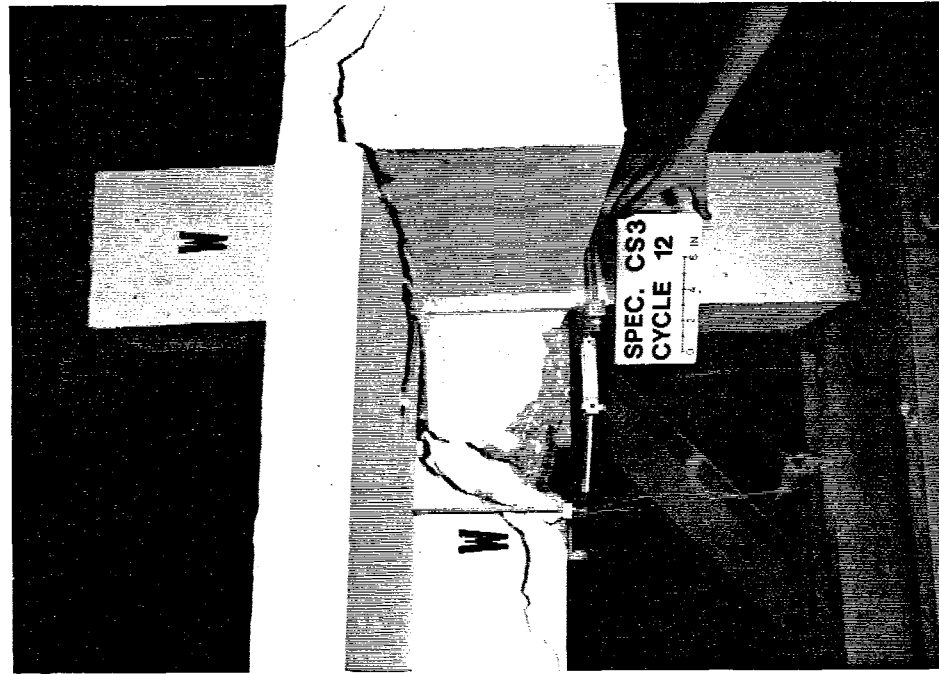
Fig. 3.6 Failure of Specimen CS3 (Right Connection)

150
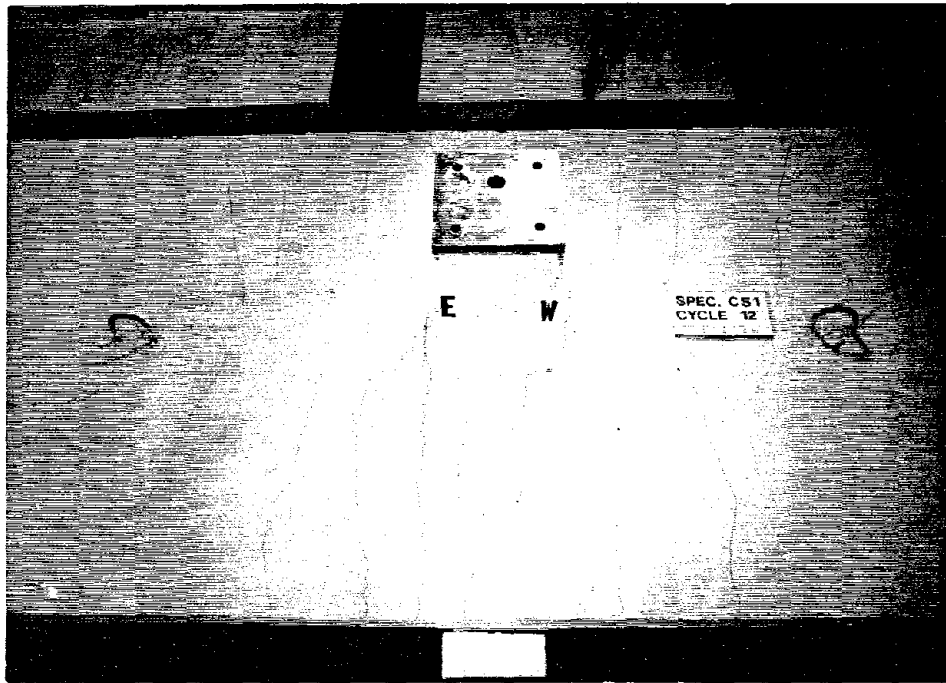
Fig. 3.8 Flexural Cracks in Slab of Specimen CS1

Fig. 3.9 Flexural Cracks in Slab of Specimen CS3

Fig. 3.10(b)   Flexural Cracks in Exterior Column of Specimen CS1
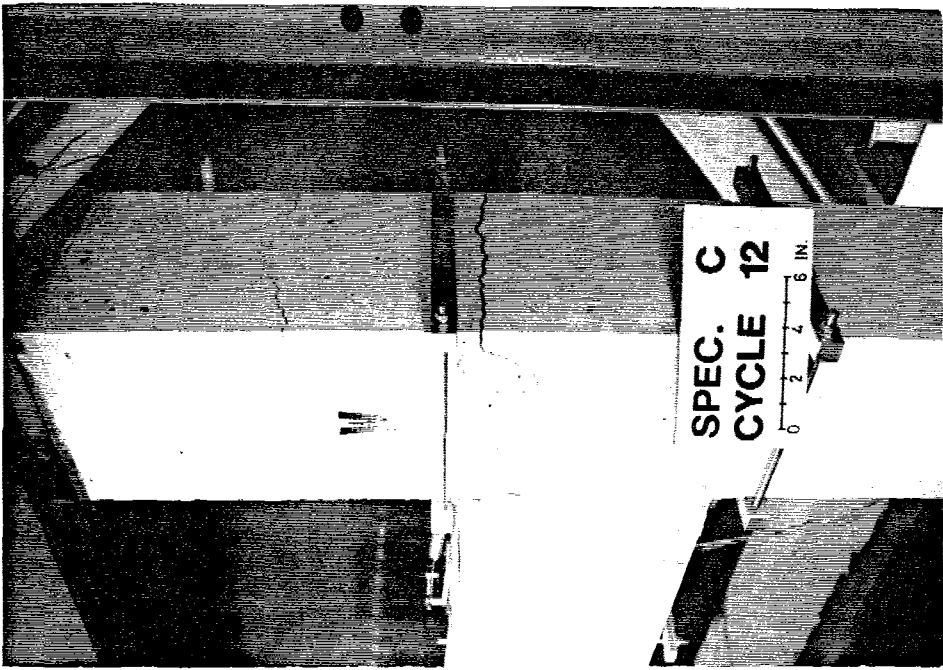
Fig. 3.10(a)   Flexural Cracks in Exterior Column of Specimen C
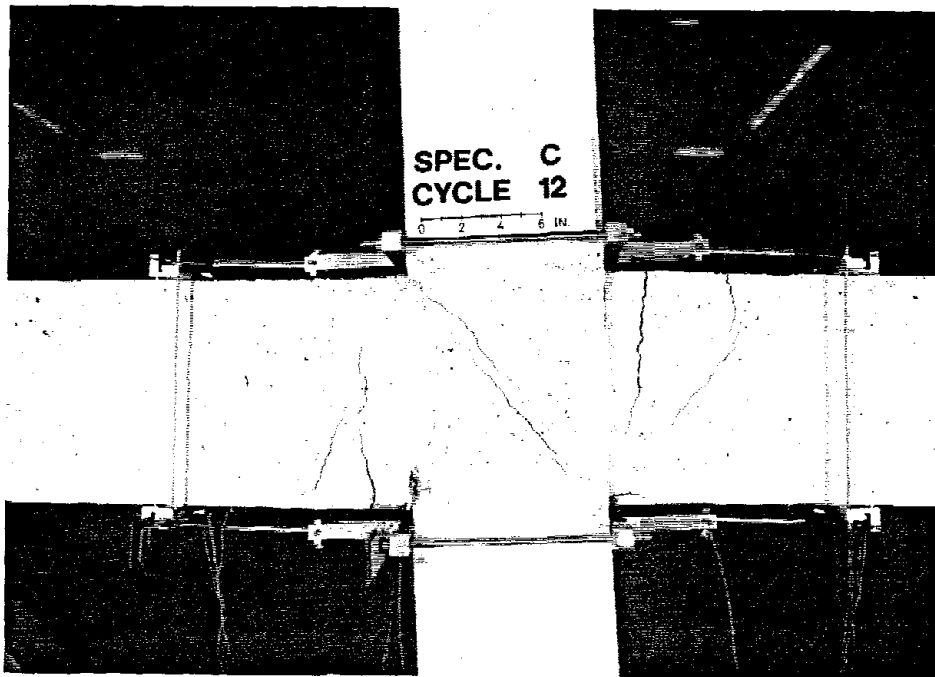
Fig. 3.11 Joint Shear Cracks of Specimen C
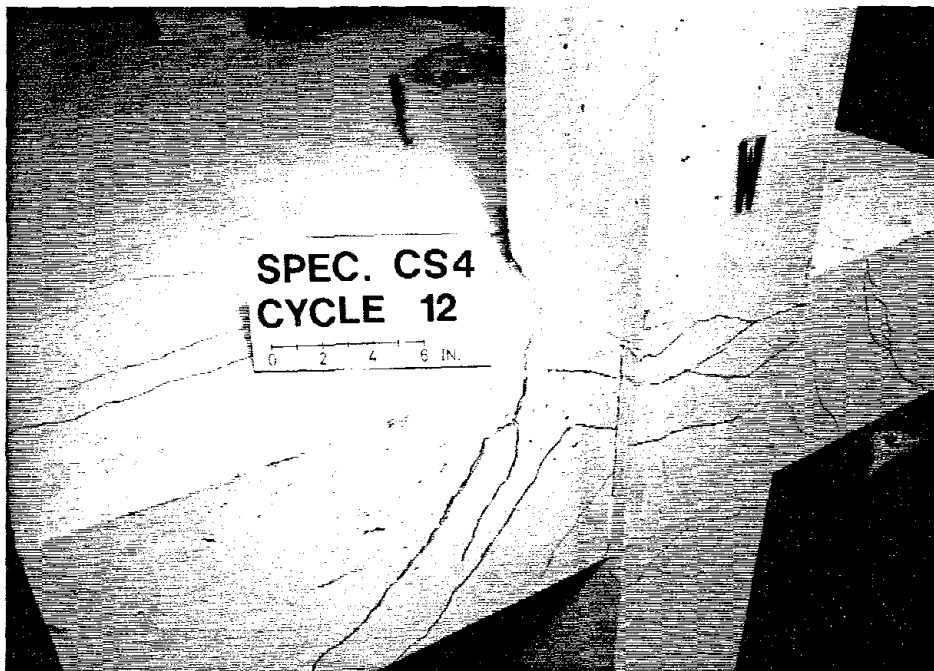
Fig. 3.12 Torsional Cracks in Transverse Beams
of Specimen CS4
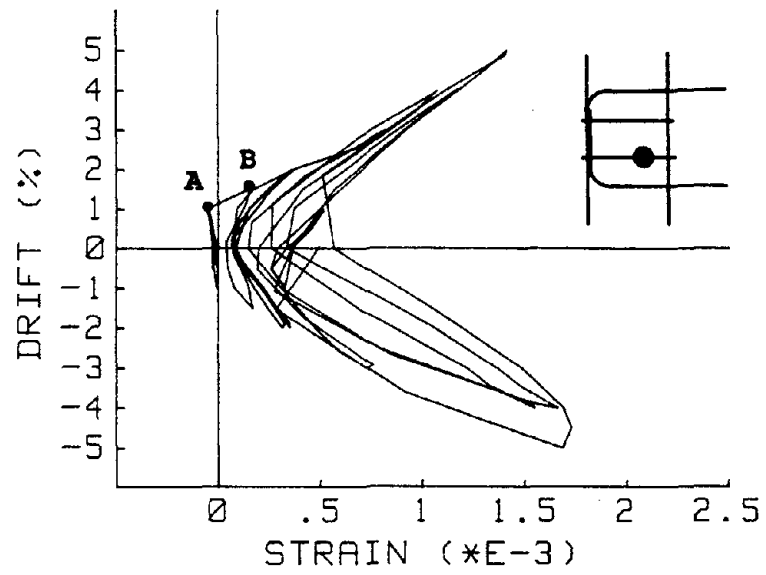
Fig. 3.13 Strain in Joint Reinforcement
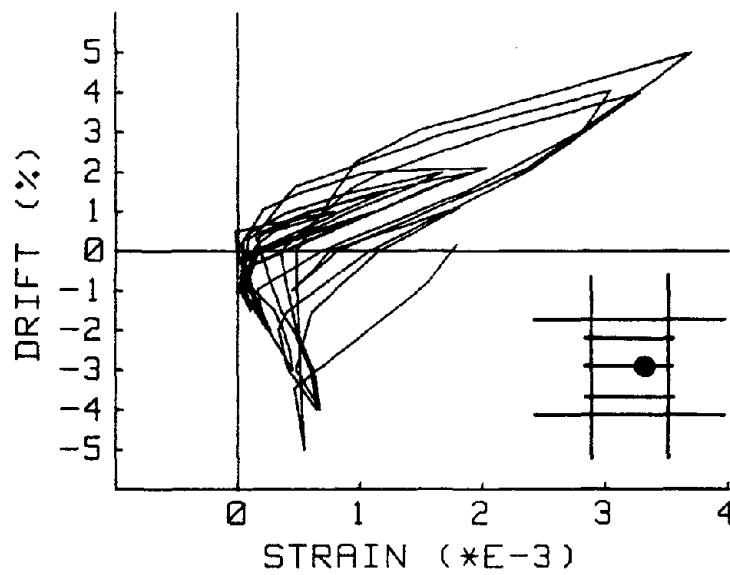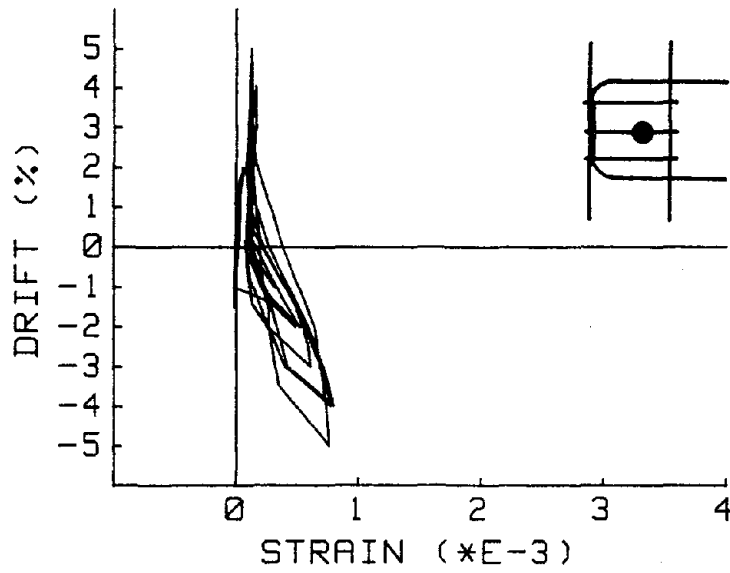
Fig. 3.14 Strain in Joint Reinforcement of Specimen C
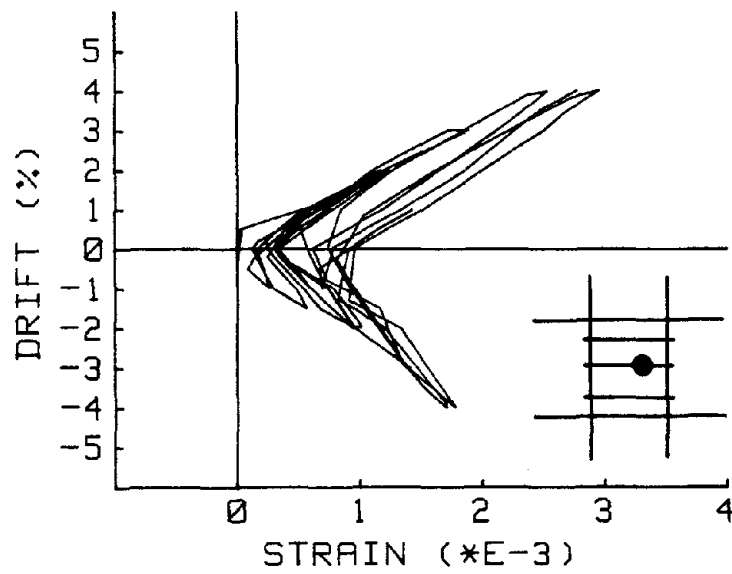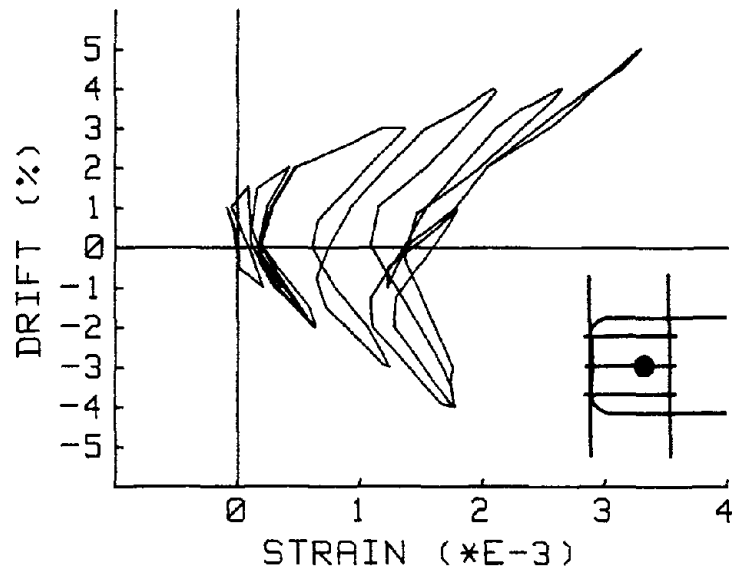
Fig. 3.15 Strain in Joint Reinforcement of Specimen CS1
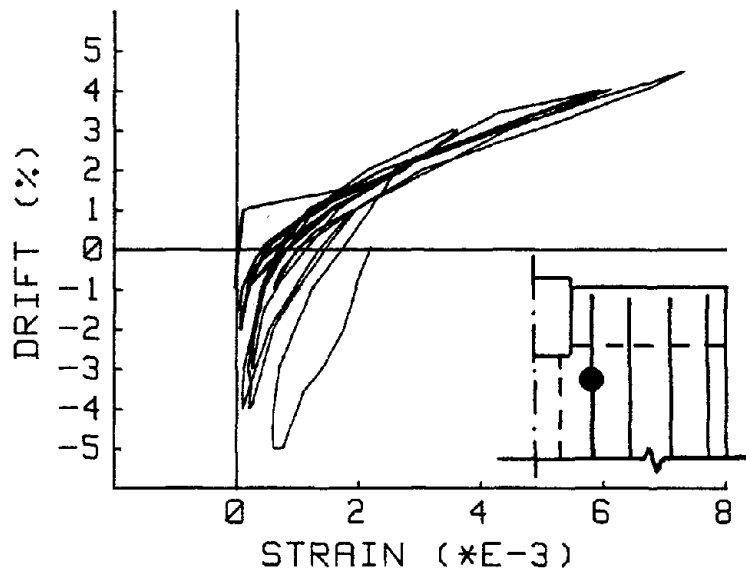
Fig. 3.16   Strain in Slab Reinforcement Near the
Main Beam
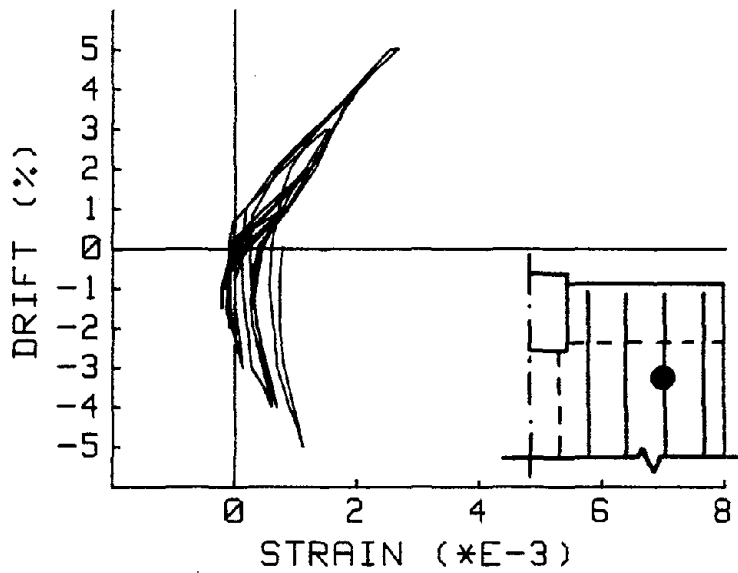
Fig. 3.17   Strain in Slab Reinforcement Away from the
Main Beam
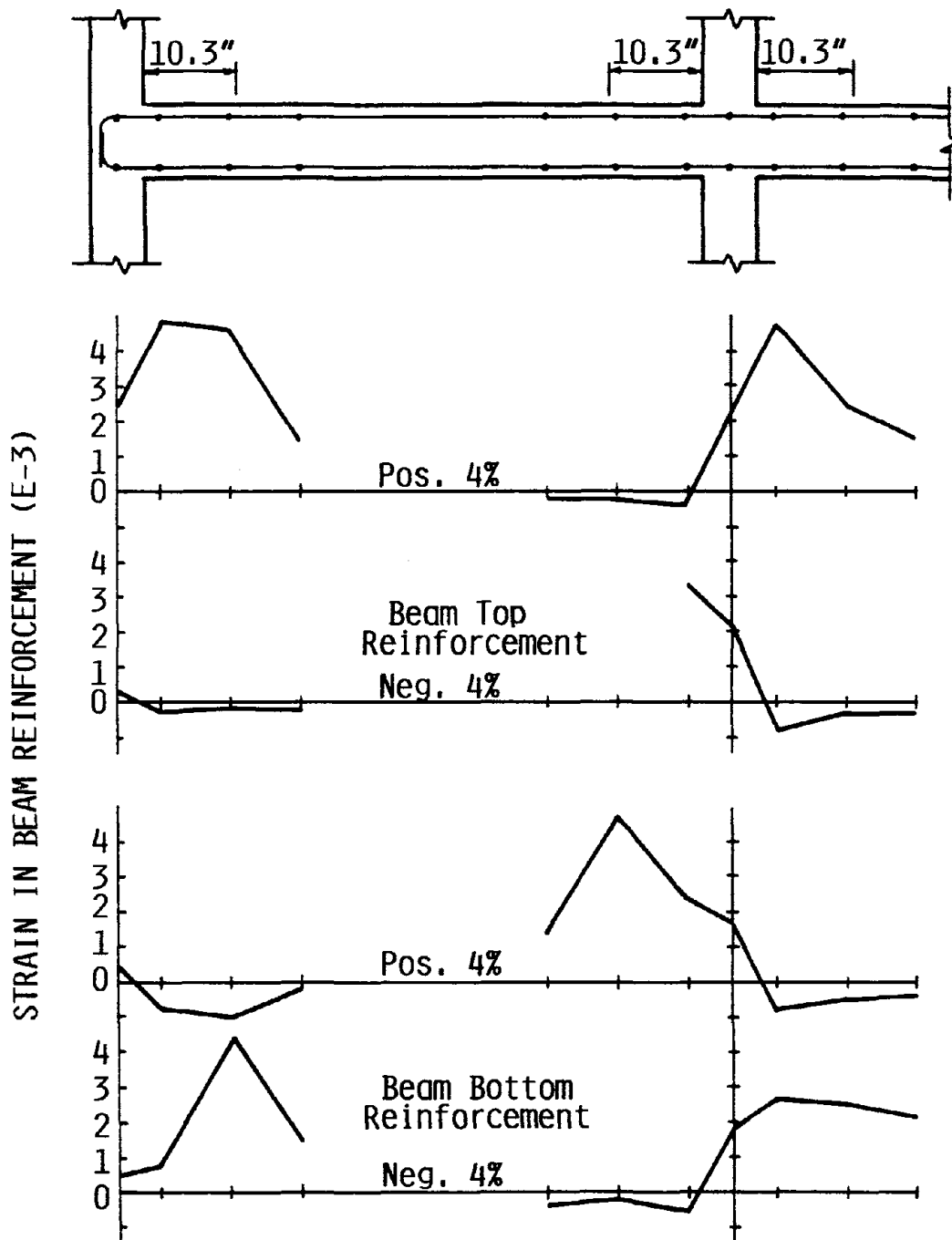
Fig. 3.18 Strain Distribution along Beam Reinforcement in Specimen CS3
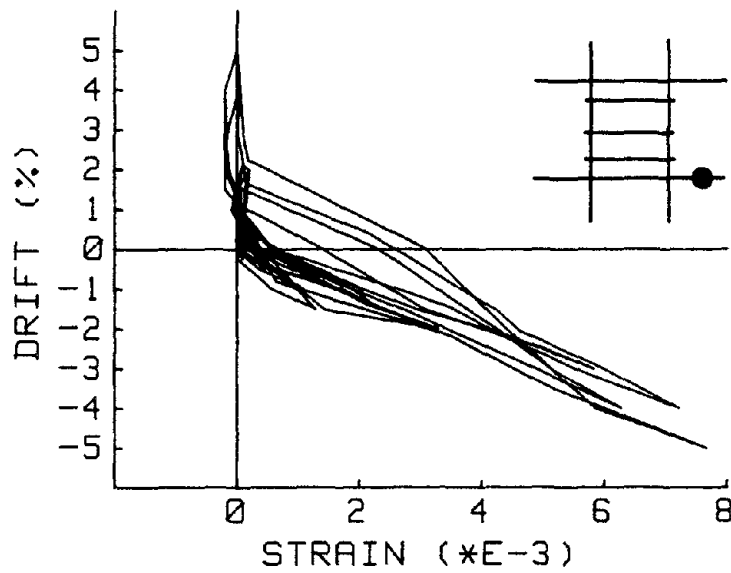
Fig. 3.19   Strain in Beam Reinforcement of Specimen C
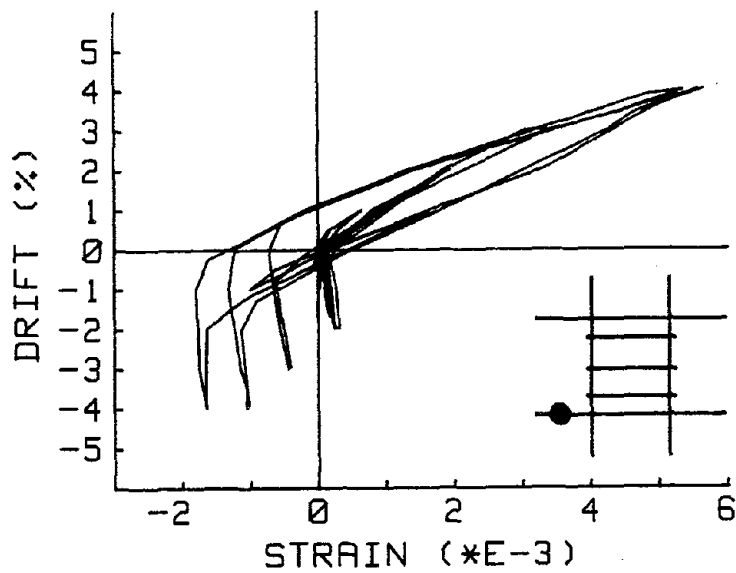
Fig. 3.20   Strain in Bottom Beam Reinforcement of
Specimen CS1 (Interior Connection)
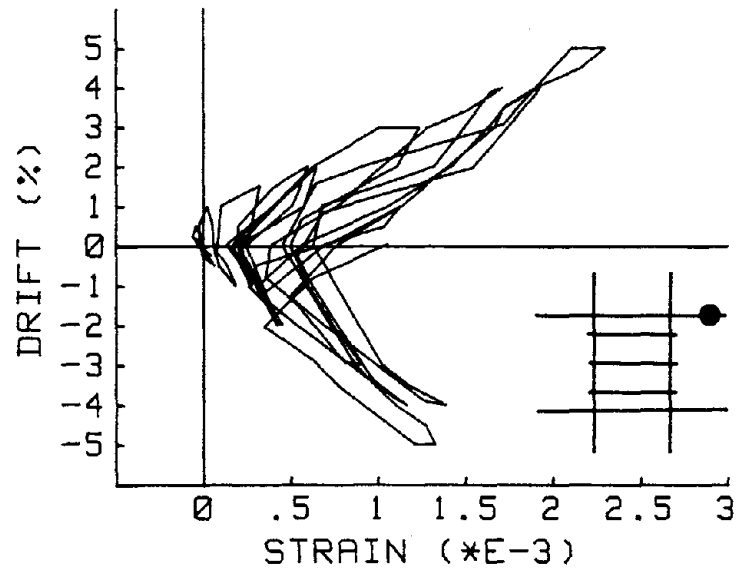
Fig. 3.21   Strain in Top Beam Reinforcement of
             Specimen CS1 (Interior Connection)
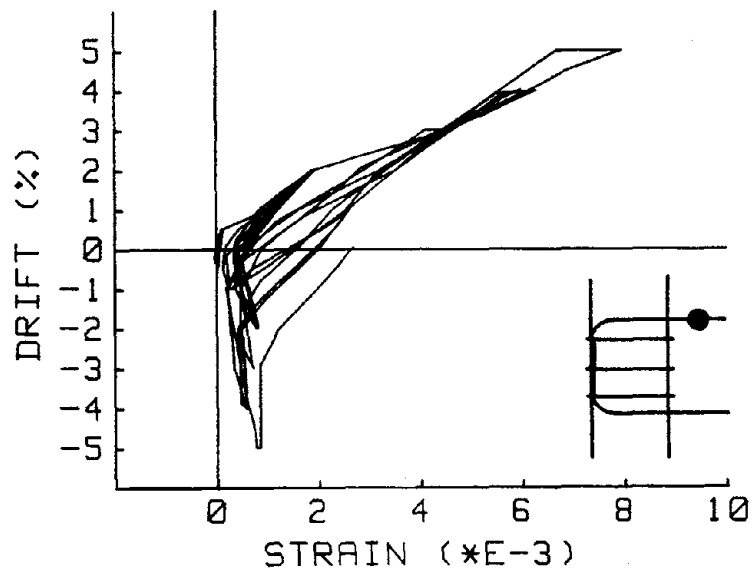
Fig. 3.22   Strain in Beam Reinforcement of Specimen
             CS1 (Exterior Connection)
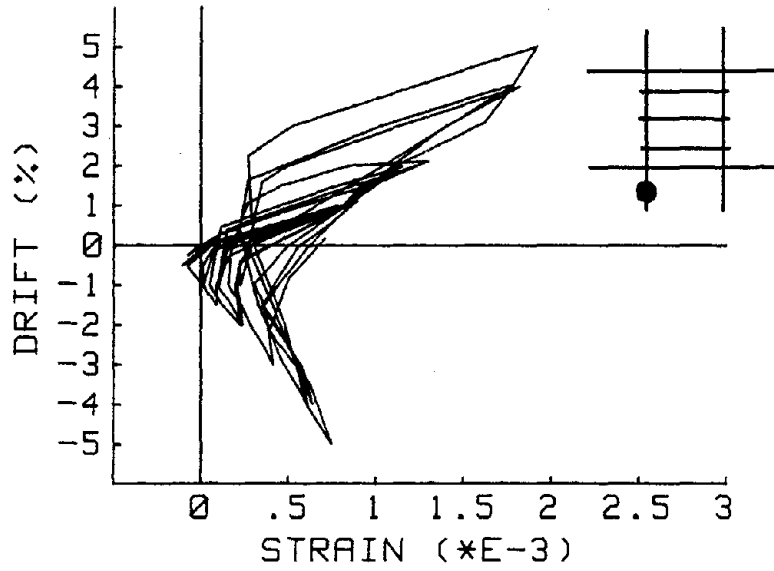
Fig. 3.23   Strain in Column Reinforcement of Specimen C
(Interior Connection)
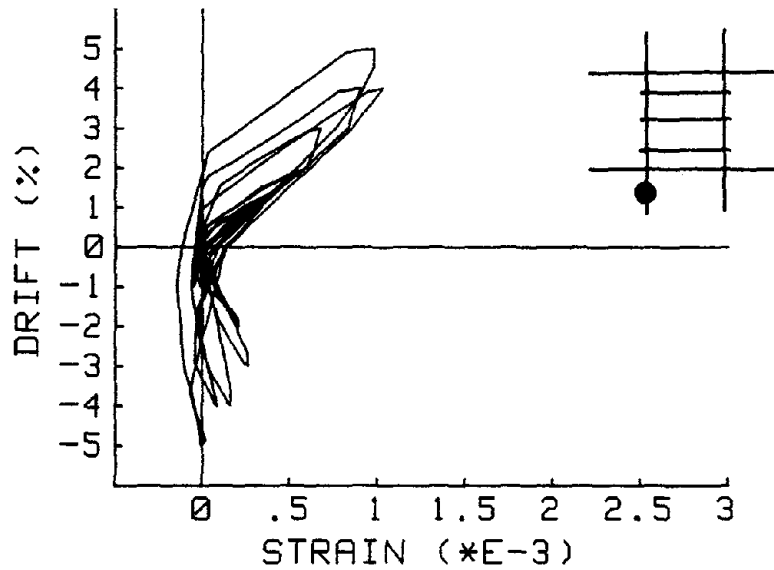
Fig. 3.24   Strain in Column Reinforcement of Specimen CTB
(Interior Connection)
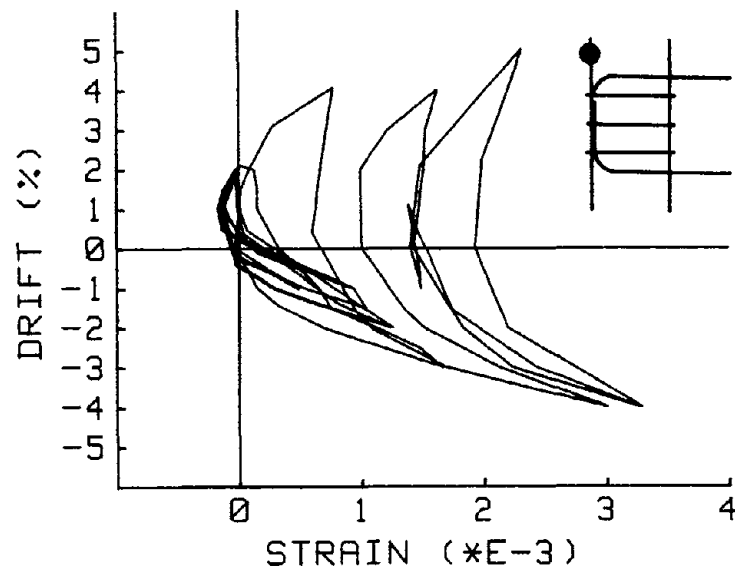
Fig. 3.25 Strain in Exterior Column Reinforcement of
Specimen C (Outer Rebar)
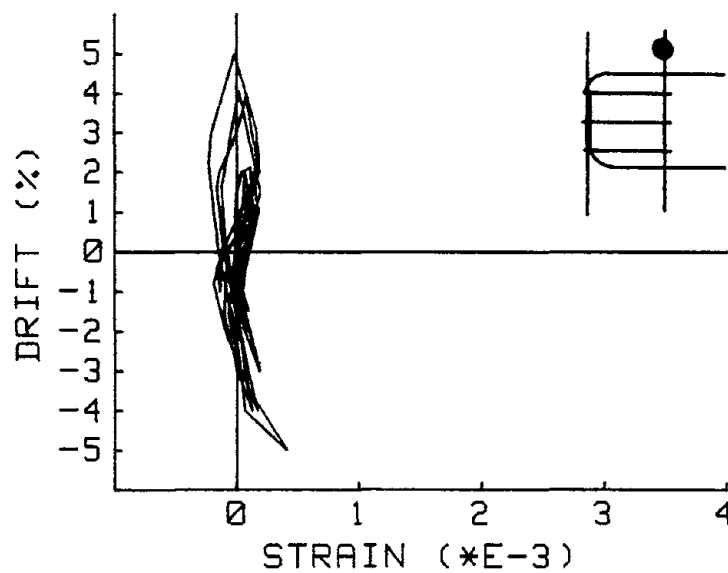
Fig. 3.26 Strain in Exterior Column Reinforcement of
Specimen C (Inner Rebar)
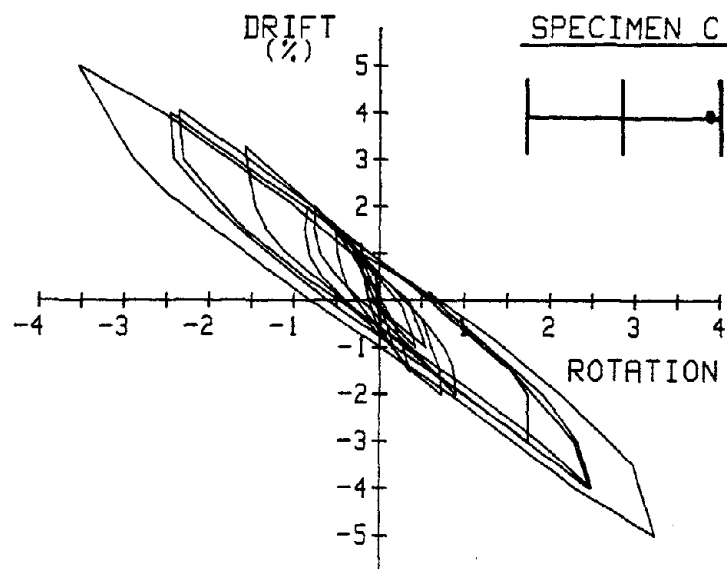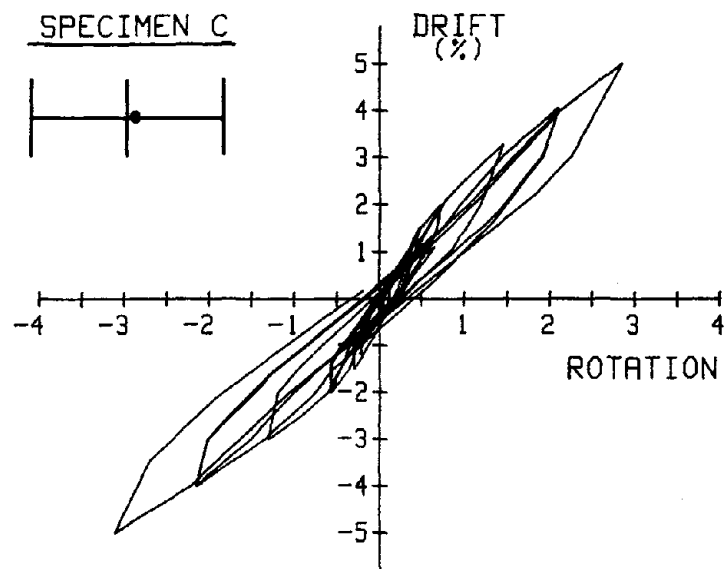
Fig. 3.27(a) Drift-Rotation plots of Specimen C
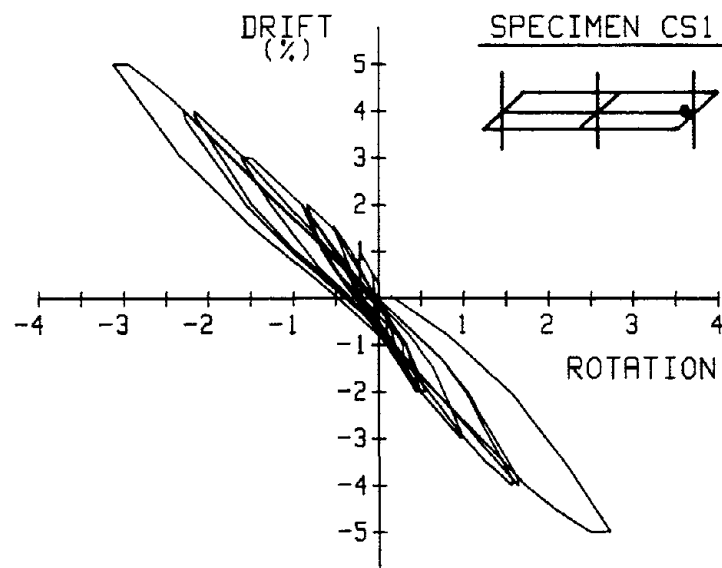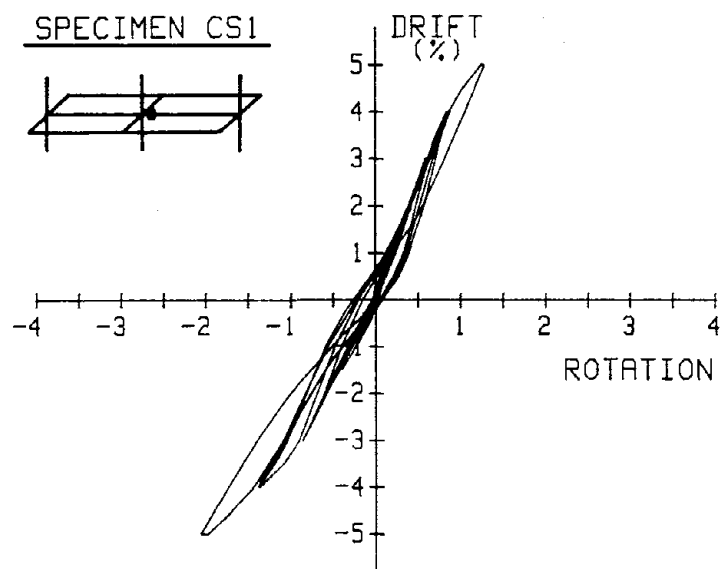
Fig. 3.27(b) Drift-Rotation plots of Specimen CS1

164
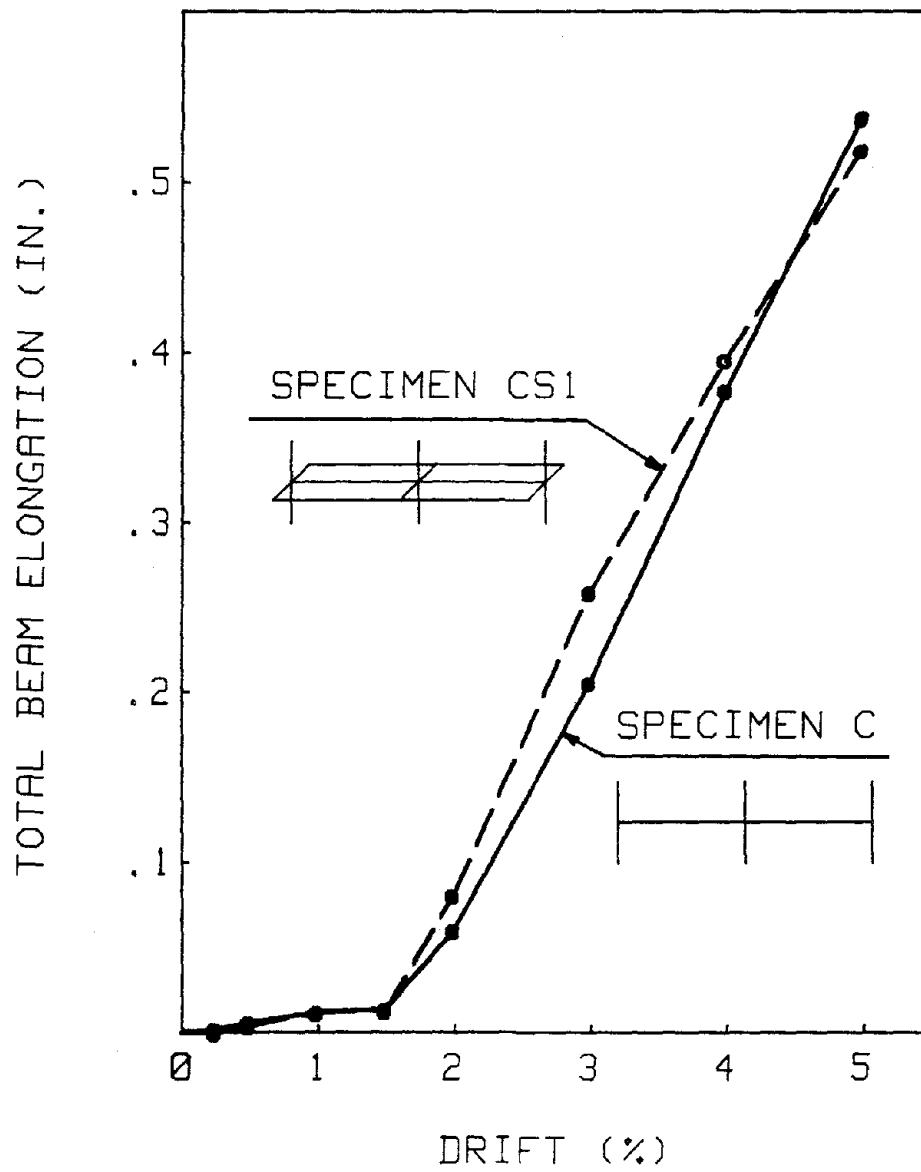
Fig. 3.28   Measured Elongation of Main beams in Specimens
            C and CS1

INTERIOR CONNECTIONS

EXTERIOR CONNECTIONS
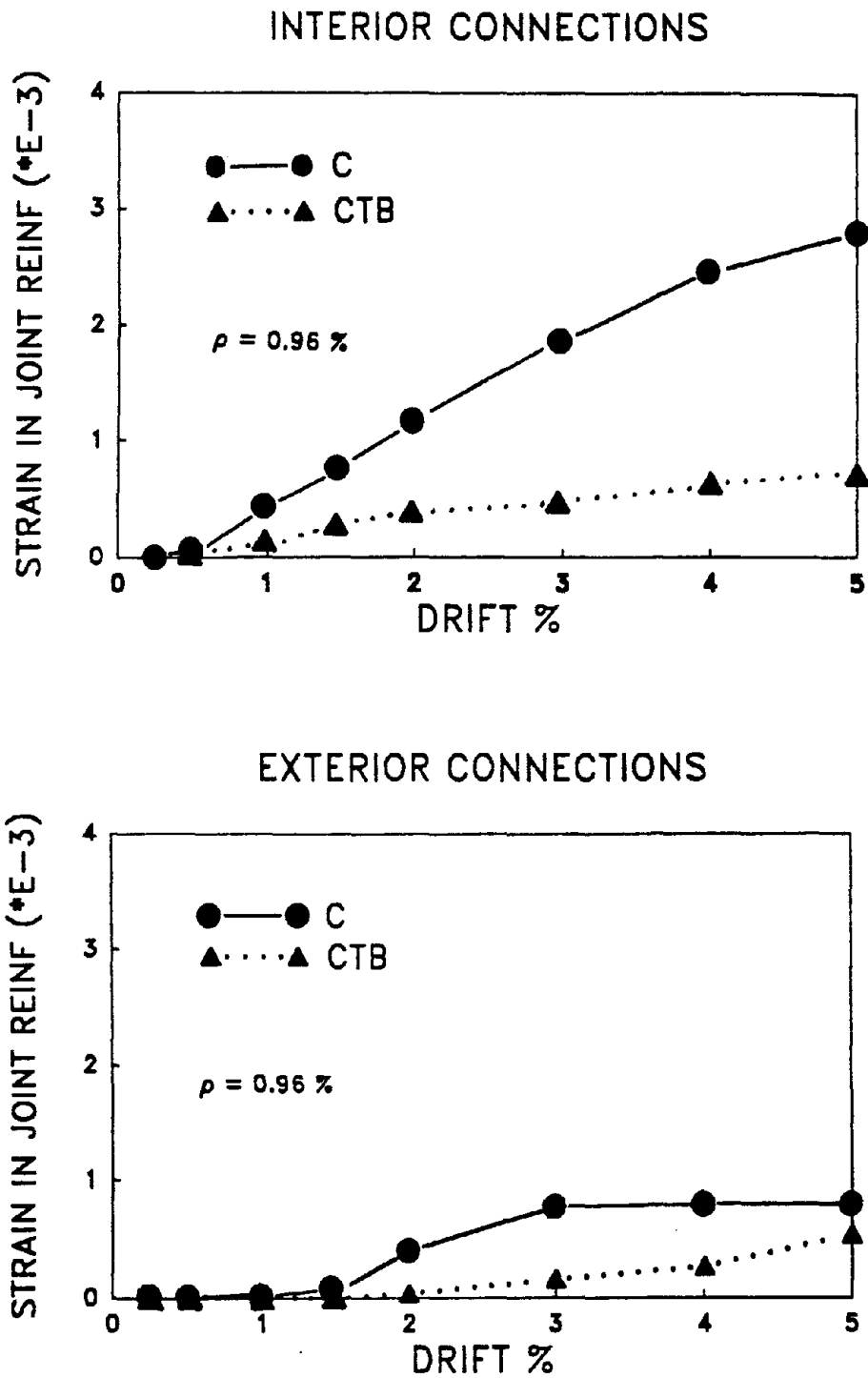
Fig. 3.29   Strain in Joint Lateral Reinforcement of
Specimens C and CTB
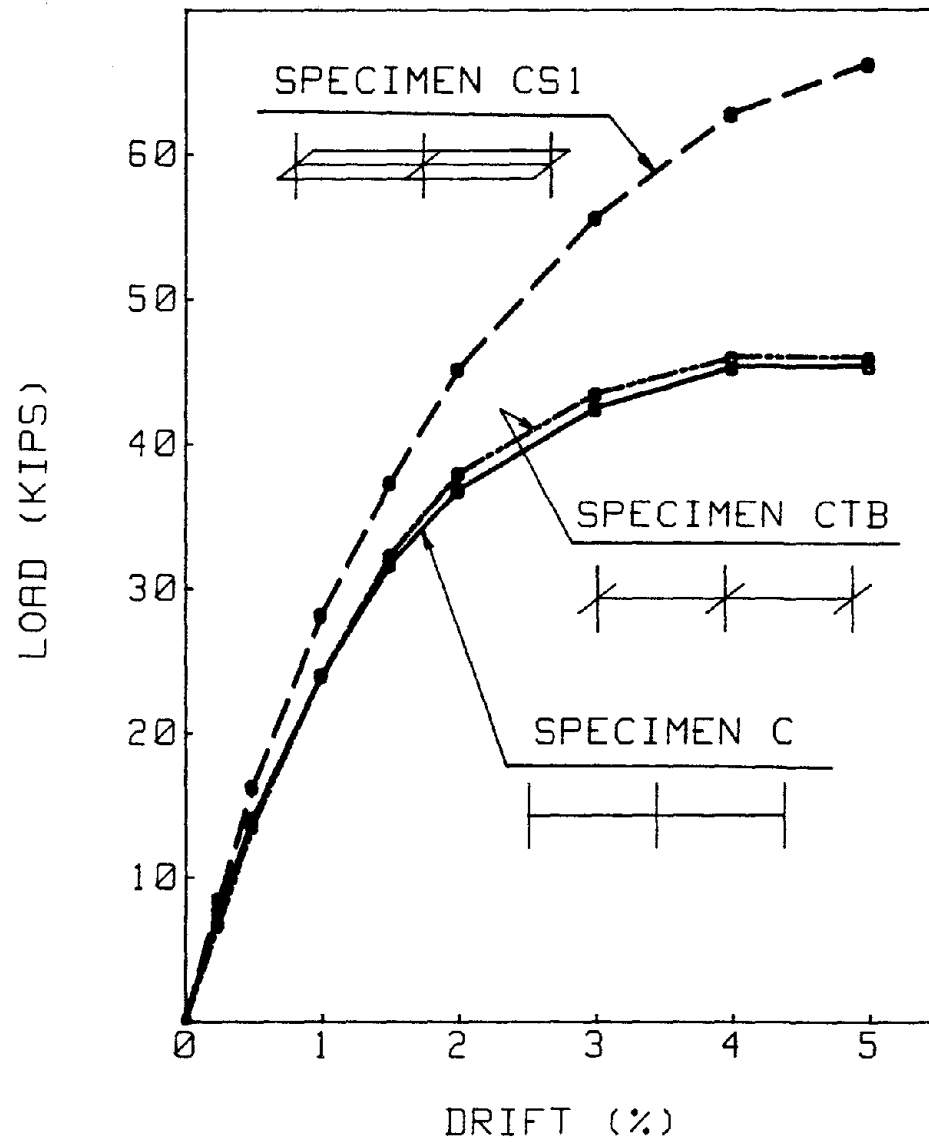
Fig. 3.30 Envelops of Load vs. Drift Curves of Specimens
            C, CTB, and CS1
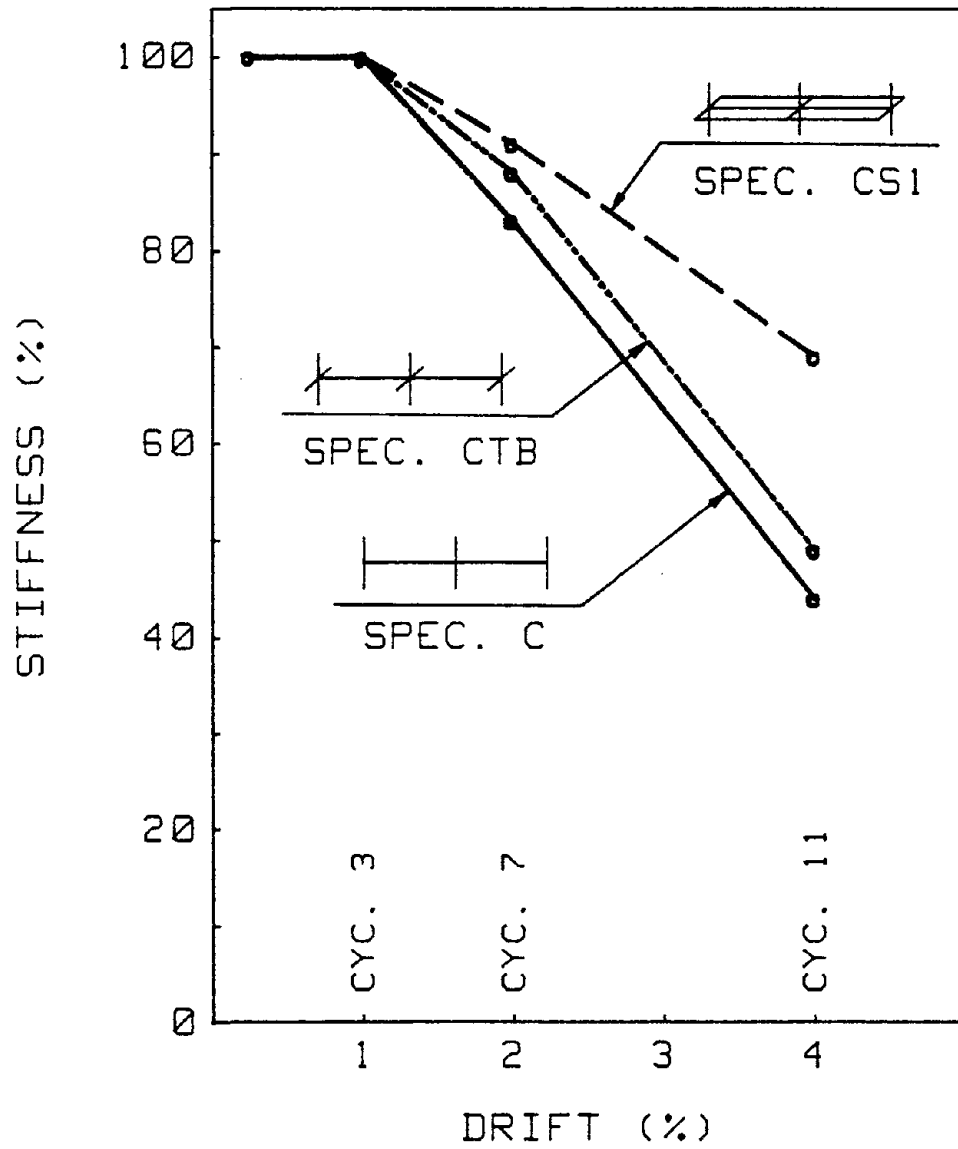
Fig. 3.31 Loss of Stiffness in Specimens C, CTB, and CS1
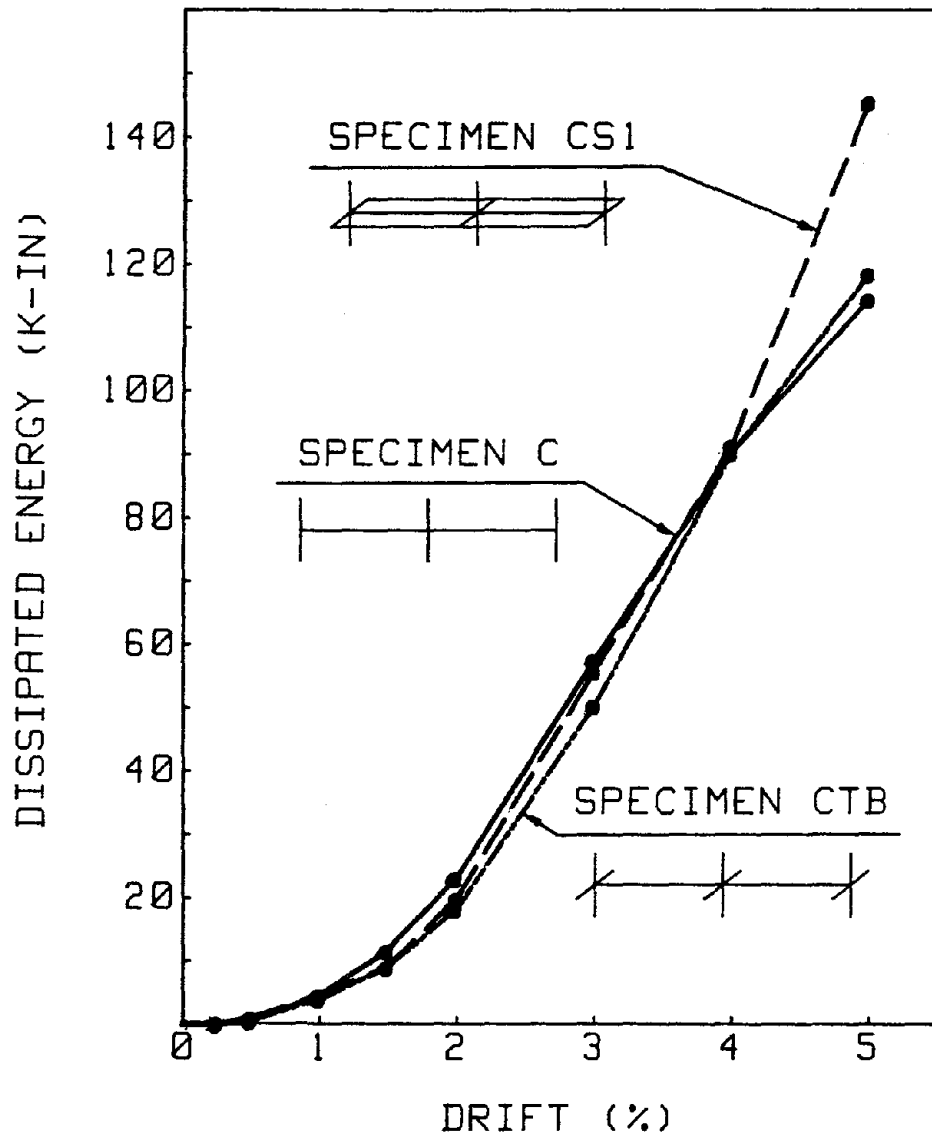
Fig. 3.32 Energy Dissipated by Specimens C, CTB, and CS1

INTERIOR CONNECTIONS

EXTERIOR CONNECTIONS
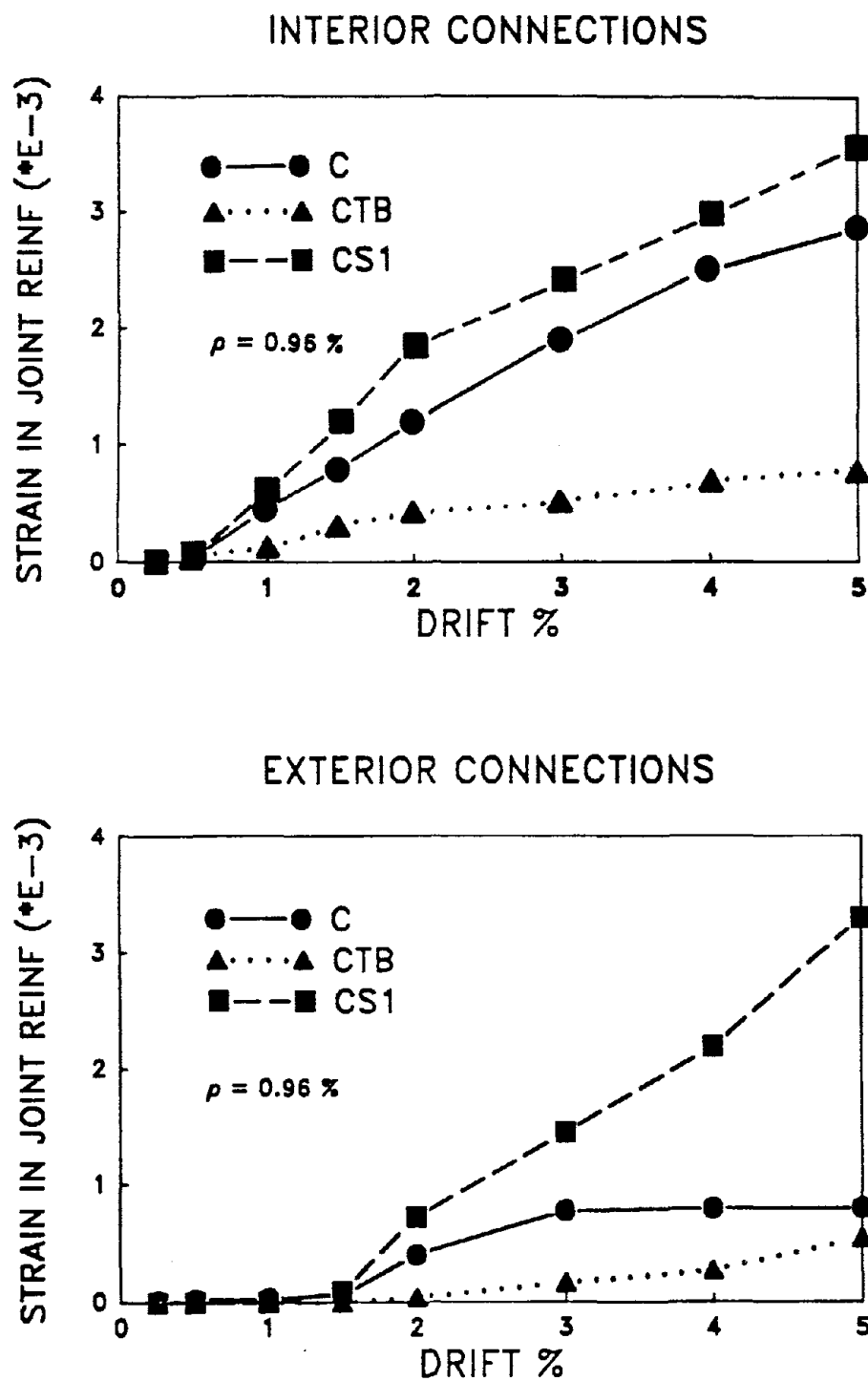
Fig. 3.33 Strain in Joint Lateral Reinforcement of
Specimens C, CTB, and CS1
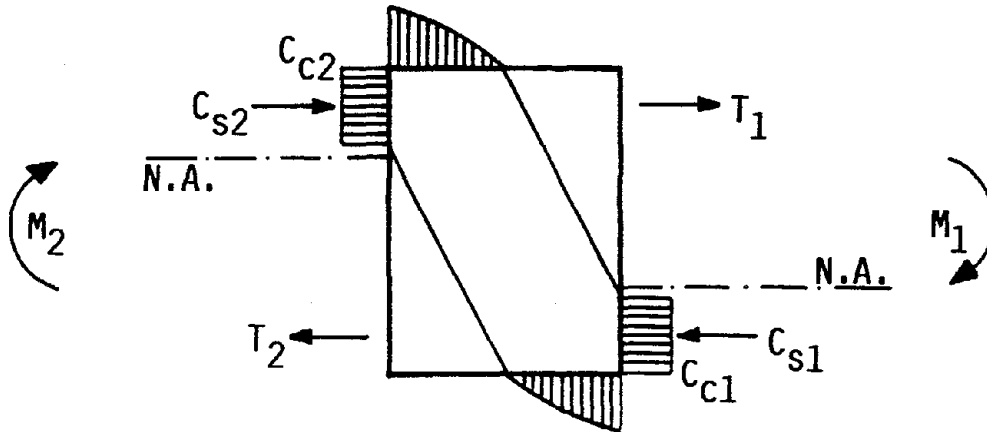
Fig. 3.34(a)   Diagonal Compression Strut in Conventional
               Interior Joint
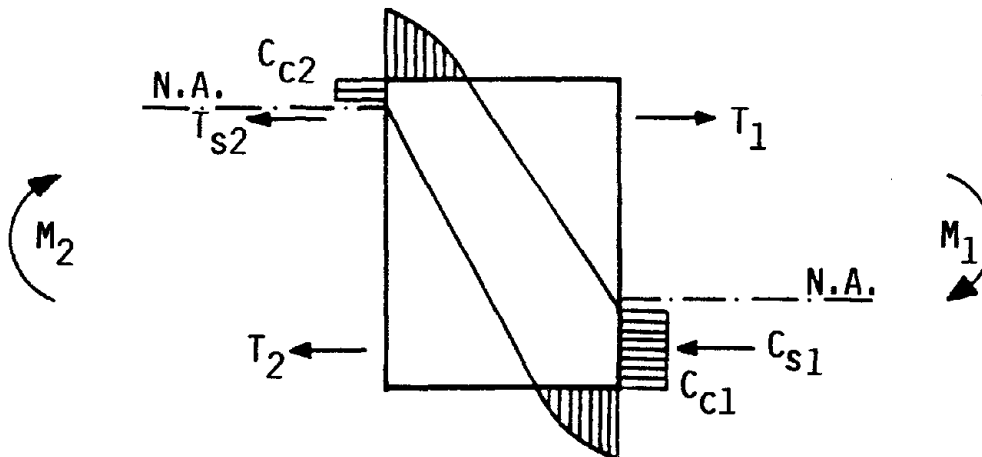
Fig. 3.34(b)   Diagonal Compression Strut in Interior Joint
               with Floor Slab

INTERIOR CONNECTIONS

EXTERIOR CONNECTIONS
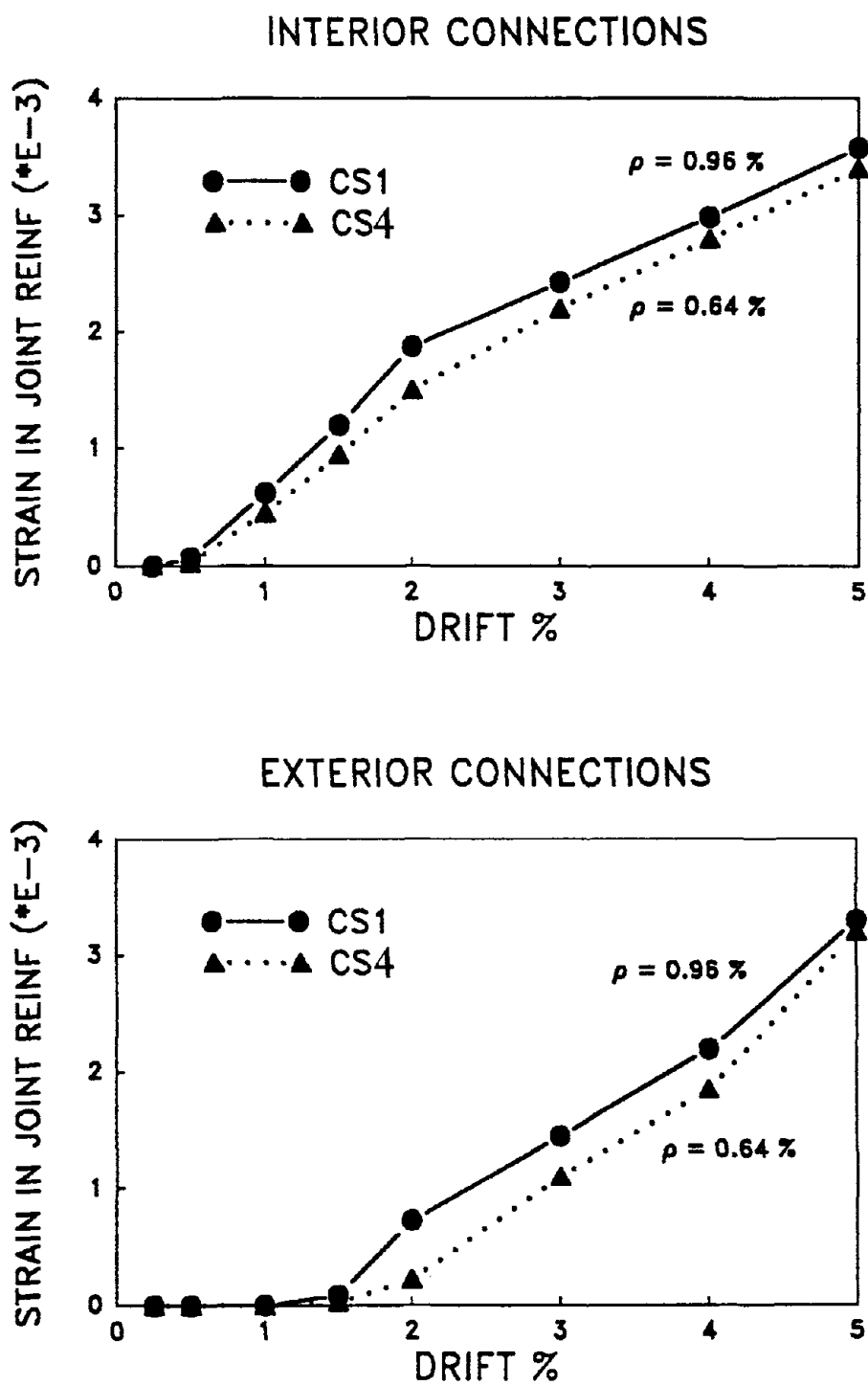
Fig. 3.35   Strain in Joint Lateral Reinforcement of
            Specimens CS1 and CS4
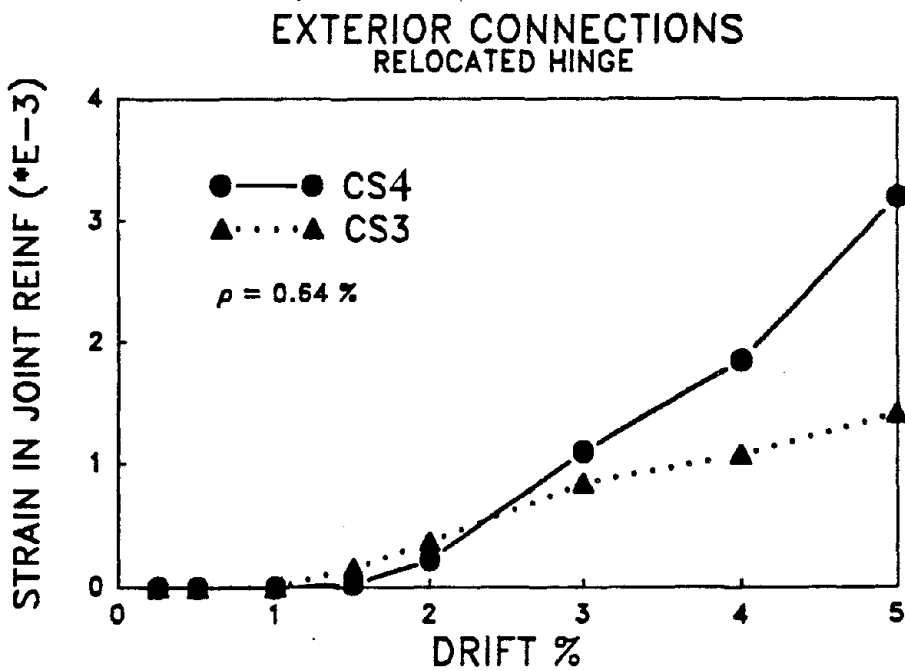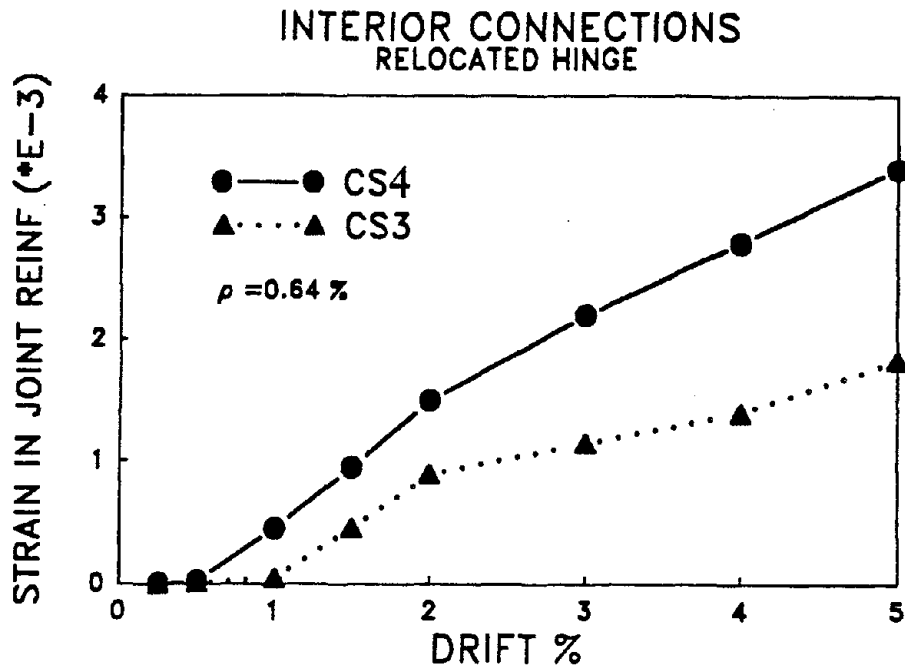
Fig. 3.36 Strain in Joint Lateral Reinforcement of
Specimens CS4 and CS3
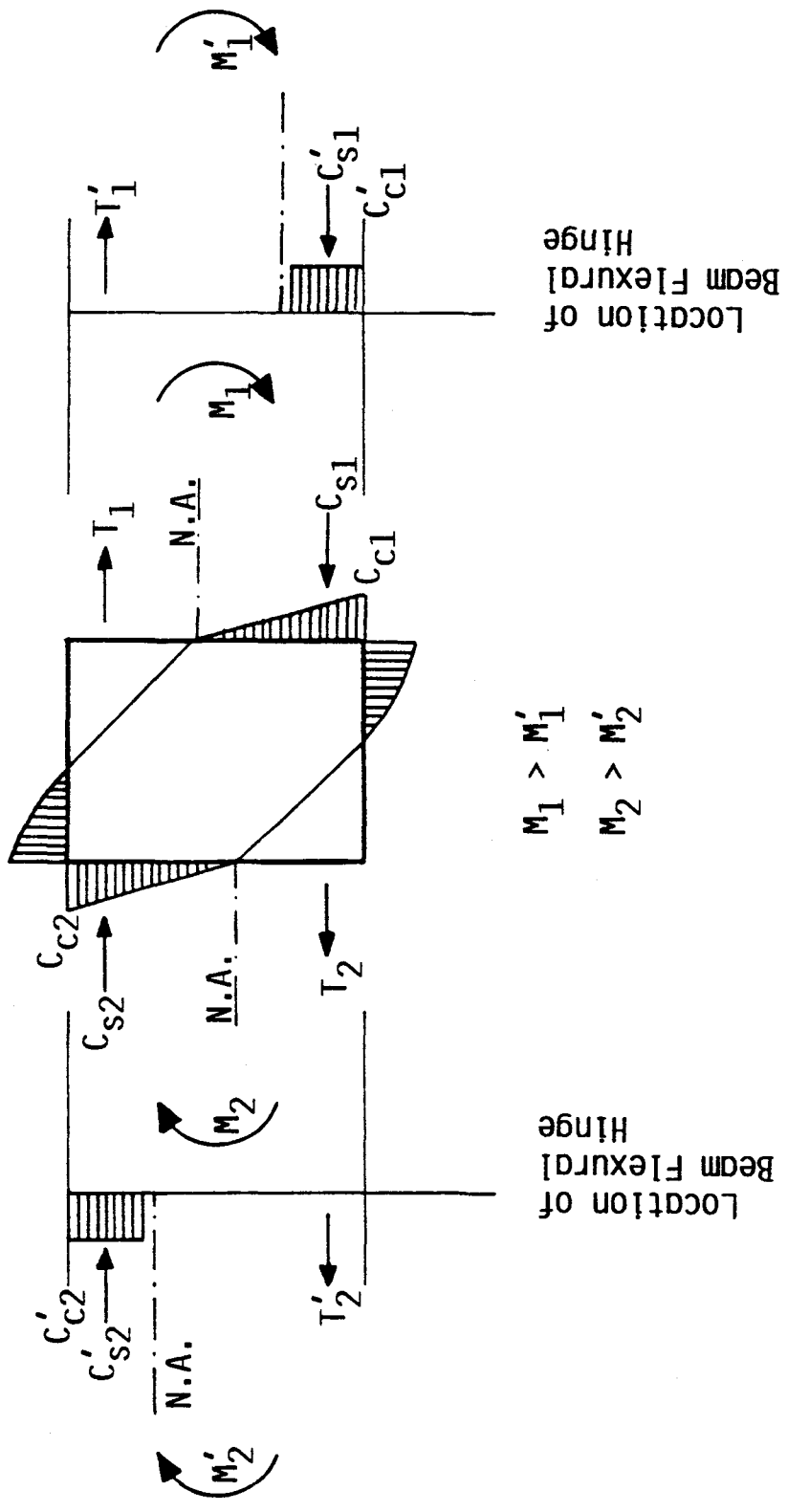
Fig. 3.37 Diagonal Compression Strut in Interior Joint with Relocated Beam Flexural Hinges

INTERIOR
CONNECTIONS

EXTERIOR
CONNECTIONS
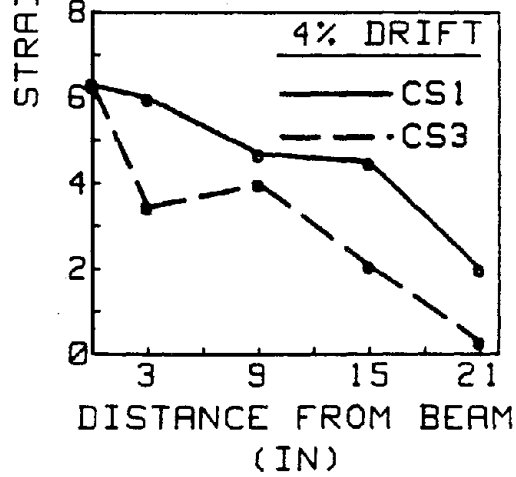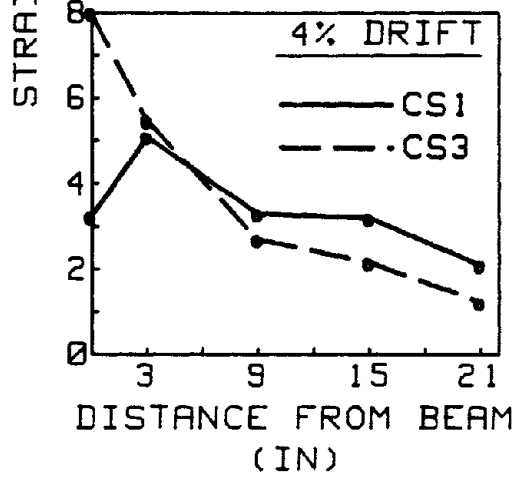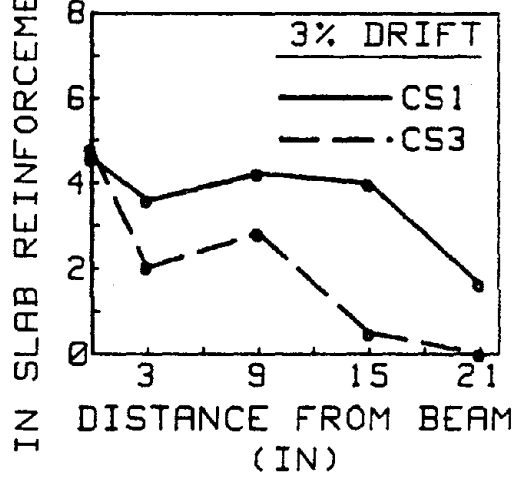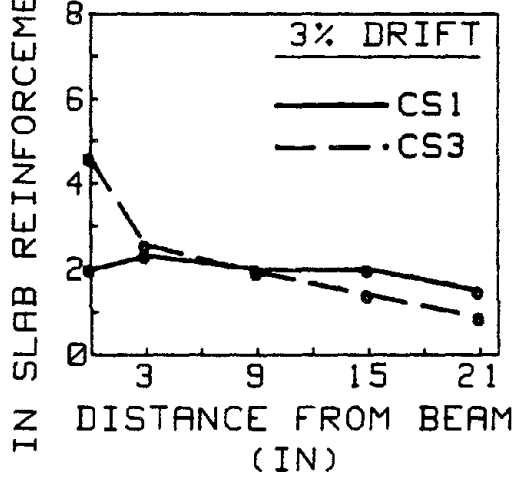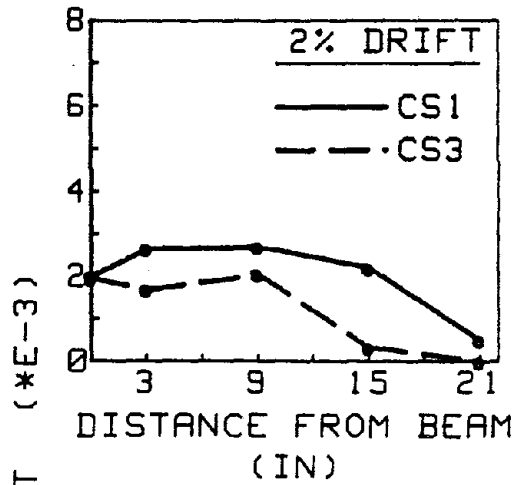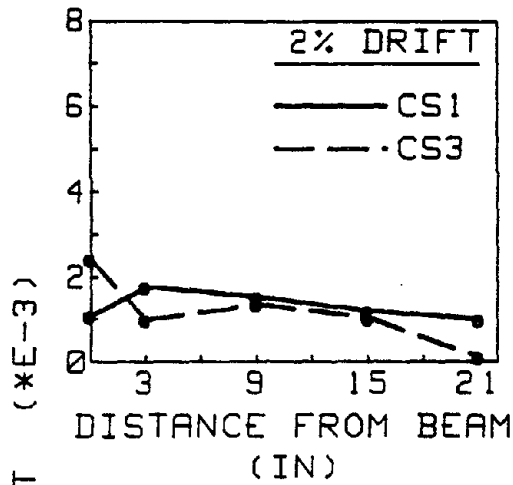
Fig. 3.38   Strain Variation in Reinforcement Across Slab Width
of Specimens CS1 and CS3

Fig. 4.1(a)   Measured Elongation of Main
              Beams in Specimens without a
              Floor Slab

Fig. 4.1(b)   Measured Elongation of Main
              Beams in Specimens with a
              Floor Slab
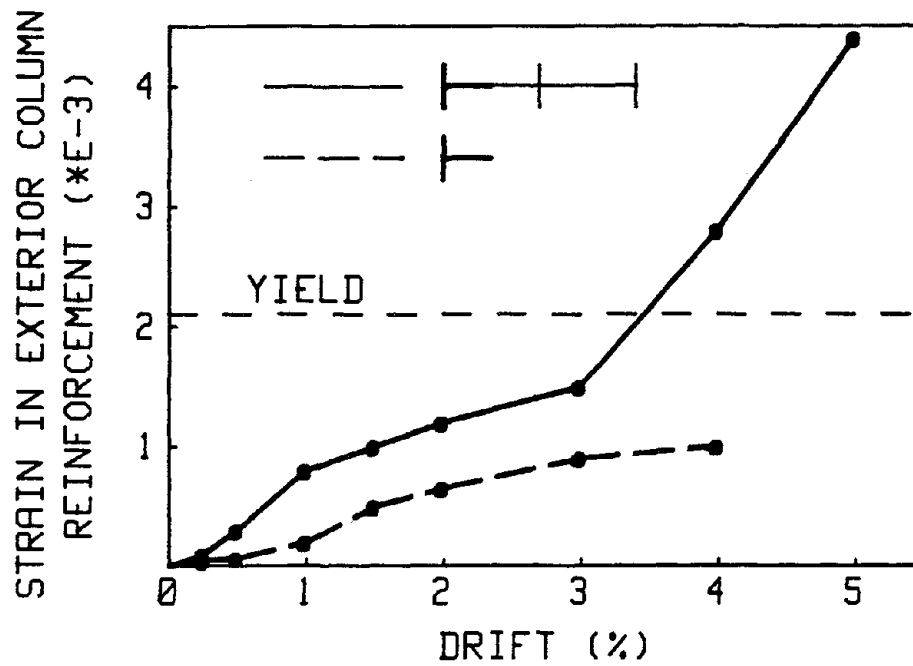
Fig. 4.2(a)   Strain in Exterior Column Reinforcement of
              Specimens C and E
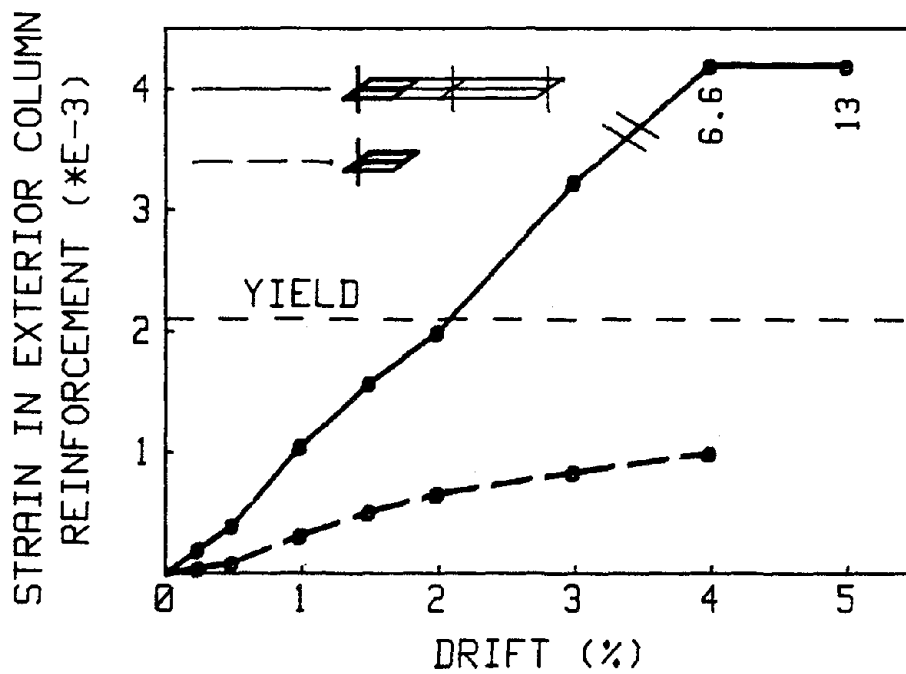
Fig. 4.2(b)   Strain in Exterior Column Reinforcement of
              Specimens CS1 and ES1
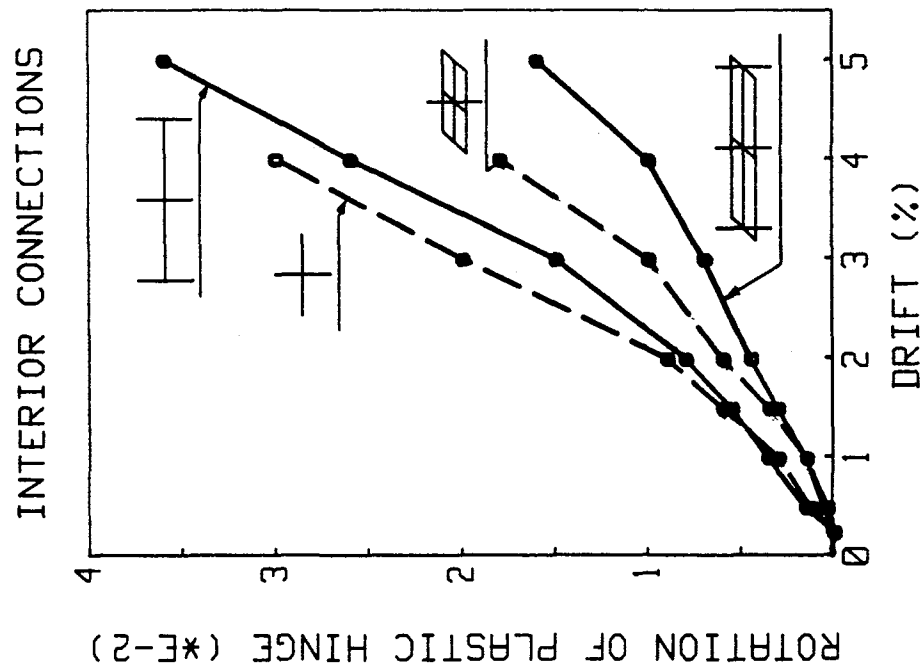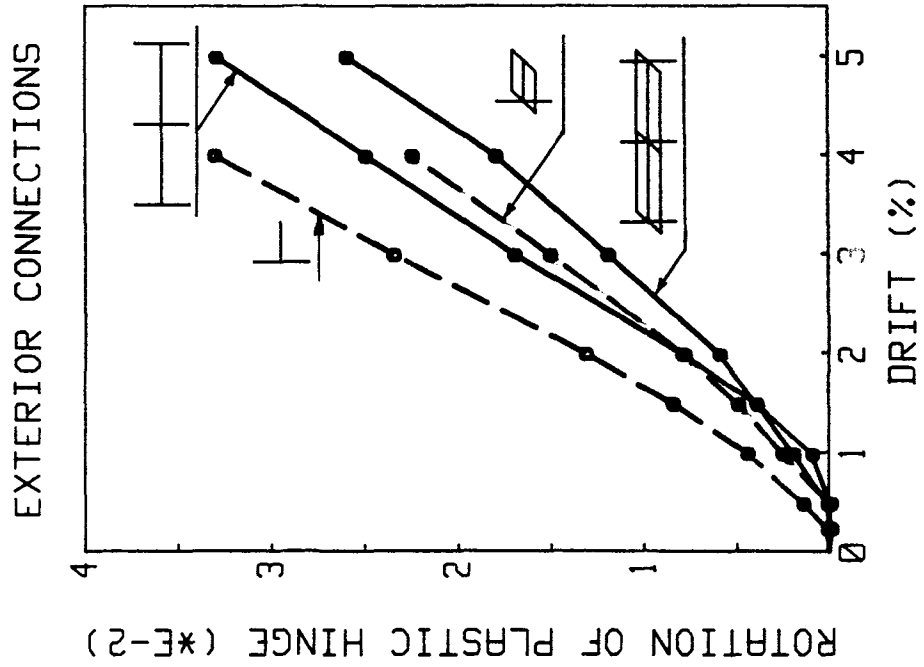
Fig. 4.3 Rotation of Beam Flexural Hinges

178

Fig. 4.4(b) Distribution of Lateral Load among Columns in Specimen CS1

Fig. 4.4(a) Distribution of Lateral Load among Columns in Specimen C
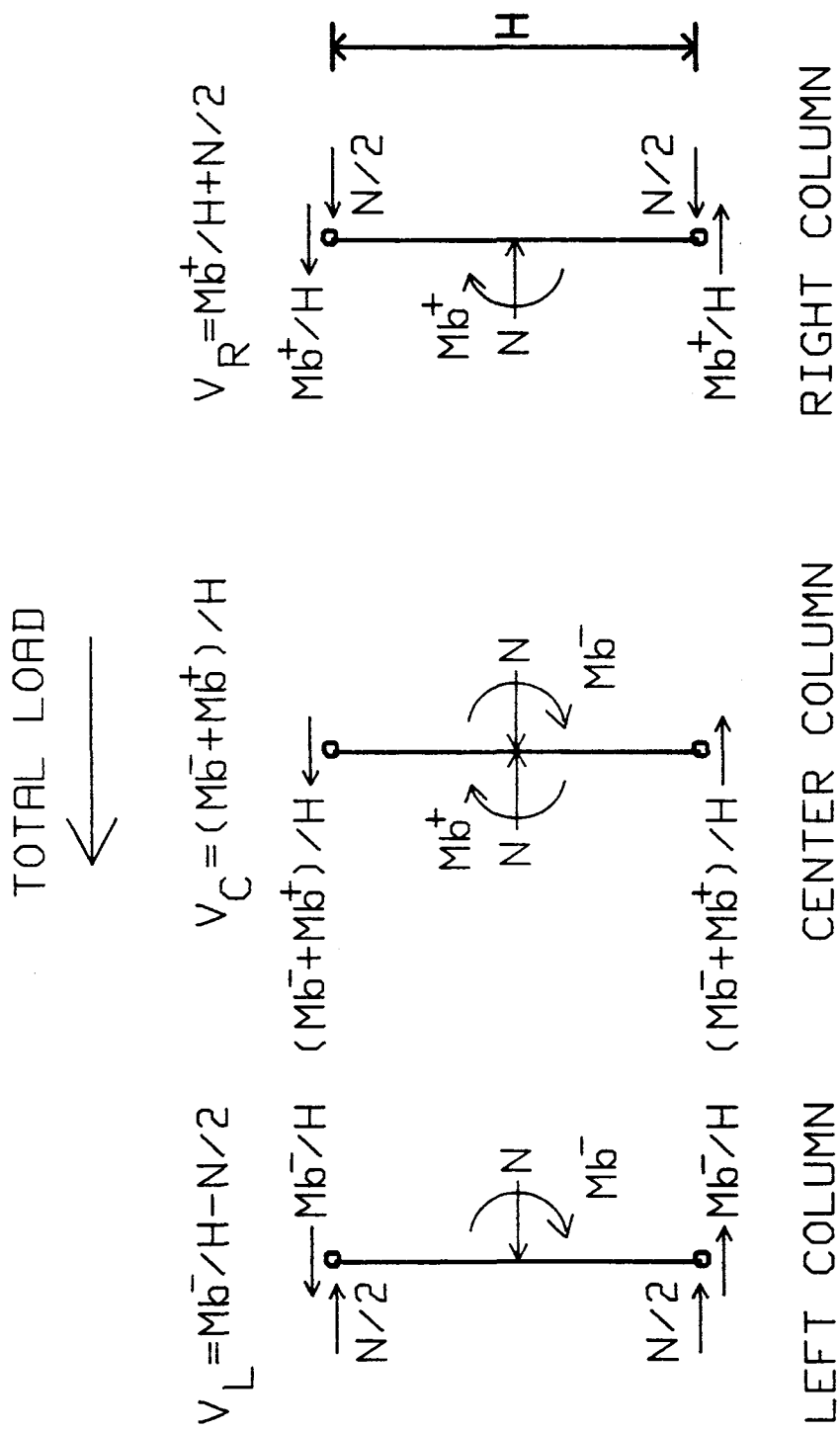
Fig. 4.5 Mechanism of Load Distribution
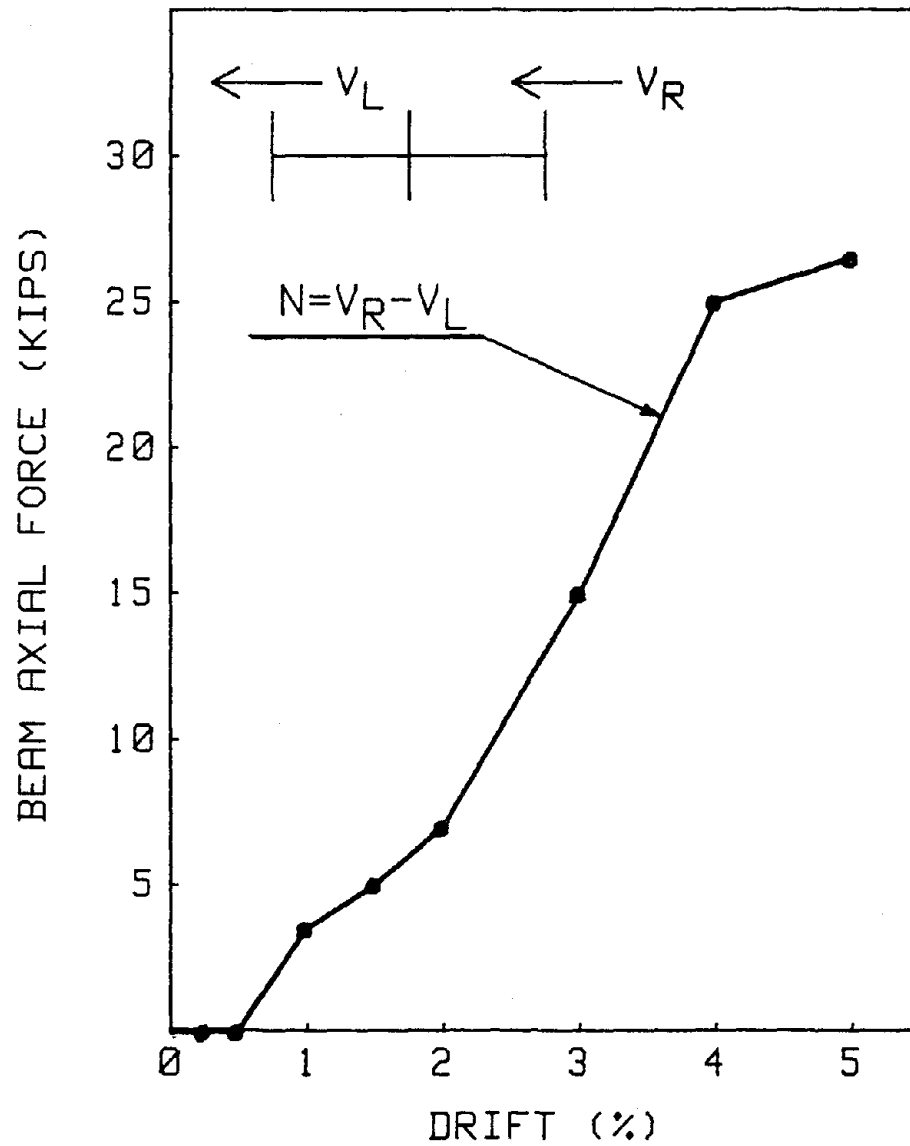
Fig. 4.6   Magnitude of Axial Force in Main Beams of
           Specimen C
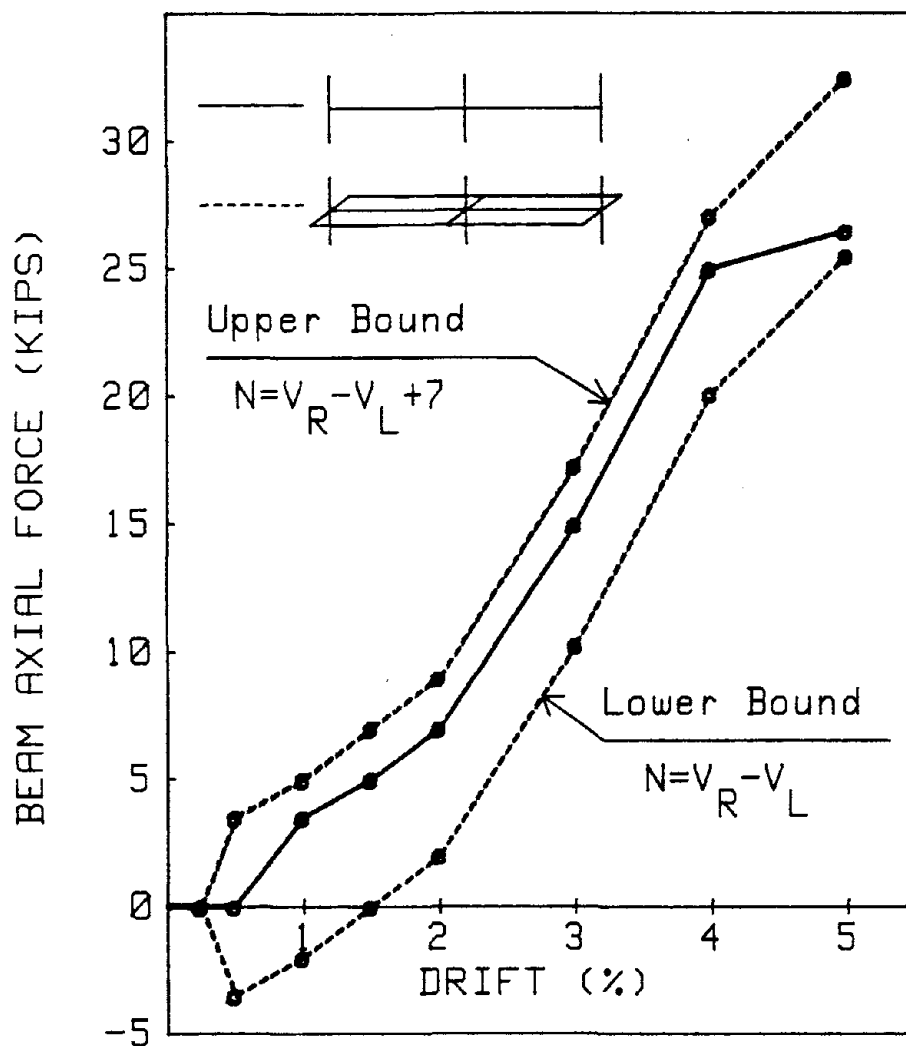
Fig. 4.7   Range of Axial Force in Main Beams of Specimen CS1
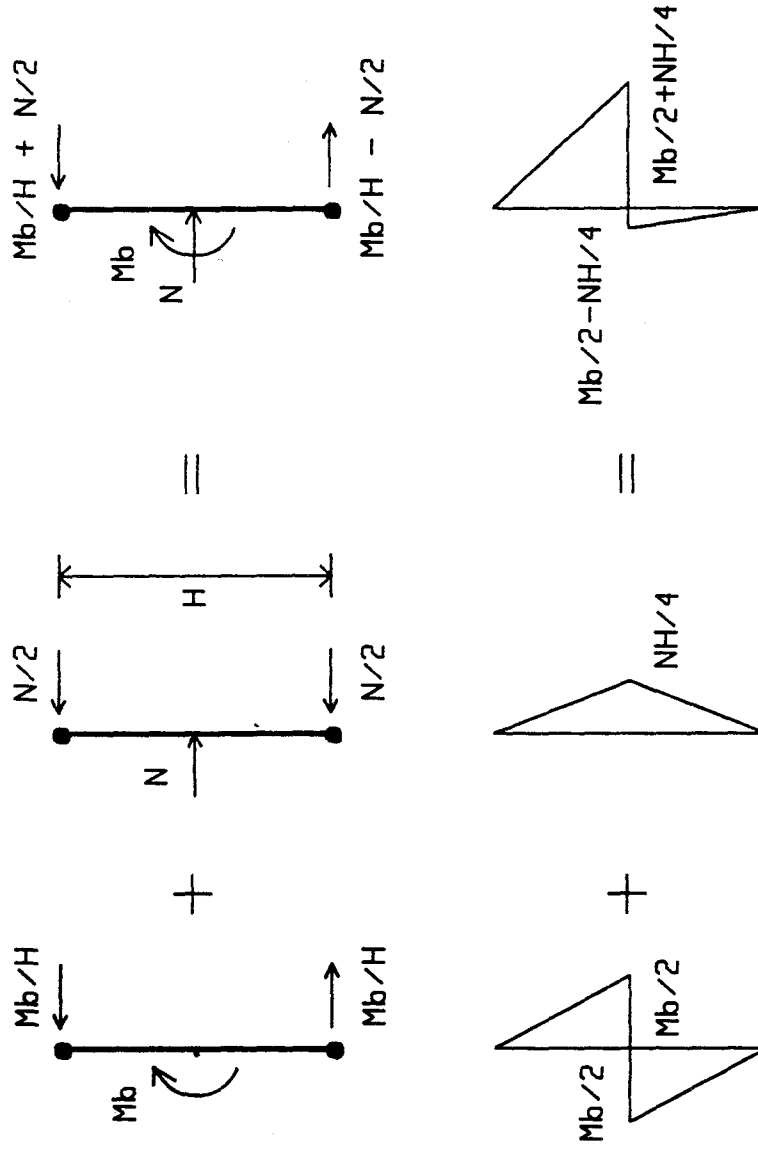
Fig. 4.8   Increase in Column Moment due to Presence of Beam Axial Force
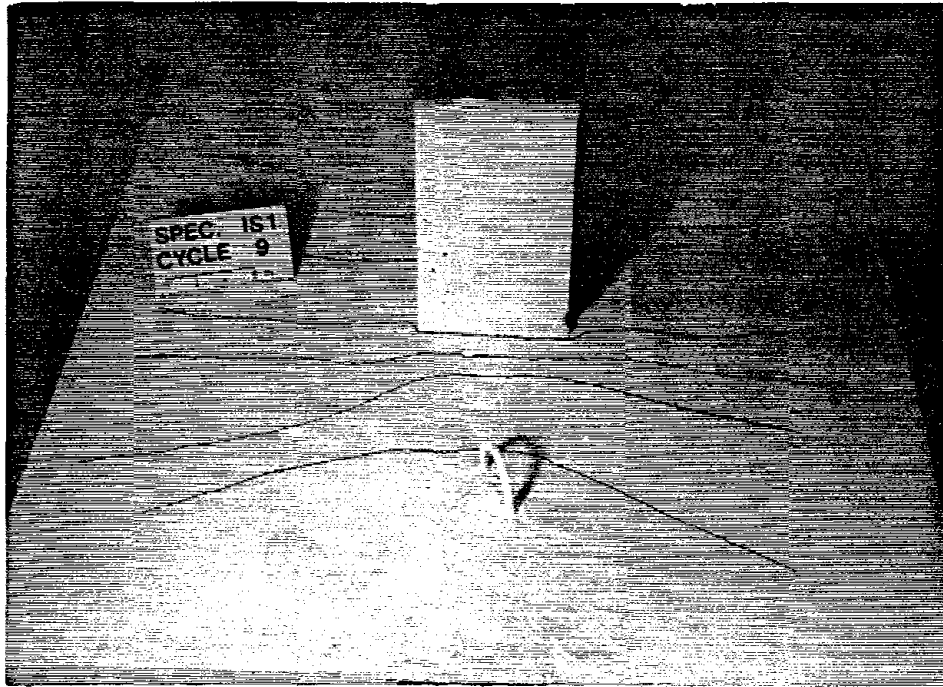
Fig. 4.9(a)   Transverse Cracks in the Slab of Specimen IS1
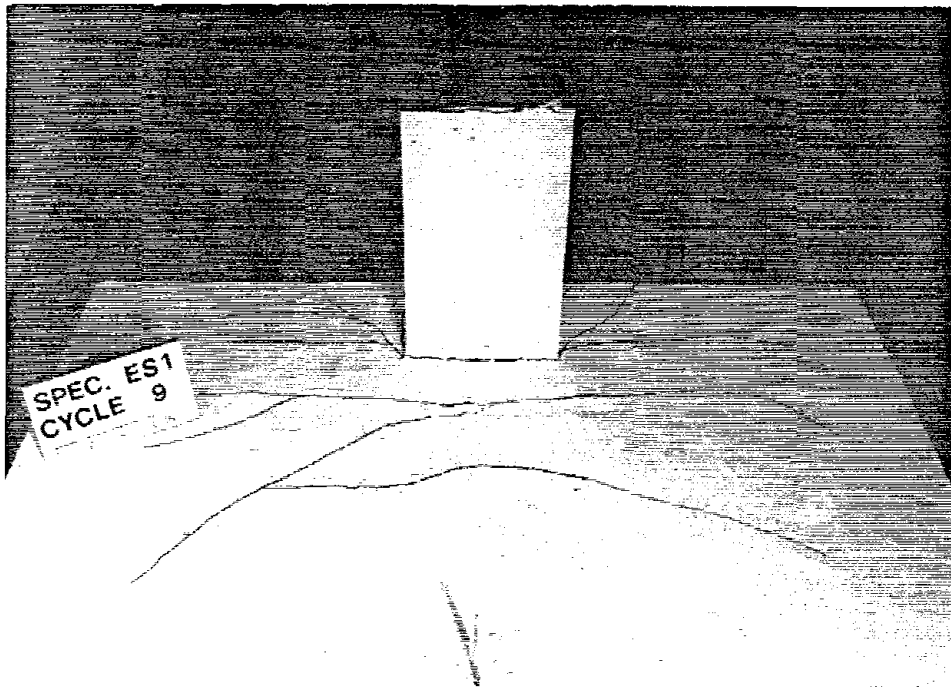
Fig. 4.9(b)   Transverse Cracks in the Slab of Specimen ES1

INTERIOR
CONNECTIONS

EXTERIOR
CONNECTIONS
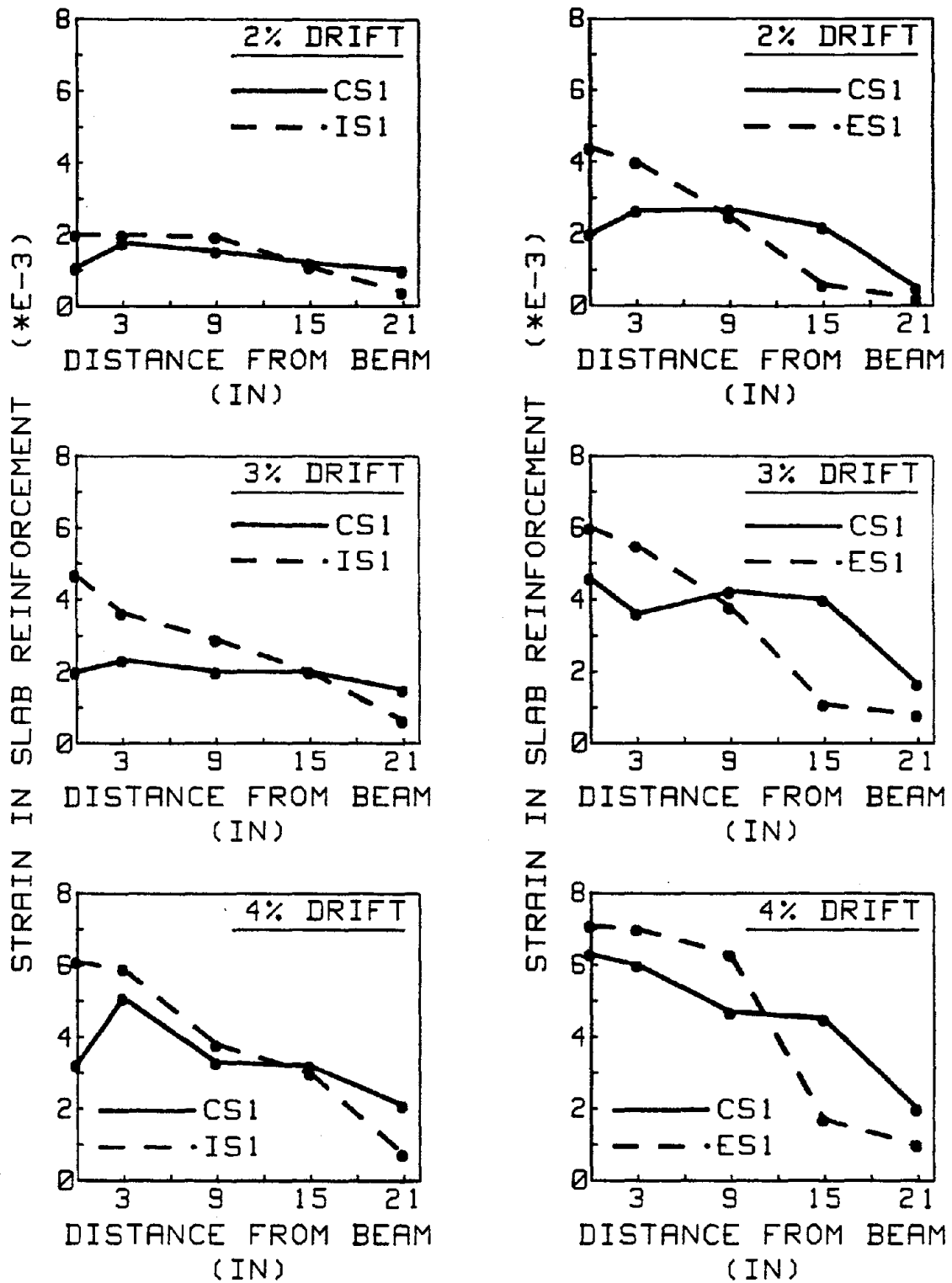
Fig. 4.10 Strain Variation in Reinforcement across Slab width
of Specimens CS1, IS1, and ES1

ISOLATED CONNECTIONS
Fixed Points of Inflection

CONTINUOUS CONNECTIONS
Floating Points of inflection
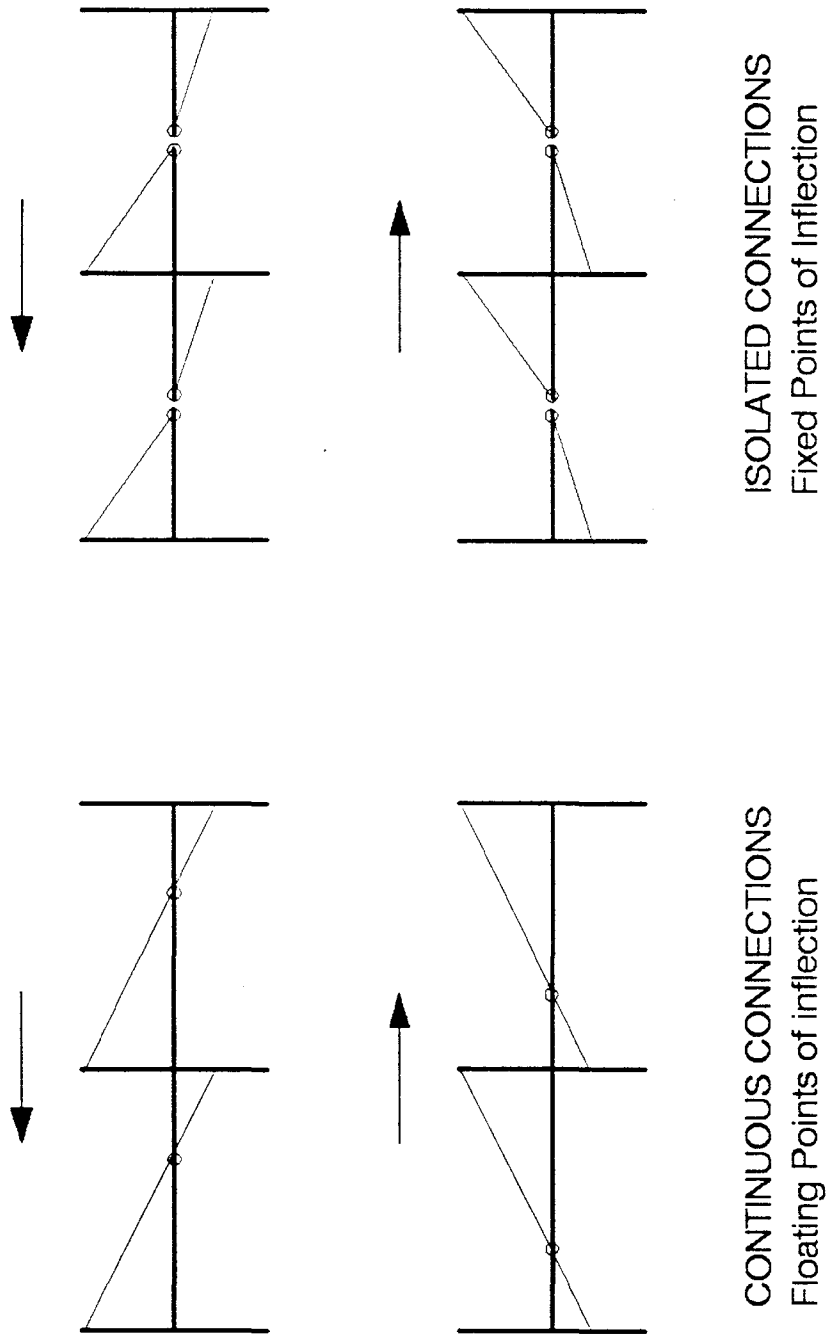
Fig. 4.11 Actual and Idealized Locations of Points of Inflection
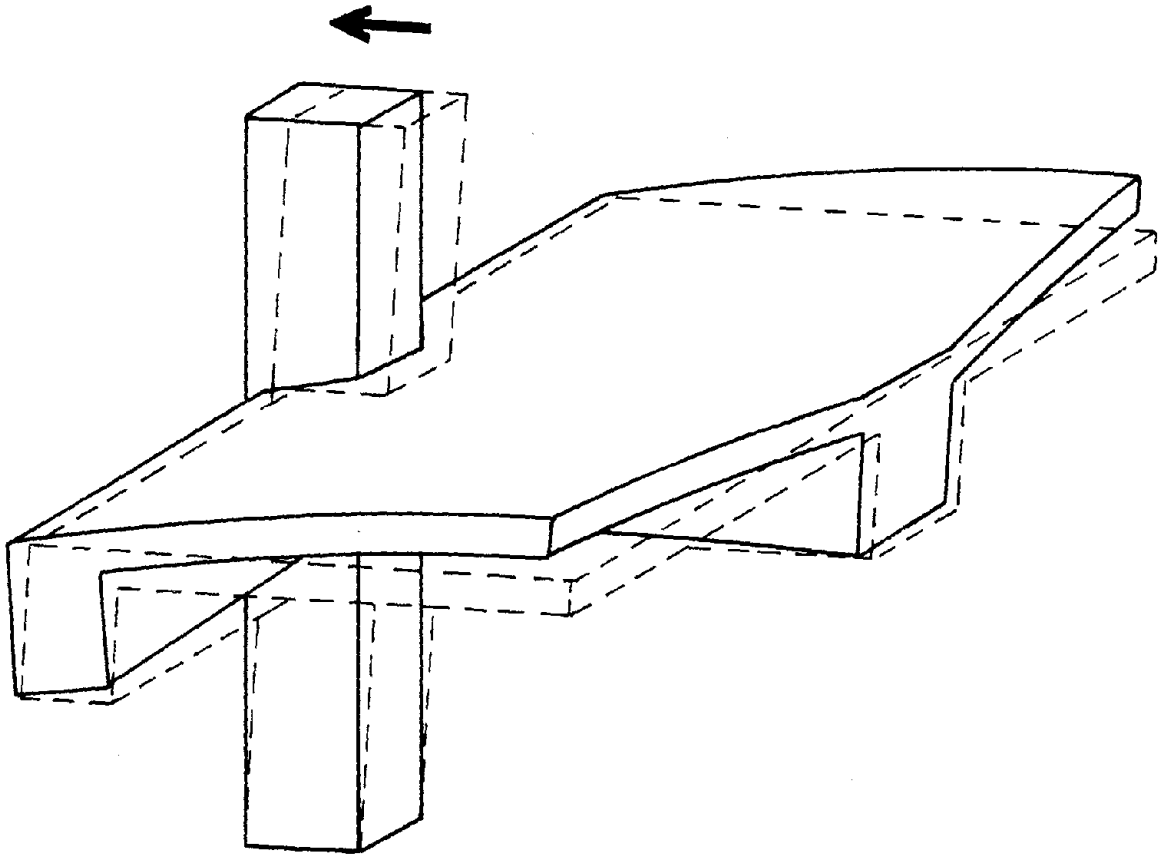
Fig. 4.12 Deflection Shape of Slab in Isolated Connections
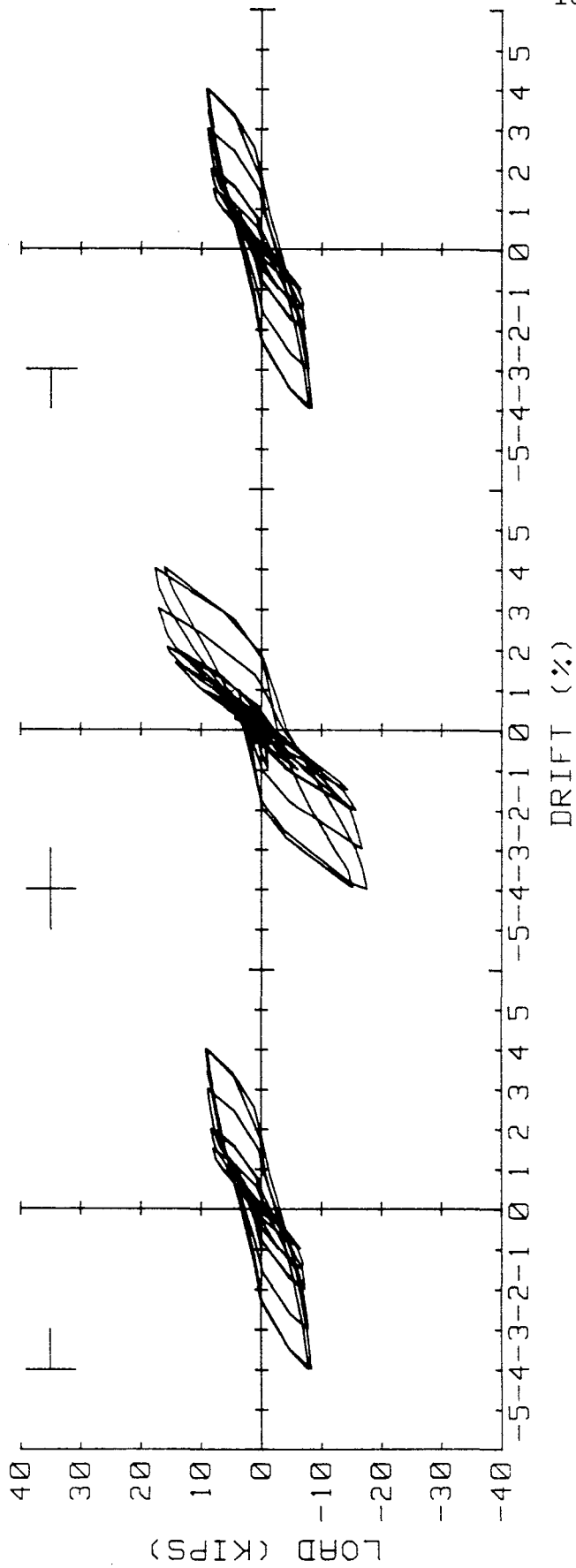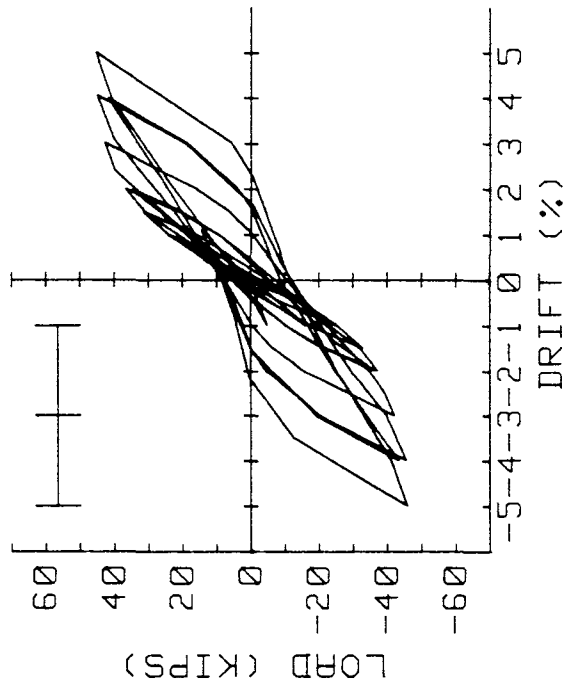
Fig. 4.13(a) Load vs. Drift curves of Specimens without a Floor Slab
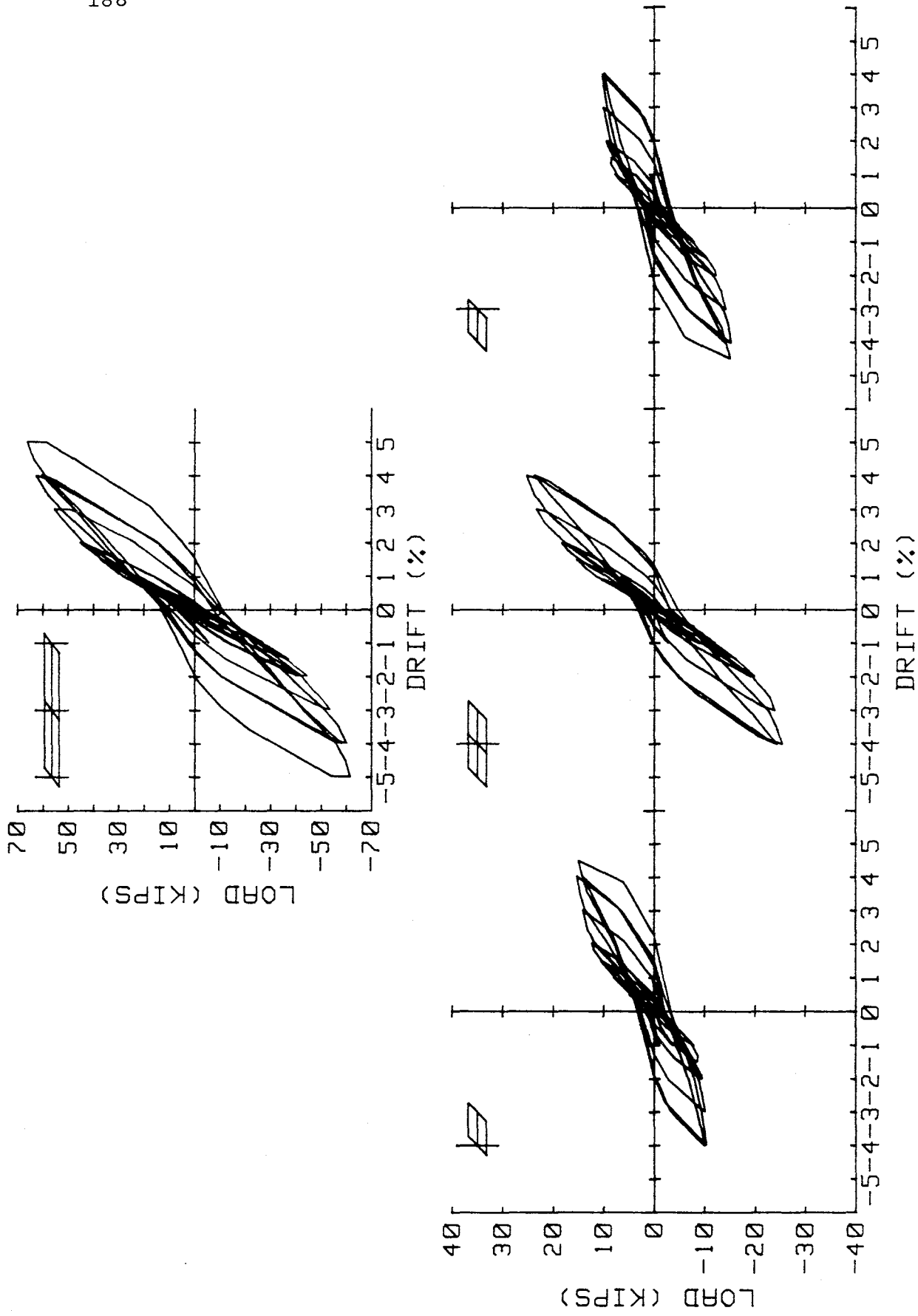
Fig. 4.13(b)   Load vs. Drift curves of Specimens with a Floor Slab
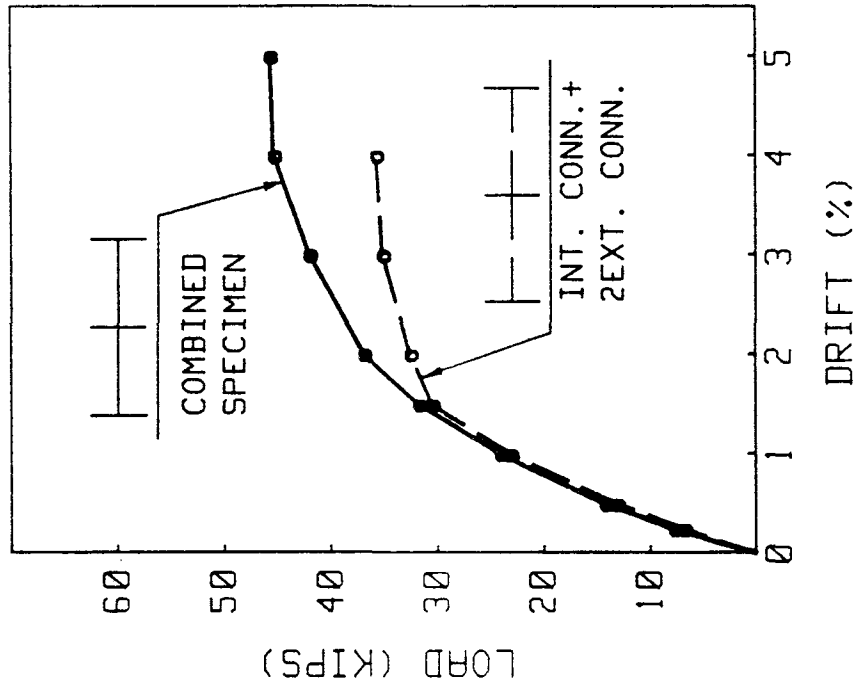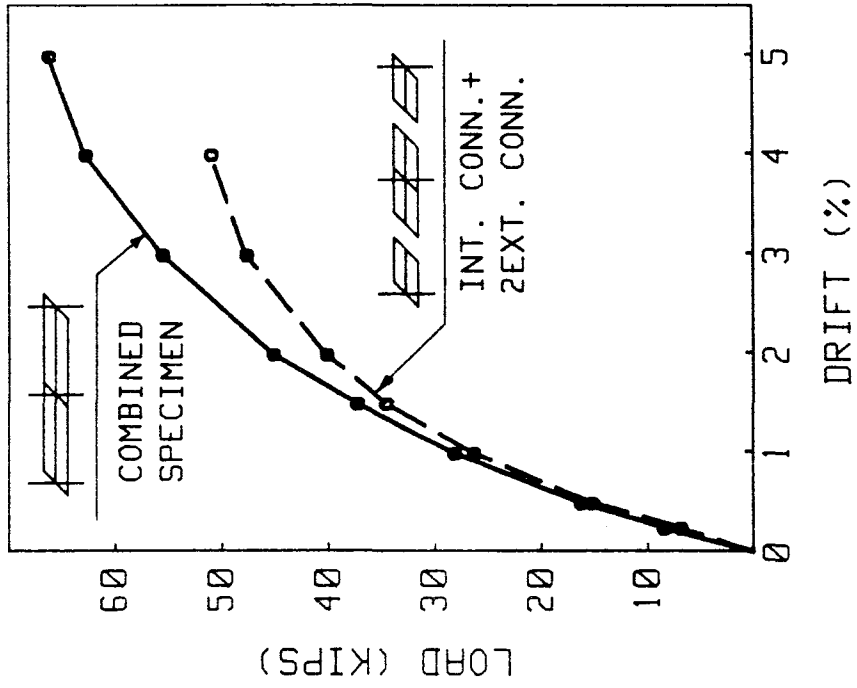
Fig. 4.14(a)   Envelops of Load vs. Drift
               Curves of Specimens without
               a Floor Slab

Fig. 4.14(b)   Envelops of Load vs. Drift
               Curves of Specimens with a
               Floor Slab
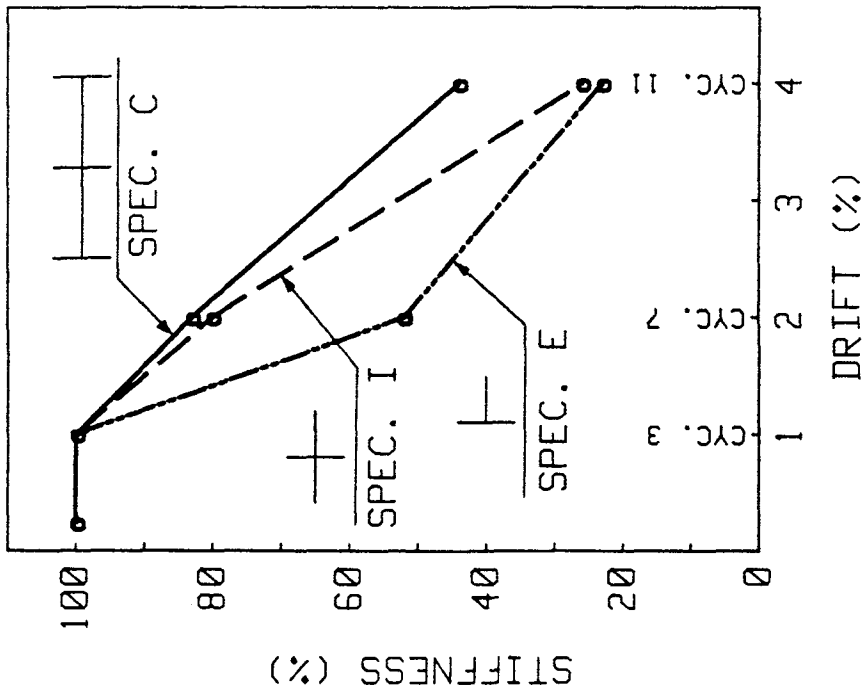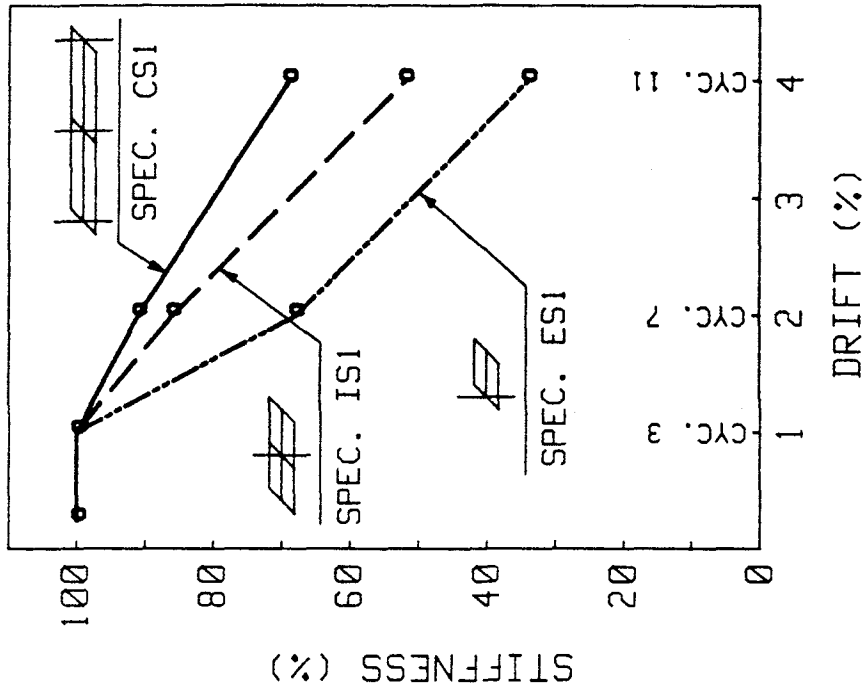
Fig. 4.15(a)   Loss of Stiffness in Specimens
without a Floor Slab

Fig. 4.15(b)   Loss of stiffness in Specimens
with a Floor Slab
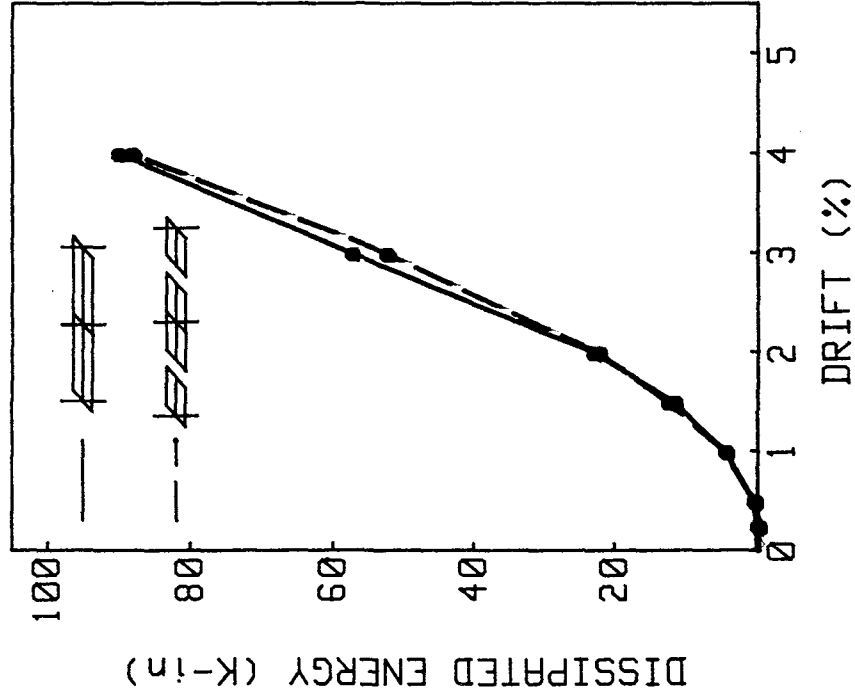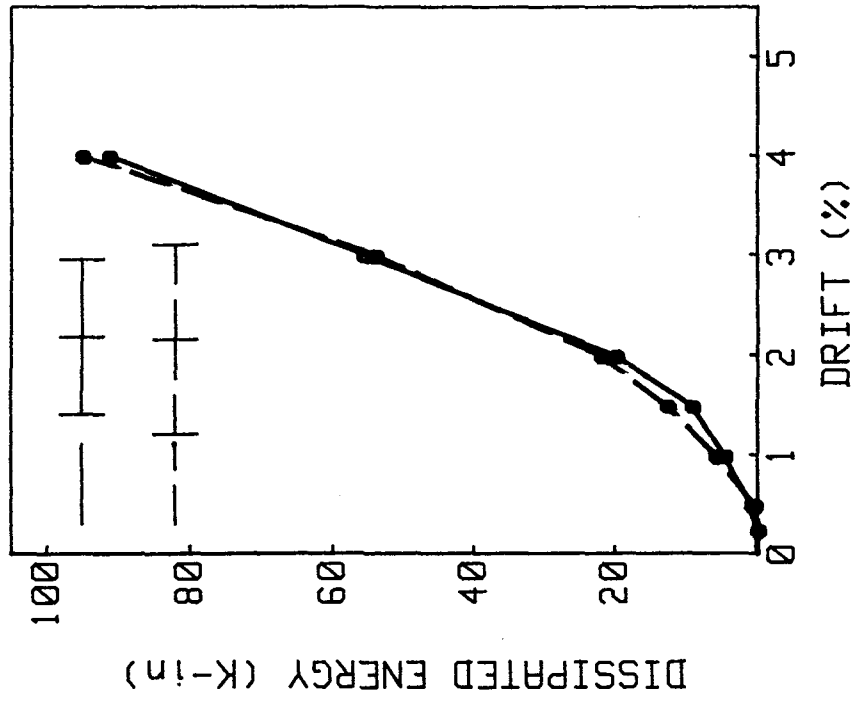
Fig. 4.16(a) Energy Dissipated by Specimens
without a Floor Slab

Fig. 4.16(b) Energy Dissipated by Specimens
with a Floor Slab
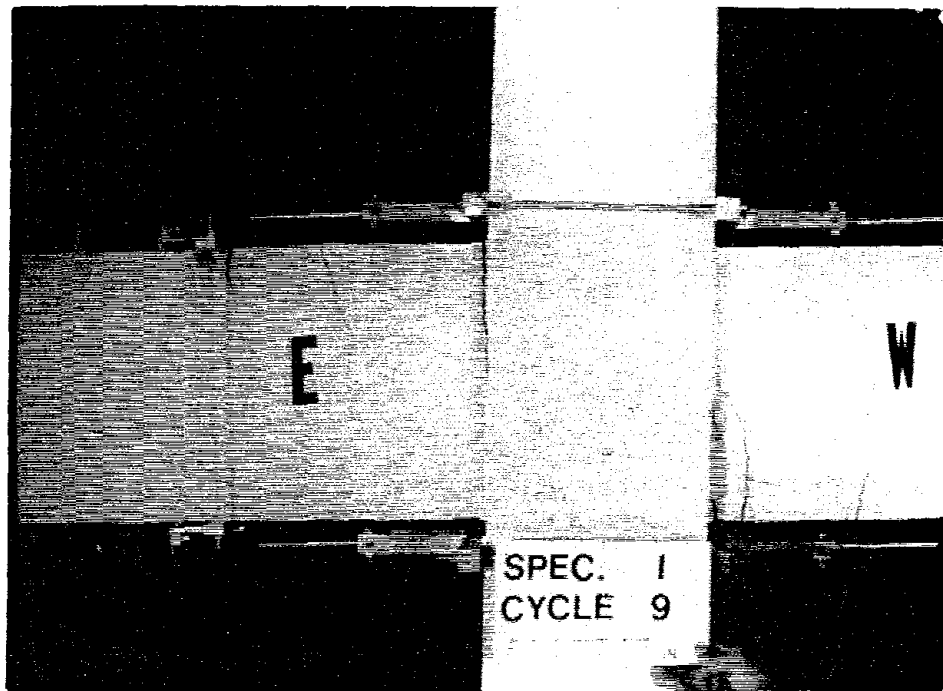
Fig. 4.17 Joint Shear Cracks of Specimen I
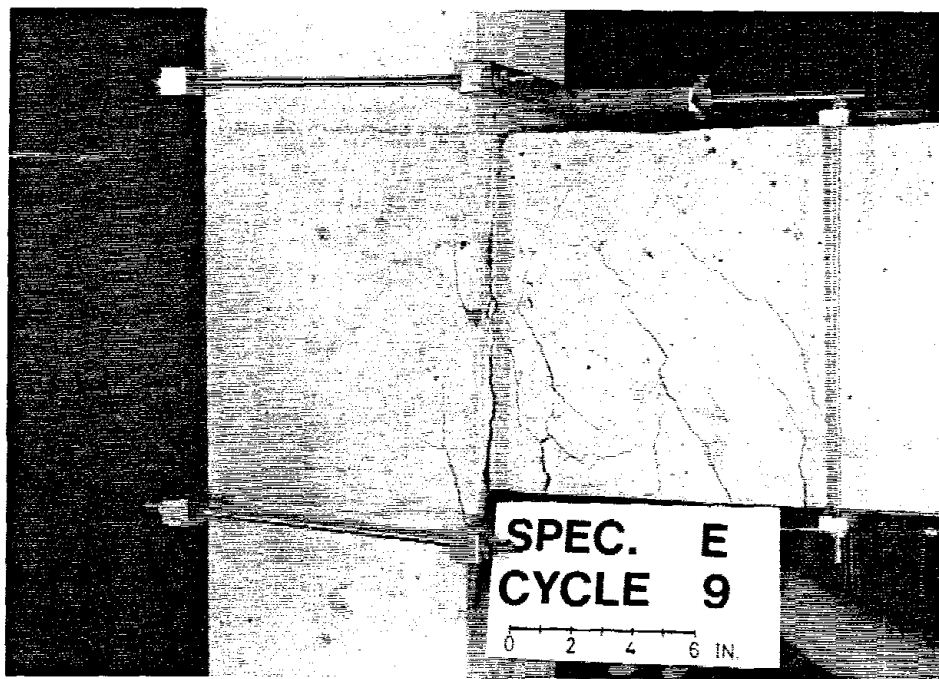
Fig. 4.18 Joint Shear Cracks of Specimen E

193
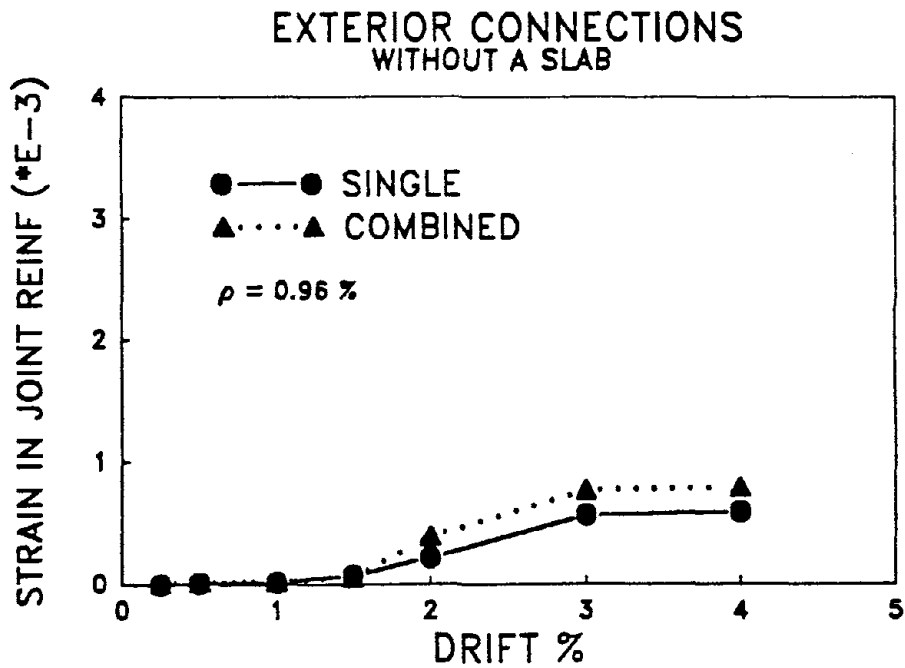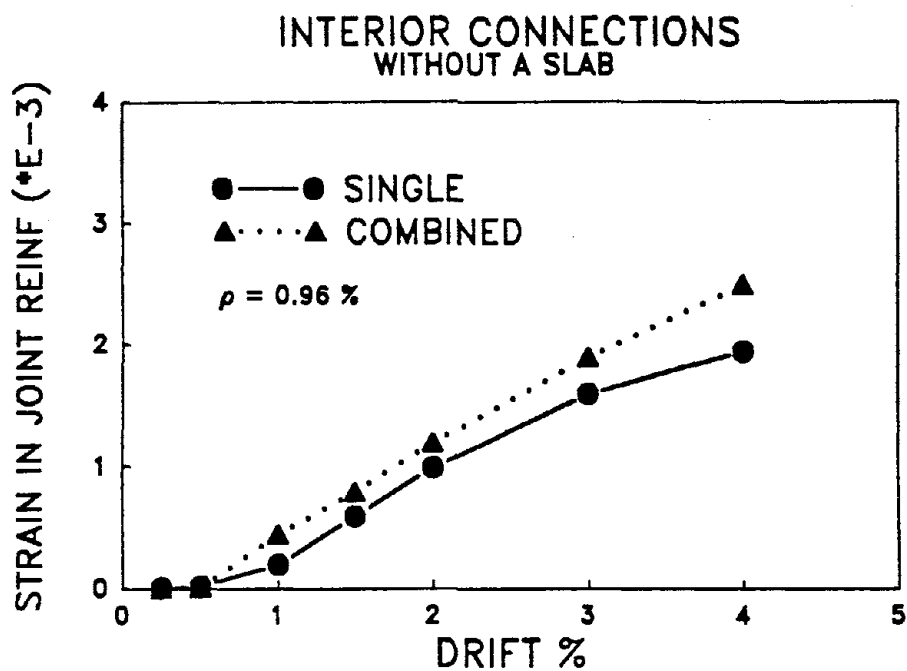
Fig. 4.19(a)   Strain in Joint Lateral Reinforcement of
              Specimens without a Floor Slab
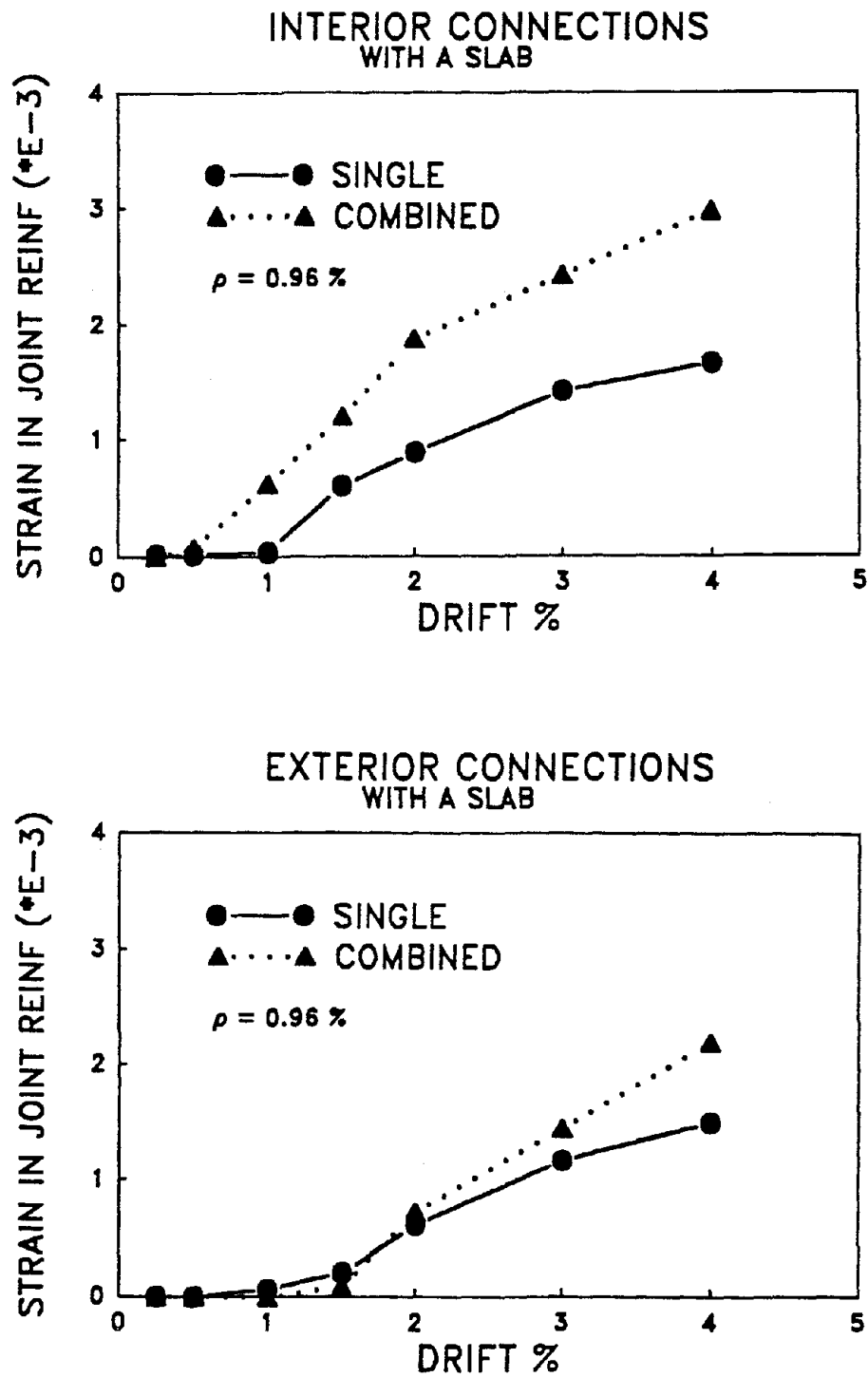
Fig. 4.19(b)   Strain in Joint Lateral Reinforcement of
              Specimens with a Floor Slab

INTERIOR JOINT   EXTERIOR JOINT
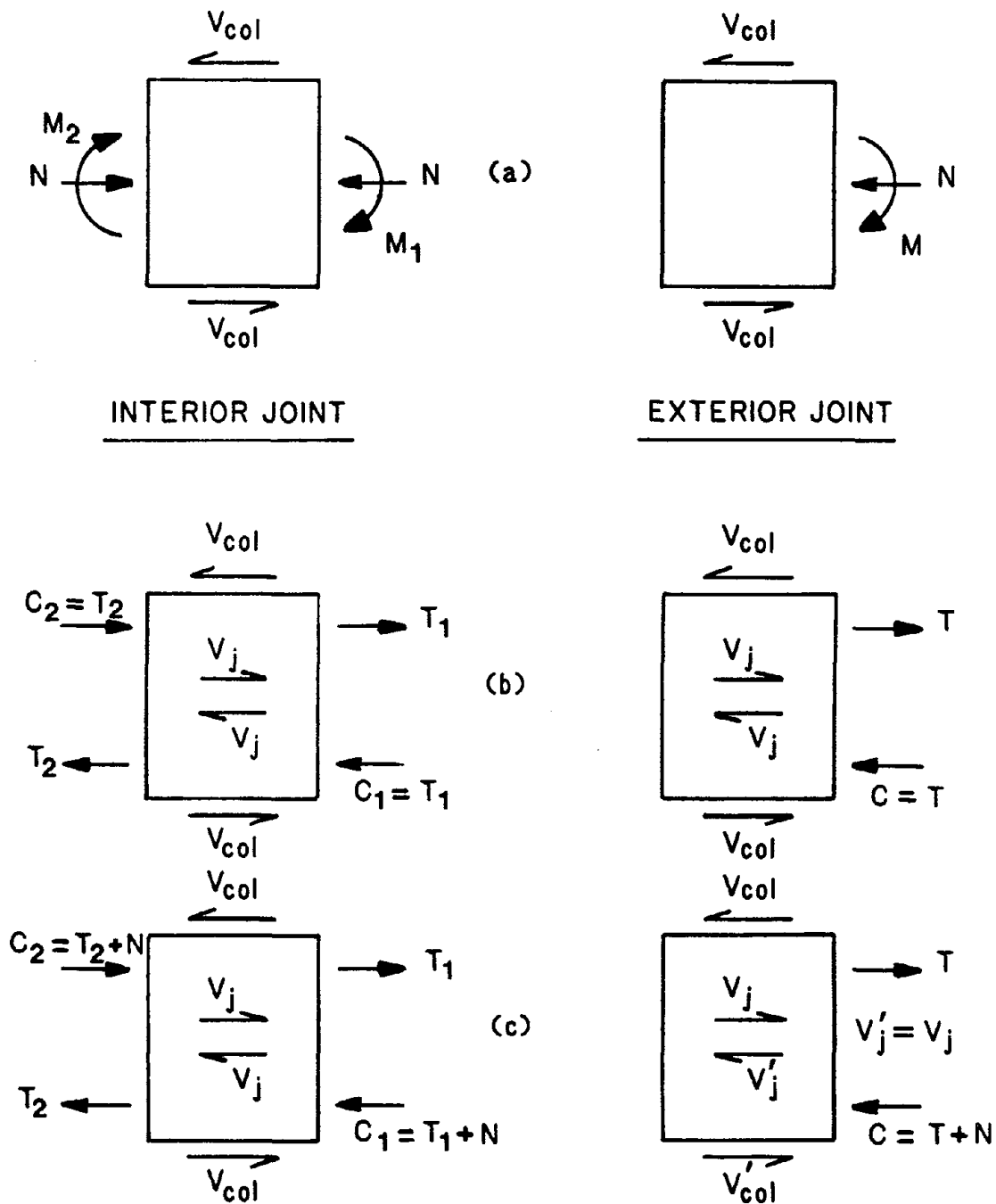
Fig. 4.20 (a) External Forces Acting in Joints, (b)
Internal Stress Resultant Excluding Beam Axial
Force, (c) Internal Stress Resultant Including
Beam Axial Force
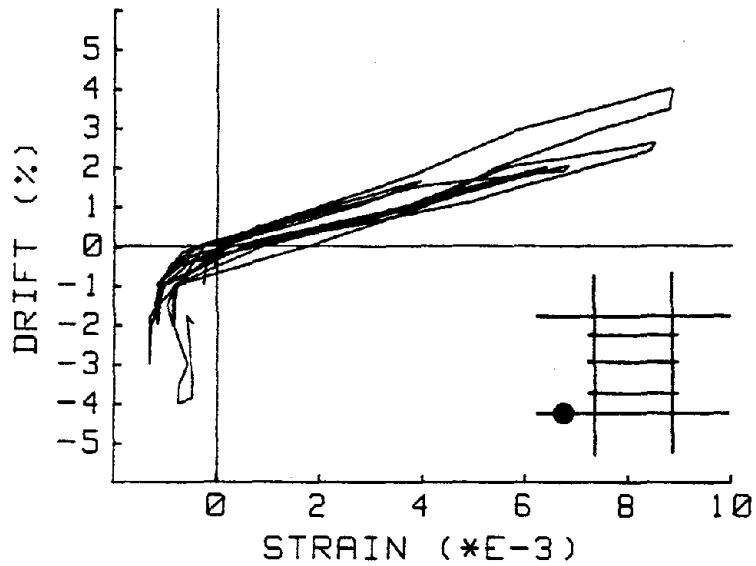
Fig. 4.21   Strain in Beam Bottom Reinforcement of
            Specimen I
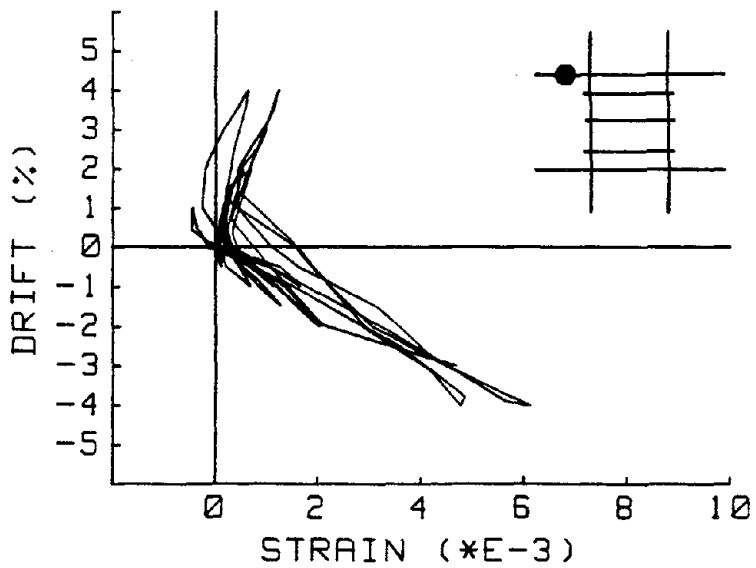
Fig. 4.22   Strain in Beam Top Reinforcement of
            Specimen IS1
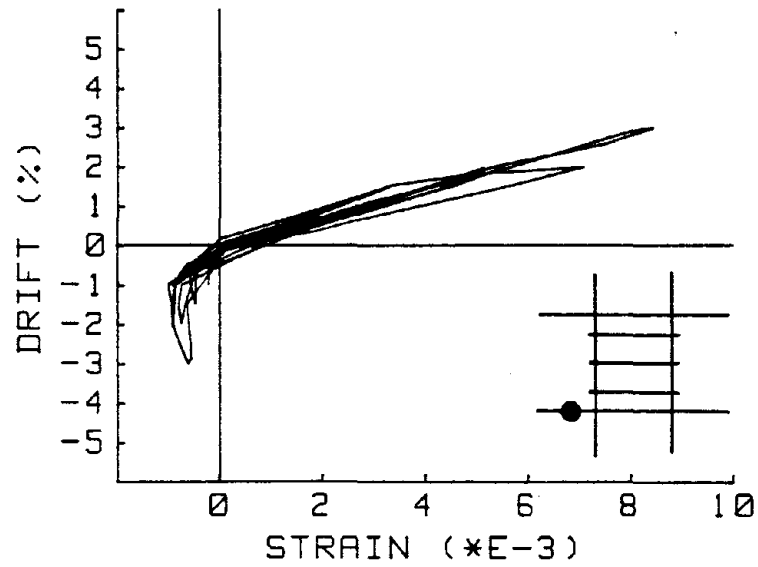
Fig. 4.23   Strain in Beam Bottom Reinforcement of
Specimen IS1
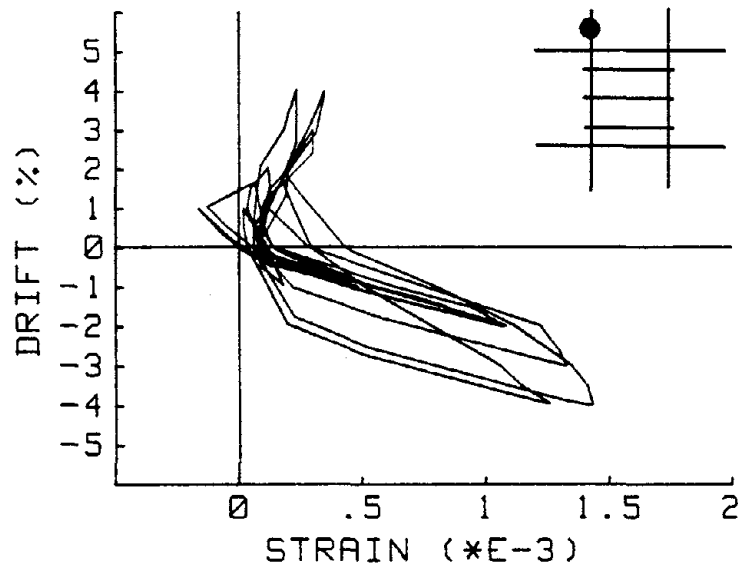
Fig. 4.24   Strain in Column Reinforcement of Specimen I
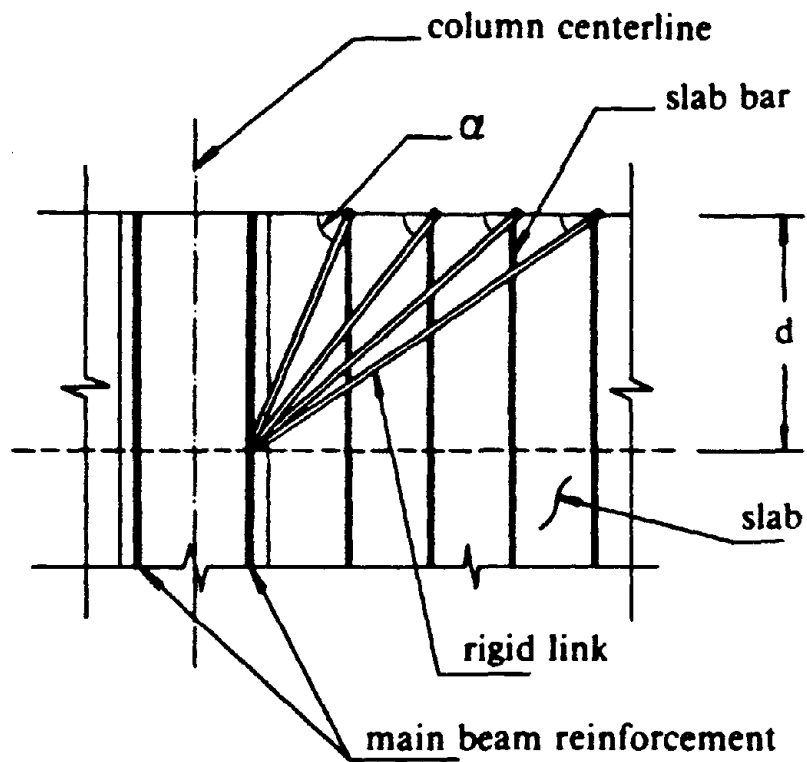
Fig. 5.1   Mechanism Assumed (Ref. 56)
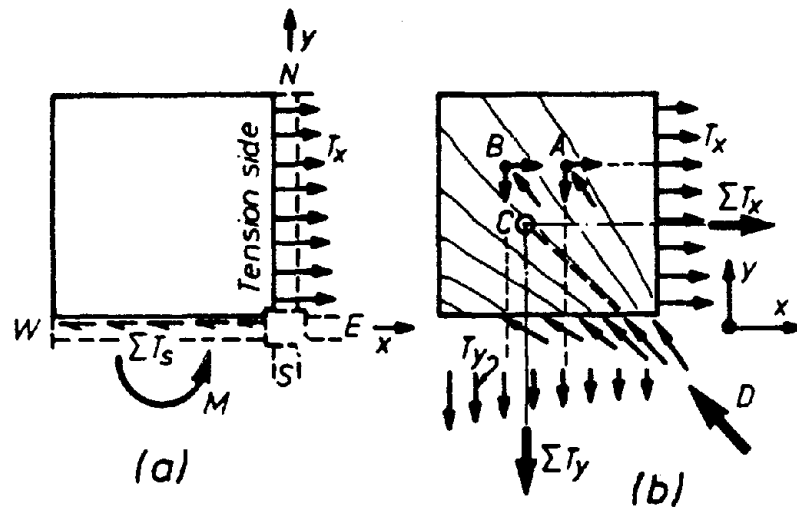
Fig. 5.2 Equilibrium Criteria for the Mechanism of Load
Resistance in one Quadrant of a Floor Slab Acting
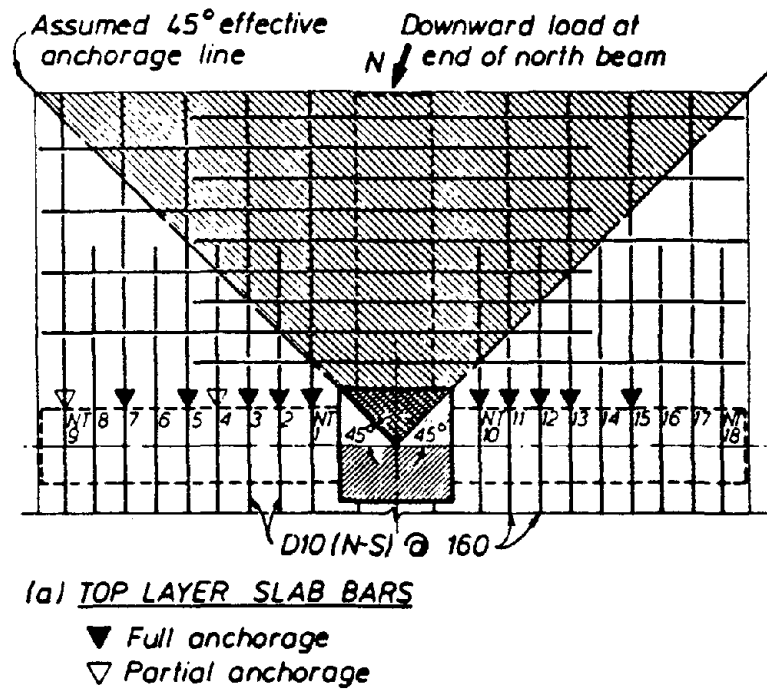as a Tension Flange of a Beam (Ref. 58)

(a) TOP LAYER SLAB BARS

▼ Full anchorage
▽ Partial anchorage

Fig. 5.3 Determination of Number of Longitudinal Slab
Bars Effectively Anchored (Ref. 58)
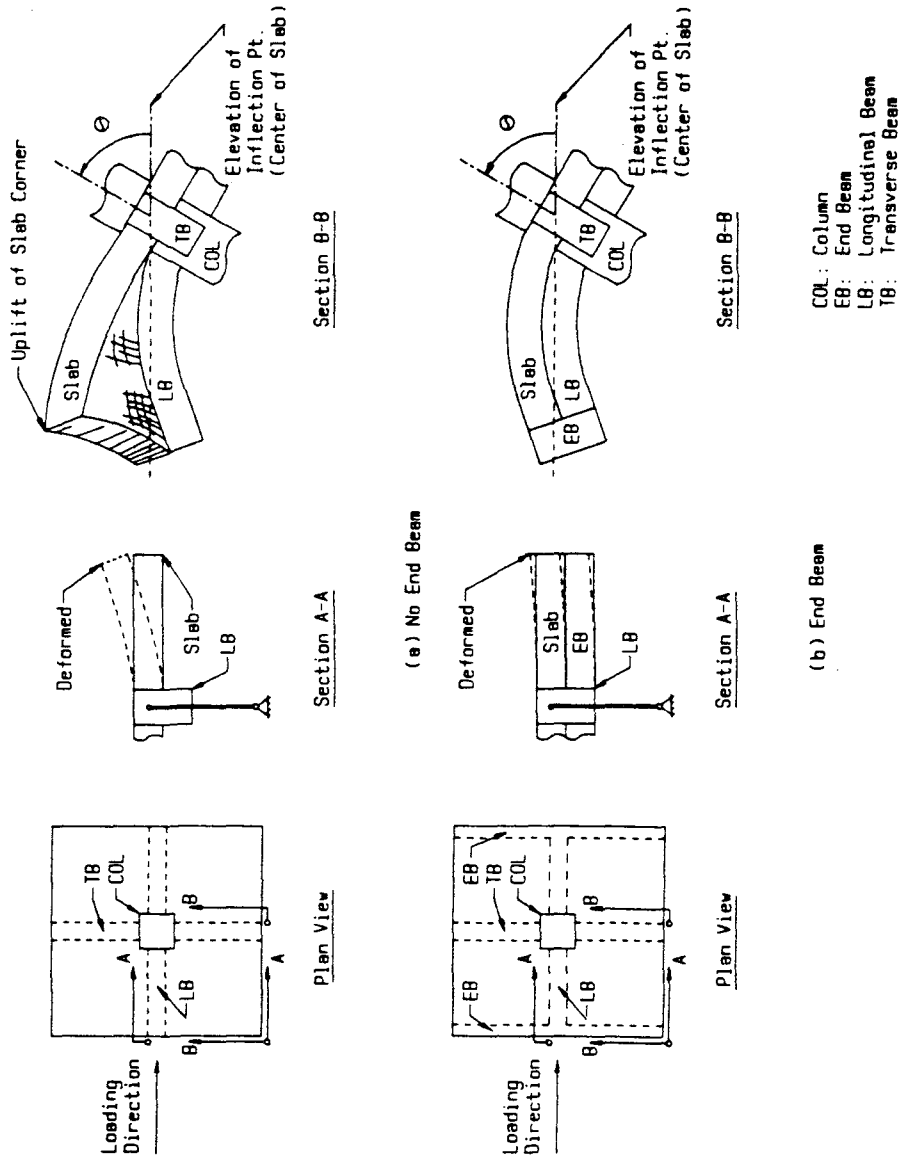
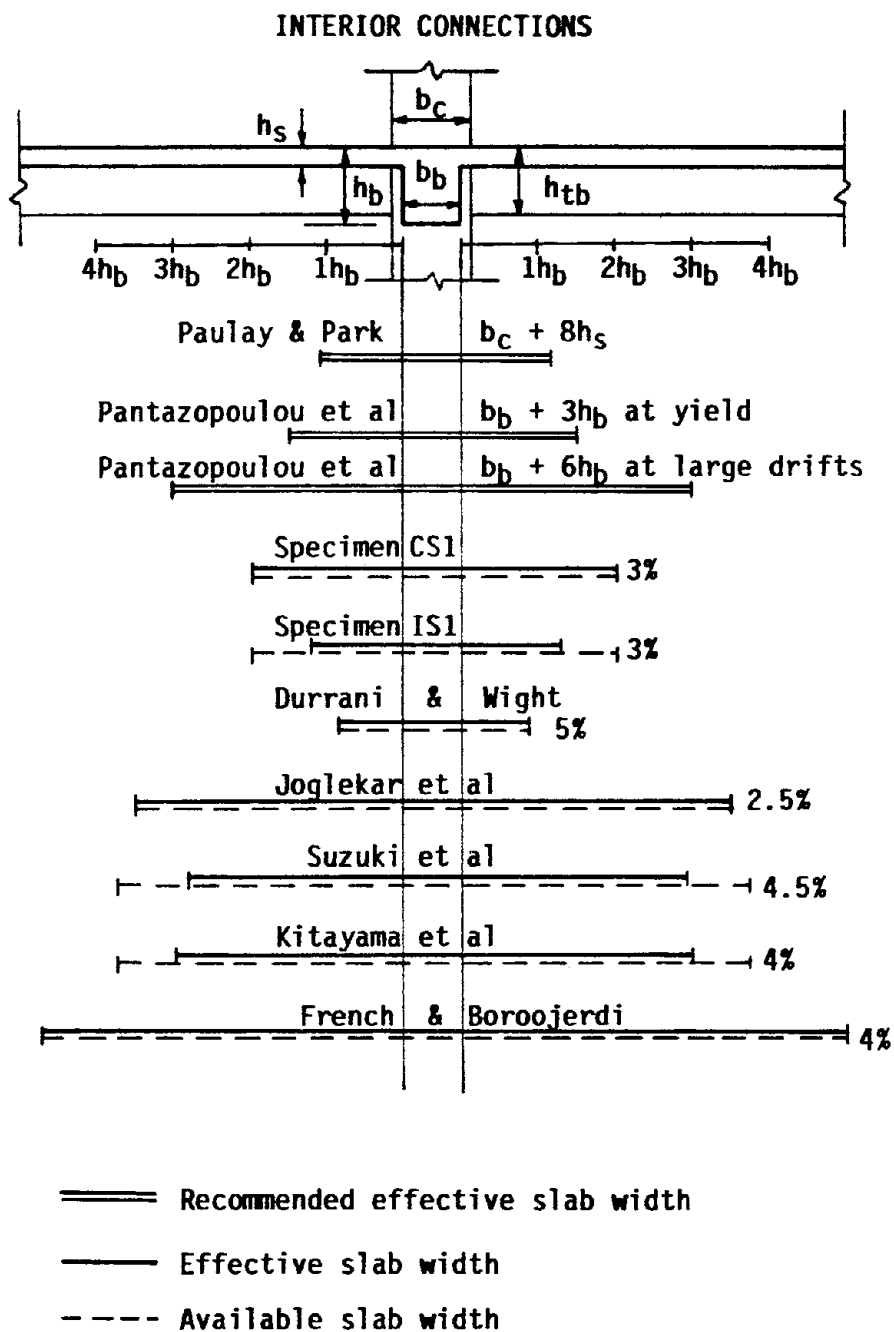Fig. 5.4 Effect of End Beam on Curvature of Slab (Ref. 51)

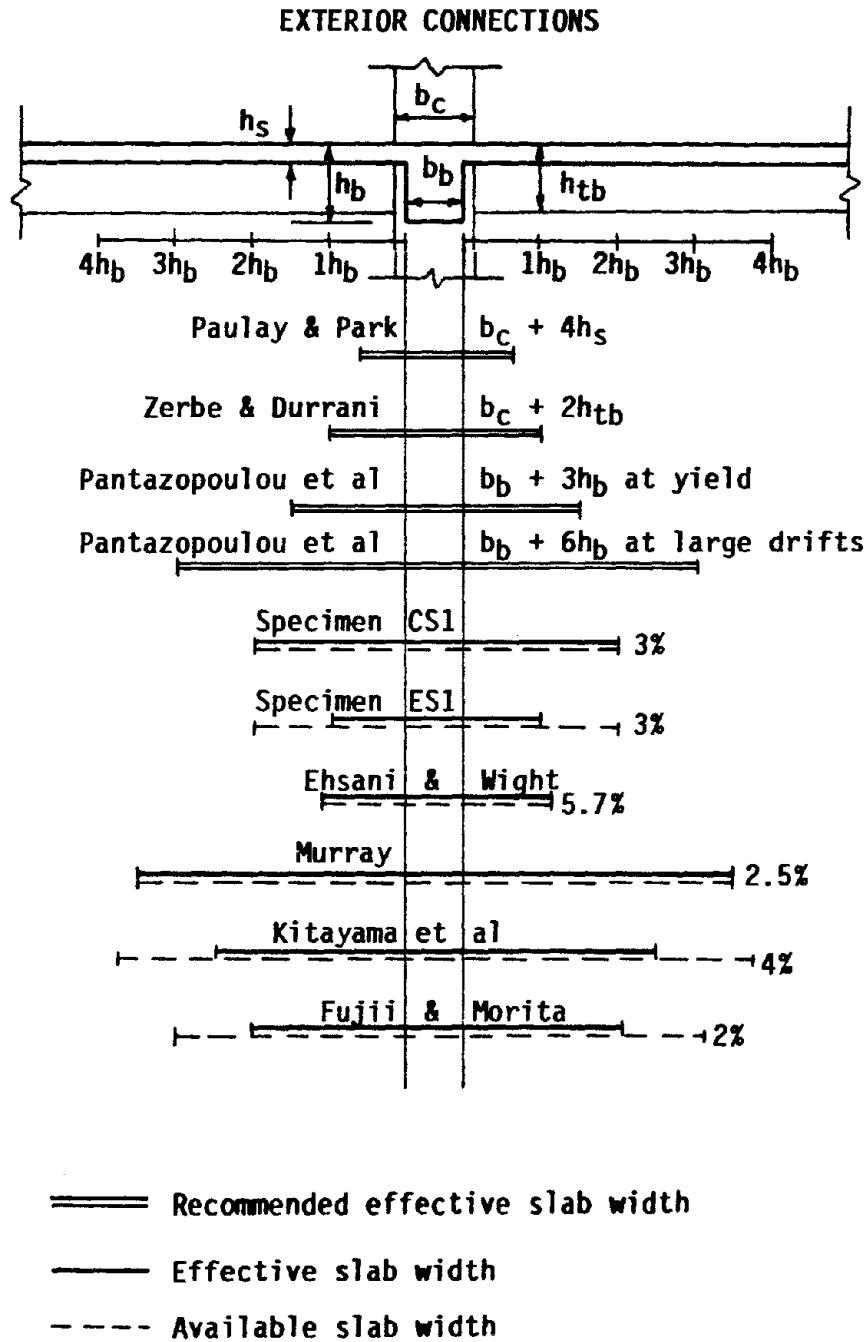Fig. 5.5(a) Effective Slab Width for Interior Connections

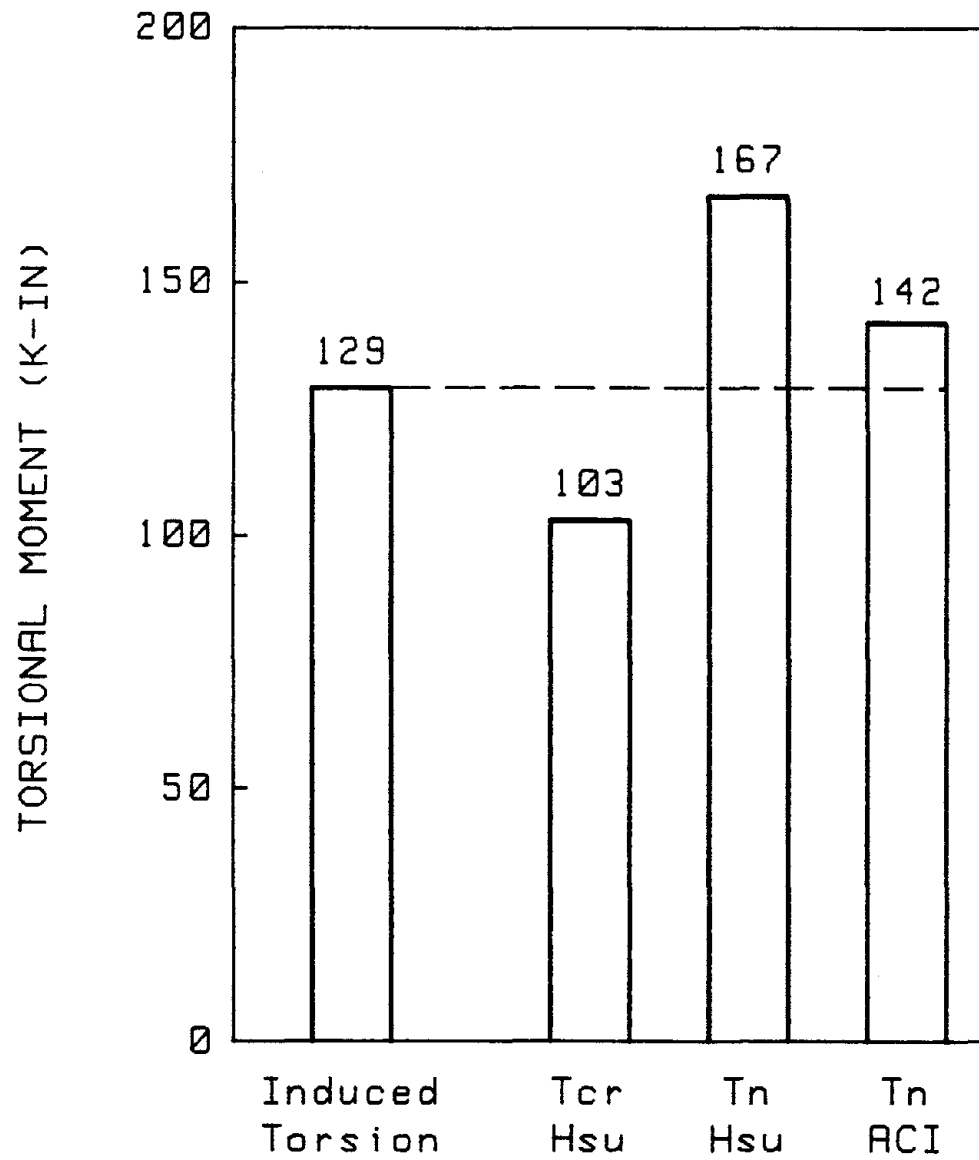Fig. 5.5(b) Effective Slab Width for Exterior Connections

Fig. 5.6 Induced Torsion vs. Torsional Strength of
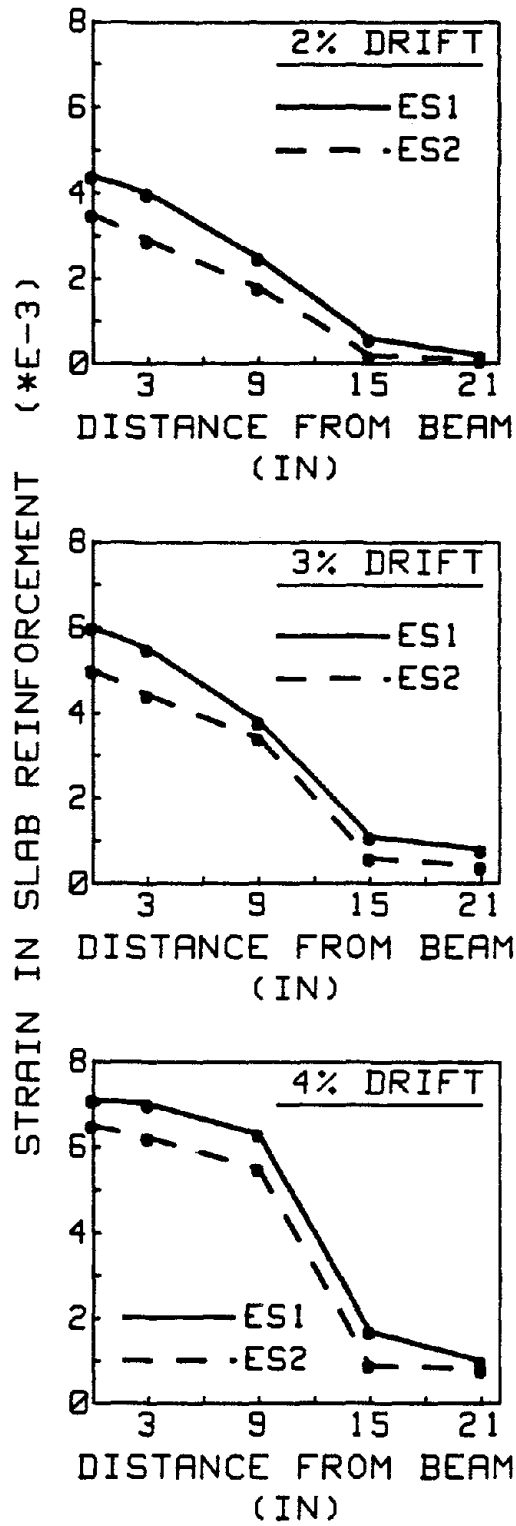Transverse Beams in Specimen CS1

Fig. 5.7 Strain in Slab Reinforcement of Specimens
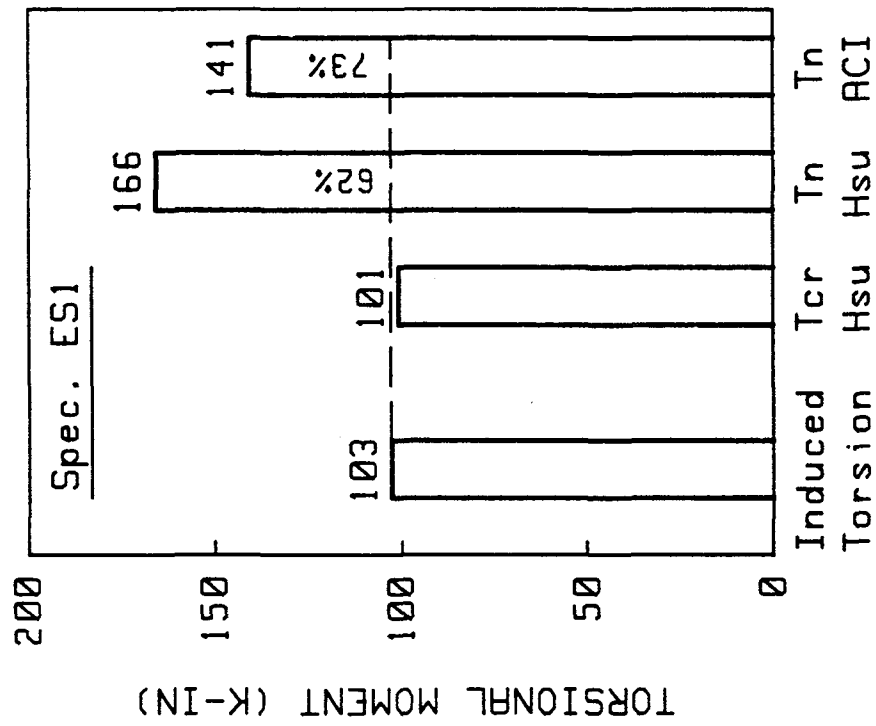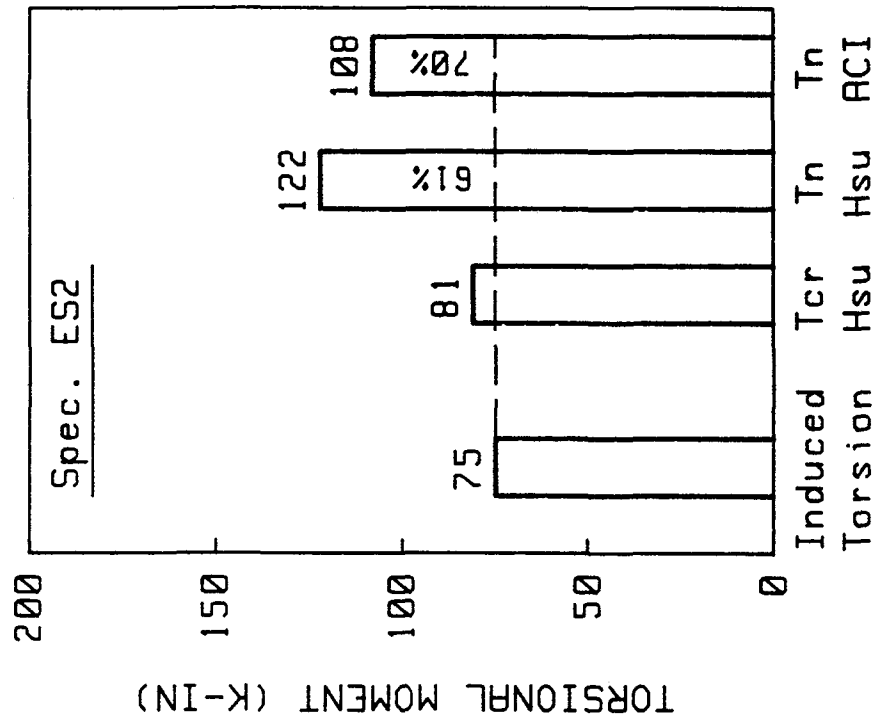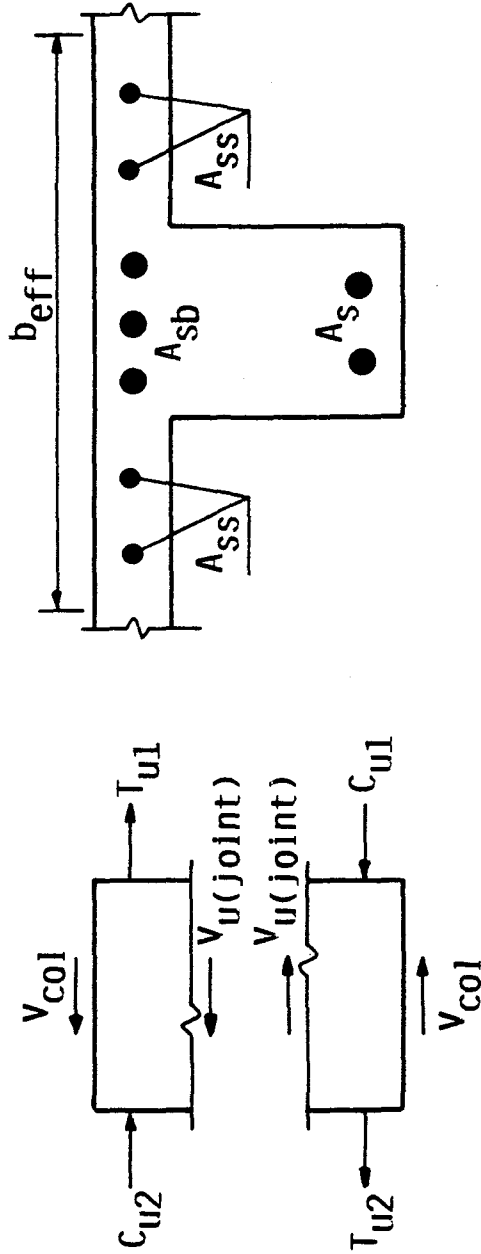ES1 and ES2

Fig. 5.8 Induced Torsion vs. Torsional Strength of Transverse Beams in Specimens ES1 and ES2

$$V_{u(joint)} = T_{u1} + C_{u2} - V_{col}$$

$$T_{u1} = A_{sb}\boldsymbol{\alpha}f_{yb} + 2A_{ss}\boldsymbol{\alpha}f_{ys}$$

$$C_{u2} = T_{u2} = A_s\boldsymbol{\alpha}f_y$$

Fig. 5.9   Evaluation of Horizontal Shear in the Joint

APPENDICES

208

Appendix A

DESIGN EXAMPLES

In order to demonstrate the effect of the slab on the design of connections two design examples are presented in this appendix. The examples are solved based on both the procedure proposed in Chapter 5 of this report and the ACI-ASCE Committee 352 design recommendations (35). The solution based on the proposed procedure is done in detail, while only the answers are given between parenthesis for the ACI-ASCE Committee 352 procedure.

In both design examples, the calculated column flexural strength is based on zero axial load for calculation of column to beam flexural strength ratio. When determining the beam flexural strength the effect of compression reinforcement in the beams is ignored.

A.1 INTERIOR JOINT

Column: 28"x28"
12#11

Slab: 7" Thick
#4@15" Top & Bottom

Main Beam: 22"x30"
4#10 Top
3#10 Bottom
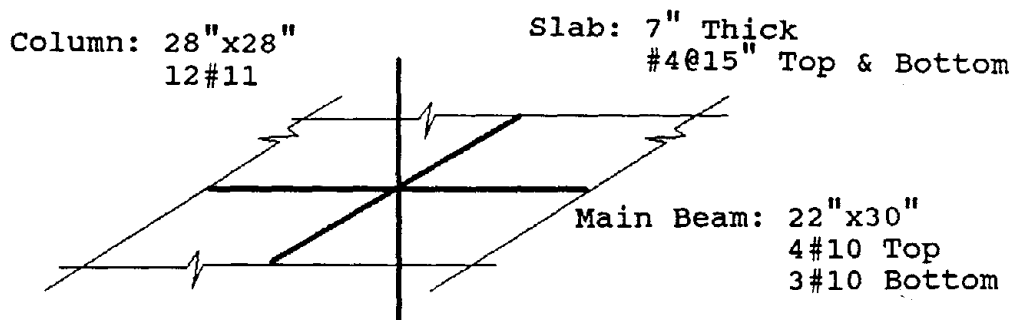
Check Joint Shear:

Find effective slab width for T-beam action with slab in compression according to ACI-318 (37) article 8.10.2

b_e = Span/4 (governs)

Assuming the Span = 25 ft., then b_e = 75 in.

$a = A_s \alpha f_y / 0.85 f'_c b_e$

$\quad = (3.81)(1.25)(60) / (0.85)(4.5)(75) = 1$ in.

$\qquad\qquad\qquad\qquad\qquad\qquad\qquad\qquad$ (3.4 in.)

$M'_{n1} = A_s \alpha f_y (d - a/2)$

$\quad = (3.81)(1.25)(60)(27.3 - 1/2) = 7658$ K-in. $= 638$ K-ft.

$\qquad\qquad\qquad\qquad\qquad\qquad\qquad\qquad$ (610 K-ft.)

Assume effective slab width in tension is equal to twice the beam depth on each side of the beam.

$A_{st} = A_{sb} + 2(A_{ss})$

$\quad = 4\#10 + 2(8\#4) = 5.08 + 3.20 = 8.28$ in.^{2}
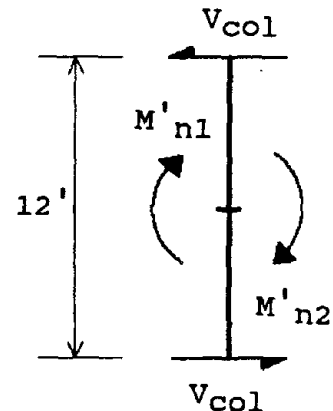
$a = (8.28)(1.25)(60) / (0.85)(4.5)(22) = 7.4$ in.

$\qquad\qquad\qquad\qquad\qquad\qquad\qquad\qquad$ (4.5 in.)

$M'_{n2} = A_{sb} \alpha f_y (d - a/2) + A_{ss} \alpha f_y (h_b - h_s/2 - a/2)$

$\quad = (5.08)(1.25)(60)(27.3 - 7.4/2)$
$\qquad\qquad\qquad + (3.2)(1.25)(60)(30 - 7/2 - 7.4/2)$

$\quad = 14464$ K-in. $= 1205$ K-ft.

$\qquad\qquad\qquad\qquad\qquad\qquad\qquad\qquad$ (795 K-ft.)
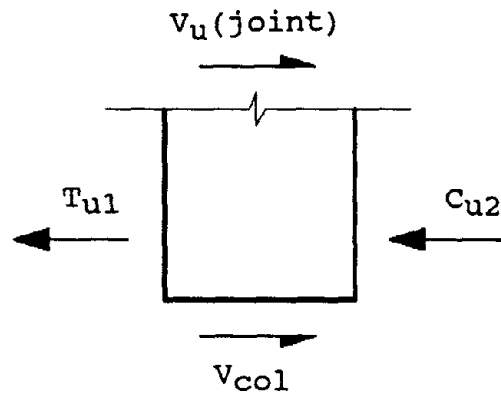
$V_u(\text{joint}) = T_{u1} + C_{u2} - V_{col}$

$T_{u1} = A_s\ \alpha\ f_y = (3.81)(1.25)(60) = 286\ \text{Kips}$

(286 Kips)

$C_{u2} = T_{u2} = A_{st}\ \alpha\ f_y = (8.28)(1.25)(60) = 621\ \text{Kips.}$

(381 Kips)

$V_{col} = (M'_{n1} + M'_{n2})/H = (638+1205)/12 = 154\ \text{Kips}$

(117 Kips)

$V_u(\text{joint}) = 286 + 621 - 154 = 753\ \text{Kips}$

(550 Kips)

$\phi\ V_n = \phi\ \gamma\ \sqrt{f'_c}\ b_j\ h_C$

where: $b_j = (28 + 22)\ /\ 2 = 25\ \text{in.} < b_b + b_c/2$

The beams have been made wide enough to classify the joint as an interior joint, so $\gamma = 20$

$\phi\ V_n = (0.85)(20)(\sqrt{4500})(25)(28)$

$= 798\ \text{Kips} > V_u(\text{joint})\quad (\text{OK})$

Check Flexural Strength Ratio:

The column flexural strength was found with α equal to 1.0. The beam flexural strengths, however, were found with α equal to 1.25. Therefore, the beam flexural strengths will be divided by 1.25 to obtain an approximate value for the beam flexural strengths if $\alpha = 1.0$.

$M_{n1} = M'_{n1}/1.25 = 638/1.25 = 510$ K-ft.

(488 K-ft.)

$M_{n2} = M'_{n2}/1.25 = 1205/1.25 = 964$ K-ft.

(636 K-ft.)

$M_n(\text{col}) = 1076$ K-ft.

Flexural Strength Ratio $= \Sigma\ M_n(\text{col})\ /\ \Sigma\ M_n(\text{beam})$

$= 2(1076)/(510+964) = 1.46 > 1.4$ (OK)
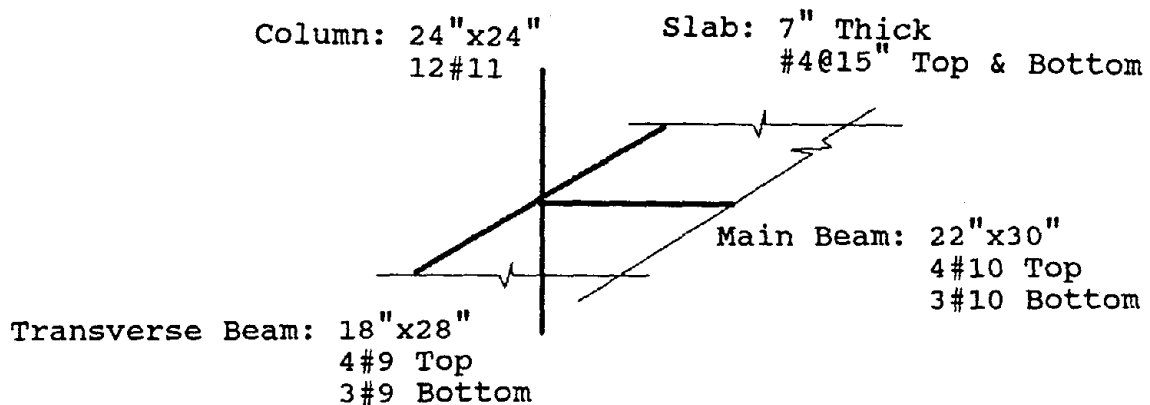
$(1.91 > 1.4$ OK)

Summary

The applied joint shear as calculated by the proposed procedure, including the effect of the slab, is equal to 753 Kips, while the applied joint shear calculated neglecting the presence of the floor slab is equal to 550 Kips. This indicates an increase in the joint shear by about 37 percent.

The ACI-ASCE Committee 352 (35) recommends a minimum value of the column to beam flexural strength ratio of 1.4. The value of the flexural strength ratio calculated including

the presence of the slab is equal to 1.46, while the value of the flexural strength ratio calculated excluding the presence of the slab is equal to 1.91. This indicates a drop in the flexural strength ratio in the order of almost 25 percent.

A.2 EXTERIOR JOINT

Column: 24"x24"
12#11

Slab: 7" Thick
#4@15" Top & Bottom

Main Beam: 22"x30"
4#10 Top
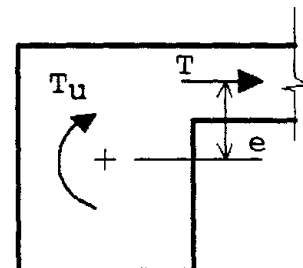3#10 Bottom

Transverse Beam: 18"x28"
4#9 Top
3#9 Bottom

Check Joint Shear:

Assume that effective slab width in tension is equal to twice the beam depth on each side of the beam.

A_{ss} = 8#4 = 8(0.2) = 1.6 in.^{2}

Assuming the entire slab reinforcement yields, the torsion, T_u, generated in transverse beams is equal to

T_u = T.e = $(A_{ss} \alpha f_y)(e)$

= (1.6)(1.25)(60)(10.5) = 1260 K-in.

According to ACI-318 (37) article 11.6.5, $\phi T_n \geq T_u$. However, $\phi T_n = 1151$ K-in. $< T_u$. Thus, torsional damage in transverse beams is expected. Use effective slab width equal to one beam depth on each side of the beam.
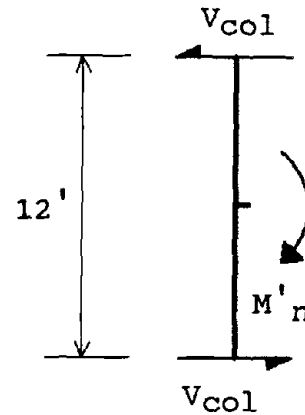
$A_{st} = A_{sb} + 2A_{ss}$

$\qquad = 4\#10 + 2(4\#4) = 5.08 + 1.6 = 6.68$ in.^{2}

$\quad a = (6.68)(1.25)(60) \, / \, (0.85)(4.5)(22) = 5.95$ in.

(4.5 in.)

$M'_n = A_{sb} \, \alpha \, f_y \, (d - a/2) + A_{ss} \, \alpha \, f_y \, (h_b - h_s/2 - a/2)$

$\qquad = (5.08)(1.25)(60)(27.3 - 5.95/2)$
$\qquad\qquad\qquad + (1.6)(1.25)(60)(30 - 7/2 - 5.95/2)$

$\qquad = 12091$ K-in. $= 1008$ K-ft.

(795 K-ft.)
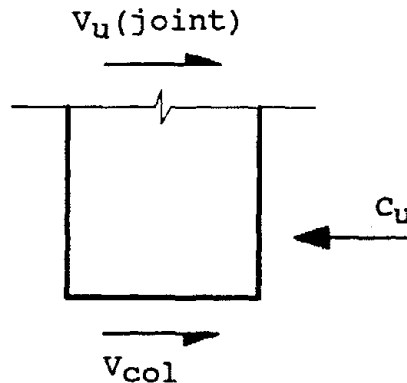
$V_u(\text{joint}) = C_u - V_{col}$

$\qquad C_u = T_u = A_{st} \, \alpha \, f_y = (6.68)(1.25)(60) = 501$ Kips.

(381 Kips)

$$V_{col} = (M'_n)/H = (1008)/12 = 84 \text{ Kips}$$

(117 Kips)

$$V_u(\text{joint}) = 501 - 84 = 417 \text{ Kips}$$

(315 Kips)

$$\phi \, V_n = \phi \, \gamma \sqrt{f'_c} \, b_j \, h_c$$

where: $b_j = (22 + 24) / 2 = 23 \text{ in.} < b_b + b_c/2$

The beams have been made wide enough to classify the joint as an exterior joint, so $\gamma = 15$

$$\phi \, V_n = (0.85)(15)(\sqrt{4500})(23)(24)$$

$$= 472 \text{ Kips} > V_u(\text{joint}) \text{ (OK)}$$

Check Flexural Strength Ratio:

The column flexural strength was found with α equal to 1.0. The beam flexural strength, however, was found with α equal to 1.25. Therefore, the beam flexural strength will be divided by 1.25 to obtain an approximate value for the beam flexural strength if $\alpha = 1.0$.

$$M_n = M'_n/1.25 = 1008/1.25 = 806 \text{ K-ft.}$$

(636 K-ft.)

$$M_n(\text{col}) = 865 \text{ K-ft.}$$

Flexural Strength Ratio $= \Sigma \, M_n(\text{col}) \, / \, \Sigma \, M_n(\text{beam})$

$$= 2(865)/(806) = 2.15 > 1.4 \text{ (OK)}$$

(2.72 > 1.4 OK)

216

Summary

The applied joint shear as calculated by the proposed procedure, including the effect of the slab, is equal to 417 Kips, while the applied joint shear calculated neglecting the presence of the floor slab is equal to 315 Kips. This indicates an increase in the joint shear by about 32 percent.

The ACI-ASCE Committee 352 (35) recommends a minimum value of the column to beam flexural strength ratio of 1.4. The value of the flexural strength ratio calculated including the presence of the slab is equal to 2.15, while the value of the flexural strength ratio calculated excluding the presence of the slab is equal to 2.72. This indicates a drop in the flexural strength ratio in the order of almost 21 percent.